Intraday pricing and mispricing of short-maturity SPX options

Christian Dorion* Piotr Orłowski† Yuhan Song‡§

Preliminary and incomplete, please do not circulate.

ABSTRACT

We study the intraday pricing and risk structure of (ultra-) short-maturity SPX options. Six factors span option returns: three powers of the underlying return and three variance-dynamics components. Using a novel factor modeling approach, we estimate high-frequency time-series of the factors' risk-neutral expectations and their unconditional risk premiums. We document significant and persistent mispricing concentrated in 0DTE options, exhibiting pronounced intraday seasonality. Regression analysis links these dislocations to intermediary leverage levels, funding costs in equity futures, and option inventories.

JEL Classification: G10; G12; G13.

Keywords: Option Returns; Factor Models; 0DTE; Tail risk.

*HEC Montréal, christian.dorion@hec.ca.

†HEC Montréal, piotr.orlowski@hec.ca.

‡HEC Montréal, yuhan.song@hec.ca.

§We thank Torben Andersen, Gustavo Freire (discussant), Robert Korajczyk, Neil Pearson, Viktor Todorov, Liuren Wu and seminar participants the FMA/Cboe 2024 Conference on Derivatives and Volatility, the 13th SoFiE Conference, HEC Montréal, Northwestern University, Queen's University, and Western University for their insightful comments and suggestions. This paper was previously presented as "The Factor Structure of 0DTE Option Returns." The three authors are with HEC Montréal; Dorion and Orłowski are with the Canadian Derivatives Institute. Corresponding author: Christian Dorion, `christian.dorion@hec.ca`, HEC Montréal, 3000 Chemin de la Côte-Sainte-Catherine, Montréal, Québec H3T 2A7, Canada. We gratefully acknowledge financial support from the Canadian Derivatives Institute and the Social Sciences and Humanities Research Council.

1. Introduction

Despite the staggering shift of SPX option market liquidity towards ultra-short maturity options, their pricing and risk structure remain largely unexplored. Using intraday data, we find that six factors span short-maturity option returns: three powers of the underlying return and three components capturing the dynamics of variance risk. Leveraging a recent factor modeling methodology, we characterize the intraday dynamics of these factors' pricing-measure (Q) expectations and provide estimates of their risk premiums. With risk compensation accounted for, we document significant and persistent seasonal mispricings of zero-days-to-expiration (0DTE) options throughout the trading day. Our analysis delivers a new high-frequency view of the option market's stochastic discount factor and of how compensation for volatility and higher-moment risks evolves within the trading day. We also link the dynamic mispricing of 0DTE options to broader financial market conditions, and especially to the funding costs of financial intermediaries.

Delta-hedging eliminates most of the variation in option positions at all maturities, including 0DTE contracts. Across maturities, we find a sharp transition in what drives delta-hedged option return variation. For 0DTE contracts, the squared underlying return is the dominant factor, reflecting the options' exposure to realizations of *prevailing* volatility. As maturity increases, *changes* in spot volatility explain most of the return variation. Conditional expectations of powers of S&P 500 index returns under the pricing measure display distinctive yet familiar dynamics: the Q-second moment co-moves with the VIX, while the Q-third moment is negative and spikes more sharply in stress periods. Importantly, these estimates arise from a paradigm not applied to option data before, and the fact that they align closely with prior literature testifies to the robustness of our approach. The premium for high frequency squared returns is estimated at essentially zero, perhaps counter-intuitively, but in line with the fact that squared returns are not correlated with either the market index return or with volatility dynamics. At this high frequency, the third power of the index return is a directional pure jump factor and we find that it also carries virtually no risk premium and carries a large positive risk premium. Among the variance-dynamics factors, the premium on spot-volatility risk turns negative around FOMC announcements yet becomes slightly positive otherwise; the short-term variance-premium factor is uniformly negatively priced, and the slope factor positively, consistent with their correlations with the market index return.

Despite the factor model's strong fit, we uncover systematic and persistent mispricing, concentrated in 0DTE option returns. We estimate high-frequency time-series of option alphas—components of expected returns unexplained by factor premiums—which we refer to as *dislocations*, and analyze their patterns across maturity, moneyness, and time-of-day. Firstly, 0DTE call dislocations average about -7% of underlying value per annum, compared with magnitudes below $\pm 1.8\%$ p.a. for other options. In puts, mean values are near zero, but at 0DTE dislocation volatility is four-to-five times higher than for one-day-to-expiration options. Despite their high volatility, these dislocations are not noise: they display significant autocorrelation and strong intraday seasonality. Zero-DTE options tend to be underpriced in the morning, overpriced around midday, and again underpriced toward market close, while the pattern disappears at longer maturities. The 0DTE pattern shifts on FOMC announcement days, when dislocations are uniformly negative—hence option prices are elevated—consistent with temporary demand pressure and sellers' inventory-management constraints. Regression evidence further links the time variation in mispricing to intermediary balance-sheet conditions: higher primary-dealer capital ratios predict higher dislocations—cheaper options—uniformly across option maturities. Another important economic link comes from the observation that in puts—but less so in calls—selling options is more attractive when open interest in like contracts is high, consistent with option sellers demanding higher premiums when option inventory is high. Taken together, these results indicate that option prices respond to intraday shifts in risk-bearing capacity, revealing a channel through which intermediary constraints transmit to the high-frequency pricing of volatility and tail risk.

Our study contributes to several strands of literature. To begin with, we add to the growing body of work on ultra-short-maturity options. We are the first to inspect intraday return dynamics through the lens of a factor model, allowing us to provide new evidence on risk premiums and mispricing in this market segment, and put them in the context of longer-maturity contracts. From a broader methodological perspective, we complement and extend the literature on Q-moment estimation: whereas the literature using static replication methods (to calculate risk-neutral variances, for instance) is limited to functions of underlying asset returns and constrained by available option maturities, imposing a factor structure unlocks the estimation of the factors' Q-expectations at a high frequency. These time-series can become an object of study in their own right, akin to the VIX, as it is likely they embed information about market expectations and risk. Taking an asset pricing view, we directly contribute to the literature recovering risk premiums from options, and our main novel stylized fact is the decomposition of the risk premium on systematic variance innovations into three components with distinct economic interpretations and risk prices. Our approach can be extended to conditional risk premiums simply by estimating predictive models for the time-series of the factors and combining their P-predictions with our estimates of the Q-expectations. In a wider asset-pricing context, our findings relate to research on the role of financial intermediaries as price-setters in securities markets, as we document how variables related to their financial health, and to quantities of options traded, influence mispricing relative to our factor model.

Our research methodology relies on the foundation of conditional factor models. When factors are not traded, their Q-expectations encode risk compensation and are unrelated to the risk-free rate. These Q-expectations can be backed out from a factor model's conditional intercepts given the assets' exposures. Option exposures are non-linear and time-varying, but tightly cross-sectionally linked, hence we model them non-parametrically as smooth functions of option characteristics; we model the conditional intercepts similarly. The Black–Scholes–Merton implied volatility is a key variable included in both exposures and intercept functions, as it summarizes market expectations of future volatility and risk. After estimating the conditional intercepts and exposures, we recover the factors' Q-expectations by estimating, at each point in time, cross-sectional regressions of the intercepts on the exposures, as implied by no-arbitrage for models with non-traded factors. To estimate pricing dislocations, we add to the cross-sectional regressions a set of fixed effects that capture common components of expected returns of options with similar characteristics not spanned by exposures.

Related literature A nascent but rapidly growing literature investigates the implications of 0DTE or ultra-short-maturity (USM) options for market dynamics and asset pricing. Considering options with conventional (non-USM) maturities, Ni et al. (2020) find that market-maker rebalancing their hedging positions significantly affects volatility dynamics of individual stocks, implying that intermediaries play a central role in volatility transmission. Lipson, Tomio, and Zhang (2023) document that retail option trading increases the volatility of the underlying securities, suggesting that the flow of speculative trades can transmit directly into underlying asset prices.

Thus, as trading in ultra-short-maturity (USM) options grew exponentially over the past few years, certain market participants raised concerns about the potentially systemic threat that same-day expiry options, in particular, could pose to markets. Whereas some media loudly echoed these concerns, careful analysis gives little credence to USM options being a destabilizing force. In particular, Adams et al. (2025) analyze the introduction of daily S&P 500 expirations and show that 0DTE trading attenuates, rather than amplifies, market volatility. They attribute this stabilizing effect to market makers' hedging flows, which typically move against contemporaneous price trends. Their results suggest that liquidity provision, rather than speculative activity, dominates the impact of 0DTE trading on the underlying index.

On the other hand, an important potential upside of having liquid USM option markets is that these options may very well contribute to making markets more complete, therefore enabling more efficient risk transfers. Recent evidence by Fu et al. (2024) indicates that realized spreads in the USM market, a measure of liquidity provider profits, are low. This finding is at odds with the widespread belief that liquidity providers exploit public customers trading 0DTE SPX options. In turn, this suggests that market makers can efficiently hedge the risks factors that, beyond the movements in the underlying, drive the returns of USM options.

To the best of our knowledge, we are the first to estimate a state-of-the-art factor model of option returns on USM options. Our work is nonetheless closely related to two contemporaneous papers. First, Bandi, Fusari, and Renò (2024) develop a novel pricing formula specifically targeted to capture the time-varying skewness and kurtosis implied by 0DTE options. They obtain prices that are within the bid-ask spread for 80% of the options in their sample. They also document significant improvements in delta-gamma hedging when using their model rather than the BMS model. Almeida, Freire, and Hizmeri (2024), on the other hand, study the asset pricing implications of a kernel that would hinge on 0DTE options. One of their important findings is that investors demand a high compensation to bear variance risk over the day.

Our approach, however, fundamentally differs from those studies. In particular, we build on Fournier, Jacobs, and Orłowski (2024) and design a model that interacts intuitive, observable risk factors with exposures estimated using machine learning methods. Such intuitive factors naturally arise in the context of classical no-arbitrage option pricing models, and in particular the Black-Scholes-Merton (BMS) model, which shapes the language and practice of derivatives trading. Using them mitigates the black-box nature of machine learning models. The decentralized option-valuation framework of Carr and Wu (2020) leverages this insight by associating risk factors to the most common BMS greeks of delta-hedged options: vega, gamma, volga, and vanna. In similar spirit, our baseline empirical model specification relies on the following six factors: the return on the underlying (DLT), its squared (GAM) and cubed (JSK) value, and changes in the market risk-neutral variance, disaggregated into three factors (labelled dSV, dVRP, and dTRM respectively). Some of the labels are chosen to evoke the greeks that are associated with these shocks in the BMS model. However, the role of the BMS model ends at providing intuition. We estimate the exposures to these shocks using machine learning methods rather than differentiating option prices implied by a pricing model.

Delta-hedged returns of at-the-money (ATM) puts (calls) exhibit roughly 95% (91%) less variation than their unhedged counterparts at maturities between 0 and 15 days to expiration (DTE). Broadie, Chernov, and Johannes (2009) nonetheless clearly established that these are the quantity of interest when assessing a model's ability to describe option returns. Delta-hedged option returns, averaging -7% per annum, encompass the very risk factors, not spanned by the underlying's market, that investors seek to hedge or speculate on by investing in options. Unsurprisingly, our variance and jump risk proxies explain roughly 85% of the variation in delta-hedged option returns on 4 to 15DTE options. On 0DTE options, this figure decreases to 70% and the mispricing is systematic, persistent, and consistent with temporary demand pressure and sellers' inventory-management constraints.

2. Data

Our dataset comprises high-frequency records of quotes of S&P 500 Index options from September 2016 to December 2023,[1] obtained from the Cboe Global Markets (further referred to as Cboe) Option Intervals dataset, which aggregates option quotes at 1-minute frequency with synchronized S&P 500 index records. We use the midpoint of the high-frequency quotes as the option price and then compute delevered returns over 30-minute intervals. As a liquid

[1] During March 2020, the S&P 500 index triggered circuit breakers four times, leading to periods of illiquidity and extreme market values. Therefore, we have chosen to exclude quotes during the four circuit-breaker dates.

and tradable proxy for the underlying we use millisecond-precision E-mini S&P 500 futures trade records from Tickdata Inc., and risk-free rates from the Fama-French Data Library, assumed constant within each day.[2]

We focus on PM-settled options with 15 or fewer business days to expiration (DTE). We set the intraday trading window to be 9:45 ET to 15:45 ET to avoid opening and closing anomalies, and sub-sample these datasets at a 30-minute frequency to mitigate microstructure noise.

We further describe the option filtering criteria which are designed to alleviate the issues of sample survivorship bias and look-ahead bias (Duarte et al., 2024). An option first enters our sample when it has 15 or fewer DTE, positive volume, and a non-zero bid price at the start of a 30-min return interval and is classified as neither in-the-money (ITM) nor extremely deep out-of-the-money (DOTM)[3] Subsequently, we monitor the option at each 30-minute interval until expiration. We record an option return at any time that the following conditions hold: (a) the option is classified as ATM, out-of-the-money (OTM) or DOTM at the start of the interval (hence we include returns that move the option into ITM or extremely DOTM territory), (b) its bid price is positive at the start of the interval (hence we include periods when the bid price ends up at zero, and use half the ask price to compute returns). Importantly, after an option is first included in the sample, we do not require subsequent positive volume. Finally, we carefully handle instances where an option might cease to trade before expiration. We treat the last interval before expiration at the start of which the option's bid price was positive, and at the end of which the bid price was zero as a total loss on the contract, i.e., a -100% raw return. This specifically addresses the survivorship bias concern. If an option's bid price remains positive through all trading periods, we keep all 30-minute returns and compute the (potentially -100%) return at expiration from the option's settlement payoff. We provide more details in Appendix A.

2.1 Option sample collection and return calculation

Our final sample contains roughly 14 million 30-minute returns on SPX puts and 6.8 million returns on SPX calls. Detailed information about the sample composition can be

[2]See https://mba.tuck.dartmouth.edu/pages/faculty/ken.french/data_library.html

[3]We exclude the options in the 1% extreme left and right tails, due to their illiquidity and lack of meaningful informational content. The tail ratio and strike boundary are defined in Section B.

found in Table I. Most of the options in our sample are relatively long-dated, with 4–15 DTE options accounting for about 85% of the total observations. If the options were evenly distributed across all the maturities in this interval, each DTE would represent about 7.1% of the total sample. In contrast, 0DTE options account for 1.4% of the put sample and 1.9% of the call sample. These numbers do not reflect actual trading activity, which is heavily concentrated in 0DTE options, but rather the limited number of distinct contracts traded at expiration day. There are two main reasons for this: first, as maturity gets very short, the strike range of actively quoted options narrows considerably; second, as the strike grid is fixed at $5, the number of strikes inside the range diminishes. We label an option as OTM or DOTM based on the distribution of normalized moneyness, $\kappa_{t,\tau}$;[4] by design, after discarding ITM options, ATM options comprise 50% of the sample, OTM options 30%, and DOTM 20%. Appendix C provides further detail; in particular, Figure A.I therein summarizes the distribution of normalized moneyness by maturity bucket (0DTE, 1-3 DTE, and 4-15 DTE). Shapes are very similar across maturities and stable across the intraday timestamps: for puts, density declines smoothly toward DOTM moneyness; for calls, density presents a steep drop beyond ATM and a short right tail.

After filtering the option sample, our analysis centers on delevered option returns defined as:

$$r_{t+1} = \frac{O_{t+1} - O_t}{S_t} = r^{raw}_{t+1} \times \frac{O_t}{S_t}\,, \tag{1}$$

The delevered return is calculated as the gain from a long position in the option divided by the price of the underlying asset at initiation, and is equal to the raw option return multiplied by the inverse of option-embedded leverage, O_t/S_t. This definition has several advantages: first, it prevents the occurrence of bias in aggregate statistics due to measurement error in a return's denominator (Duarte, Jones, and Wang, 2024); second, under this definition, return exposures to risk factors do not depend on the ratio of the stock price to an option's price, which simplifies modeling, and are stationary;[5] third, FJO document that it delivers more robust and plausible estimated exposures, most likely due to the fact that it down-weights extreme

[4]We define normalized moneyness as $\frac{\ln(K/F_{t,\tau})}{\sqrt{\tau CIV_{t,\tau}}}$, where CIV is a variance proxy (Andersen, Bondarenko, and Gonzalez-Perez, 2015) described in Appendix B.

[5]For example, under the Black–Scholes–Merton model, an index option's beta, more generally referred to as an option's elasticity, is equal to the product of its delta and the option's embedded leverage, S_t/O_t. Therefore, the delevered return's beta is simply equal to delta, and this estimand is easier to reliably recover, as documented by FJO and Dickerson et al. (2025).

returns on very deep OTM options with very low prices. We track the delevered returns of the option positions described in Section 2. We compute the delevered intraday returns at a 30-minute frequency. To maximize coverage and avoid discarding observations due to zero bids at exact timestamps, we allow a 5-minute tolerance window: at each timestamp, we select the last positive bid in the preceding 5 minutes; if none exists, the recorded quote is zero.[6] We match the ES future prices with the option quotes at the selected timestamps to ensure consistency under the tolerance window.

2.2 Descriptive statistics of option returns

We report on both (i) delevered, but unhedged 30-minute returns defined in equation (1) and (ii) delevered delta-hedged 30-minute returns defined as:

$$r^{dh}_{i,t+1} = \frac{O_{t+1} - O_t}{S_t} - \widehat{\beta}_{\mathrm{DLT},i,t}\mathrm{DLT}_{t+1} = r^{raw}_{i,t+1} \times \frac{O_t}{S_t} - \widehat{\beta}_{\mathrm{DLT},i,t}\mathrm{DLT}_{t+1}; \tag{2}$$

where DLT denotes the 30-minute return on the E-mini S&P500 futures contract, and the hedge ratio, $\widehat{\beta}_{\mathrm{DLT},i,t}$, is estimated using the factor model described in Section 3. Table I contains the summary statistics of the returns by moneyness and maturity, reported in percentage terms and annualized. For the unhedged series, put returns are uniformly negative across all moneyness and maturity buckets (overall mean of −4.12%), whereas call returns are positive for all maturities except 0DTE (overall mean of 2.28% for 1–3DTE; 3.10% for 4–15DTE; but −5.11% for 0DTE). The negative returns on 0DTE calls are surprising because calls are on average positively exposed to the market return, which has a positive risk premium. The return magnitudes are the highest for ATM options and intensify as maturity shortens, making 0DTE ATM options the most extreme: mean returns of −13.32% for puts and −6.26% for calls. After delta-hedging, mean returns for both puts and calls are negative and substantially less dispersed: mean returns are −1.46% for puts and −1.22% for calls, while standard deviations decline from 7.07% to 1.74% for puts and from 5.52% to 2.04% for calls. These intraday return patterns contrast with the findings of Muravyev and Ni (2019), who document positive intraday delta-hedged option returns for SPX. Two design differences reconcile the results: (i) their shortest maturity is 4DTE, whereas our

[6] Such procedures are common in the asset pricing literature, see for instance notes on calculation of bond returns in Dickerson, Mueller, and Robotti (2023).

sample includes shorter-maturity options whose hedged returns are uniformly negative, with 0DTE contracts exhibiting the most negative values; and (ii) their sample period is earlier (2004–2013), whereas ours covers a more recent period with markedly different intraday trading dynamics in USM options.

3. Factor structure in option returns

3.1 A factor model inspired by classical option pricing

To anchor the specification of our model, we start with a familiar Taylor expansion of the option value dynamics:

$$\mathrm{d}O = O_S\,\mathrm{d}S + O_t\,\mathrm{d}t + O_V\,\mathrm{d}V + \frac{1}{2}O_{SS}\,(\mathrm{d}S)^2 + \frac{1}{6}O_{SSS}(dS)^3 + \ldots, \tag{3}$$

where O_x, O_{xy}, and O_{xyz} denote derivatives of the option price with respect to pricing inputs x, y, and z up to third order; in our case the inputs being the underlying value, S, and the level of variance of the underlying, V. Equation (3) accounts for the nonlinear impact of the underlying asset's dynamics and the first-order effect of variance changes on option prices.[7] To obtain the delevered option return defined in equation (1), we multiply both sides of equation (3) by $\frac{1}{S}$ and collect terms in such a manner that the expansion is in terms of the powers of the underlying return $\mathrm{d}S/S$ and changes in variance $\mathrm{d}V$:

$$\frac{\mathrm{d}O}{S} = O_S\frac{\mathrm{d}S}{S} + \frac{O_t}{S}\,\mathrm{d}t + \frac{O_V}{S}\,\mathrm{d}V + \frac{1}{2}S \times O_{SS}\left(\frac{\mathrm{d}S}{S}\right)^2 + \frac{1}{6}S^2 \times O_{SSS}\left(\frac{dS}{S}\right)^3 + \ldots \tag{4}$$

Equation (4) states that an option delevered return's direct sensitivity to the underlying asset return is equal to its delta, while its sensitivity to the second and third powers of the underlying return are scaled versions of its gamma and third-order price sensitivity, respectively. For the sake of brevity, throughout the rest of the paper, we refer to the squared and cubed underlying returns as gamma and jump skew risk.[8] Furthermore, the option's

[7] Our choice of O_{SSS} rather than variance vanna O_{SV} or variance volga O_{VV} is motivated by empirical analysis (cf. Table A.II) showing the superior explanatory power of O_{SSS} in our context.

[8] At high frequency, the cubed return captures the directional jump risk, as the diffusion component is negligible; see, for instance, Aït-Sahalia and Jacod (2014).

sensitivity to changes in variance is proportional to its scaled variance-vega. One of the benefits of the delevered return representation is that the sensitivities in equation (4) do not depend on the level of the underlying asset if one considers a fixed moneyness level $\kappa = K/S$. For instance, in the Black–Merton–Scholes model, $O_{SS} = \frac{\phi(d_1(\kappa,\tau))}{S\sigma\sqrt{\tau}}$, where σ is the implied volatility and τ the option's maturity. In equation (4), after scaling by S and accounting for the Taylor expansion, we obtain $\frac{\phi(d_1)}{2\sigma\sqrt{\tau}}$. Finally, in the factor model, the option's time decay term O_t/S is accounted for by the conditional intercept of the option.[9]

Using the BMS pricing formula as a bijection between the space of options prices and that of implied volatilities, Carr and Wu (2020) introduce a decentralized option valuation framework where V in equation (3) is replaced by each option's implied volatility, and where exposures are calulated using the BMS model. Our approach differs by constructing a set of factors that are common to all options and employing a nonparametric estimation of the scaled risk exposures. Equations (3) and (4) imply that, absent any frictions, an option return's dynamics should be determined by the dynamics of the underlying asset and its time-varying variance.

Accordingly, we construct factors that are proxies for these joint dynamics. The first factor is a proxy for the return on the underlying asset, akin to $\mathrm{d}S/S$ in equation (4): the return on the front S&P E-Mini futures contract, labeled DLT. For the gamma and jump skew risk factors, we use the squared and cubed returns on the same futures contract, and label them GAM and JSK, respectively.

Recognizing that the option pricing literature documents that variance dynamics of the S&P 500 index are likely determined by multiple factors, we split the second factor, $\mathrm{d}V$, into three components. The first, labeled dSV, captures the changes in the spot variance of the index return.[10] The second component, labeled dVRP, is the change in the difference between short-maturity risk-neutral variance and spot variance; it captures the short-term dynamics of the variance risk premium and of the risk-neutral expected quadratic variation of jumps. The third component, dTRM, reflects the shifts in the term structure of expected risk-neutral variance and its risk compensation and is defined as the change in the difference

[9]See the derivation of the expected return on an option in Broadie, Chernov, and Johannes (2009). In this derivation, the time decay is substituted out via the pricing PDE to accommodate the Q-expectations of the factors.

[10]Spot variance is the instantaneous variance of the continuous component of the underlying return process, see Aït-Sahalia and Jacod (2014).

between long- and short-maturity risk-neutral variances. Importantly, each of these variance factors is the same for all options, and only the exposures of each option to these factors will differ in the cross-section. In what follows, we will sometimes refer to the sum of dSV, dVRP, and dTRM as VAR, a total variance dynamics factor similar to VAR in the FJO paper.

We operationalize the three variance factors as follows. First, we estimate spot variance (SV) following Cboe's methodology for the calculation of the SPOTVOL index, based on the nonparametric spot variance estimator proposed by Todorov (2019).[11] Cboe calculates initial estimates from options with the two shortest maturities exceeding 2DTE (labeled 2^+) and averages them to obtain the final value, SV_{2^+}. Using these estimates, we define dSV $:= SV_{2^+,t+1} - SV_{2^+,t}$. To calculate risk-neutral variance at different maturities, we use the Andersen, Bondarenko, and Gonzalez-Perez (2015) corridor implied variance (CIV) estimator. For the short-maturity risk-neutral variance, we repeat the procedure used for spot variance and denote the averaged estimator as CIV_{2^+}. The dVRP factor is then defined as dVRP $:= (CIV_{2^+,t+1} - SV_{2^+,t+1}) - (CIV_{2^+,t} - SV_{2^+,t})$. Finally, for the long-maturity risk-neutral variance, we use the CIV estimator calculated from options with the longest available maturity (14–15DTE), denoted CIV_{14^+}. The dTRM factor is defined as dTRM $:= (CIV_{14^+,t+1} - CIV_{2^+,t+1}) - (CIV_{14^+,t} - CIV_{2^+,t})$.

It is also instructive to discuss the conceptual difference between the variance dynamics factors and GAM, the squared return realization. The GAM factor captures the realized variation in the underlying return over a short interval, akin to the quadratic variation process in continuous-time models. It can be interpreted as a high-frequency realization of the prevailing instantaneous variance of the underlying at the beginning of the interval. In contrast, the variance dynamics factors capture changes in the variance process itself, i.e., changes in expectations about the future realizations of GAM. dSV and dVRP capture changes in short-term variance expectations, and together with dTRM they capture changes in longer-term variance expectations. From an intertemporal asset-pricing perspective, they are associated with changes in the investment opportunity set, and thus are likely to command risk premiums.

Finalizing our model requires choosing a set of instruments that impact the risk exposures. We use the same signals for each factor; in estimation this will result in different exposures because of the non-parametric nature of the model. In the BMS framework, the greeks are

[11] https://www.cboe.com/us/indices/dashboard/spotvol/

all functions of time to expiration ($\tau_{i,t}$), adjusted moneyness ($\kappa_{i,t}$, defined in equation (C3) in Appendix C), and implied volatility ($IV_{i,t}$). In our setting, implied volatility serves as an aggregating characteristic which captures the state of the market (as the implied volatility itself depends on the level of the underlying's volatility) and other relevant information about the option that arises from the investors' pricing activity. As demonstrated by Chen et al. (2023), machine learning models can significantly benefit from being "taught" structural models. In that spirit, whereas we do not learn the BMS greeks themselves before estimating our model's sensitivities, it seems natural to instrument our model with $\boldsymbol{c}'_{i,t} = [\ln \tau_{i,t},\ \kappa_{i,t},\ \ln IV_{i,t}]$, the determinants of BMS greeks. While our estimation method is non-parametric, we use logarithms of τ and IV to improve estimation outcomes. For time to maturity, this increases the method's flexibility in capturing the dynamics of 0DTE options as maturity approaches zero. For implied volatility, this prevents overfitting extreme values during the COVID-19 pandemic.

3.1.1 Factor dynamics

Table II reports, among others, the physical means of the factors ($\overline{f}$), in annualized percentage points. The average realization of DLT, 4.5%, is the expected excess daytime return on the nearest-maturity S&P 500 futures contract. The 1.6% mean of GAM is consistent with the annualized variance of the S&P 500 intraday index return being around 13%. The sample means of the variance dynamics factors are more difficult to interpret directly. In particular, the fact that after annualization these means are large in magnitude signals that there are large fluctuations in the levels of variance outside of our intraday sample, but within our sample period. The means of dSV and dVRP are large and negative: dividing by 252, they imply an average decrease in variance of about 8.3 and 10.6 basis points, respectively, between 9:45 ET to 15:45 ET. Over the same period, the mean of dTRM is positive, and corresponds to an average daily increase in the term structure of variance of about 12.3 basis points. These observations are consistent with strong seasonal patterns in intraday variance dynamics documented in the literature.

The factors are not strongly persistent. Table III reports the first-order (30-minute) and one-day lag autocorrelations; only GAM exhibits moderate persistence (30% at both frequencies); surprisingly, dTRM has a negative one-day autocorrelation of a similar order, but a first-order autocorrelation close to zero. The remaining autocorrelations are all at most

10% in absolute value.

The joint correlation structure of the factors (tabulated in Table A.III), contains several notable features. First, DLT is negatively correlated with dSV (-0.56) and dVRP (-0.38), and positively correlated with dTRM (0.41) and JSK (0.42). Second, GAM—the realization of prevailing instantaneous variance—is, in practical terms, uncorrelated with all factors except for JSK (0.37). This correlation structure has implications for one's expectations about the factors' risk premiums, which we confront with empirical estimates in Section 4.

3.2 Model implementation and estimation

We employ the conditional factor model from FJO to capture the non-linear nature of option exposures to risk factors and potential time-variation in risk premiums. The delevered excess option returns are modeled as:

$$\begin{aligned} r^e_{i,t+1} &= r_{i,t+1} - E^Q[r_{i,t+1}] \\ &= \sum_l \left(-E^Q[f_{l,t+1}] \times \beta_{l,i,t} + \beta_{l,i,t} \times f_{l,t+1}\right) + \varepsilon_{i,t+1} \\ &= c_{i,t} + \sum_l \beta_{l,i,t} f_{l,t+1} + \varepsilon_{i,t+1} \end{aligned} \tag{5}$$

where $E^Q[r_{i,t+1}]$ is the risk-neutral expectation of the option return, $f_{l,t+1}$ represents the risk factor realization between time t and $t+1$, $c_{i,t}$ is the conditional intercept, and $\varepsilon_{i,t+1}$ denotes the model residual that satisfies $E^P[\varepsilon_{i,t+1}] = E^Q[\varepsilon_{i,t+1}] = 0$. The conditional intercept, $c_{i,t}$, should equal the negative of $\sum_l E^Q[f_{l,t+1}]\beta_{l,i,t}$, the sum of the products of negative risk neutral expectation of the factors and their corresponding exposures.

Following FJO, we model option exposures as functions of option characteristics using the thin plate regression spline (TPRS) basis. The risk loading of option i can be written as

$$\beta_{l,i,t} \approx \boldsymbol{\phi}'_{i,t}\boldsymbol{b}_l \tag{6}$$

where $\boldsymbol{b}_l$ is a $k \times 1$ vector of factor-specific parameters capturing the basis representation of $\beta_{l,i,t}$ across i and t, $\boldsymbol{\phi}_{i,t}$ is $\phi(\boldsymbol{c}_{i,t})$, a "feature" vector in a higher-dimensional space, and $\boldsymbol{c}_{i,t}$ is the vector of option characteristics. As a result, the exposure to a given risk factor l is linear in $\boldsymbol{b}_l$, the parameter vector. Combining equations (1) and (6), and setting $E^Q[f_{l,t+1}] = \mu_{l,t}$

implies the following conditional factor structure for the delevered option return:

$$r^e_{i,t+1} = \sum_l \left(-\mu^Q_{l,t} \times \boldsymbol{\phi}'_{i,t} \boldsymbol{b}_l + f_{l,t+1} \times \boldsymbol{\phi}'_{i,t} \boldsymbol{b}_l \right) + \varepsilon_{i,t+1}\,. \tag{7}$$

To express equation (7) as linear in parameters, we first define $\boldsymbol{F}_{l,i,t+1} = f_{l,t+1} \times \boldsymbol{\phi}_{i,t}$, a $k \times 1$ vector of scaled factor realizations. The conditional intercept $c_{i,t}$ is the sum of products of interactions between $\boldsymbol{\phi}'_{i,t}$, and the conditional risk-neutral expectations. Because our option characteristics contain the option implied volatility, the conditional intercept contains information relevant for risk-neutral moment and risk premium estimation, and we set $\mu_{l,t}$ to constants. With $\boldsymbol{\phi}_{i,t}$ identical for each factor, we rewrite the conditional intercept as $c_{i,t} = \boldsymbol{\phi}'_{i,t}\boldsymbol{q}$, where $\boldsymbol{q} = \sum_l -\mu_l \times \boldsymbol{b}_l$. With these definitions, we rewrite equation (7) as:

$$r^e_{i,t+1} = \underbrace{\boldsymbol{\phi}'_{i,t} \sum_l \boldsymbol{q}_l}_{c_{i,t}} + \sum_l \boldsymbol{F}'_{l,i,t+1} \boldsymbol{b}_l + \varepsilon_{i,t+1}\,. \tag{8}$$

In this form, we obtain a scaled factor model with a time-varying intercept. The model is linear in parameters $\boldsymbol{q}$ and $\boldsymbol{b}_l$ but the risk-neutral means are not uniquely identified. They can be estimated separately: we obtain period-by-period estimates of $\mu^Q_{l,t}$ from Fama-MacBeth regressions, whereas FJO impose more structure on risk premium dynamics and run an extra set of regressions.[12] OLS estimation of equation (8) yields coefficients $\widehat{\boldsymbol{q}}$ and $\widehat{\boldsymbol{b}}_l$ which can be used to recover the conditional intercept and option exposures. These two quantities can be coupled with factor realizations to examine the explanatory power of the model.

3.3 Empirical results

To assess various aspects of the model's explanatory power, we compute the R^2 in percentage terms as:

$$R^2\% = \left[1 - \frac{\sum_{i,t} \left(r_{i,t+1} - \widehat{r}_{i,t+1} \right)^2}{\sum_{i,t} (r_{i,t+1})^2} \right] \times 100, \tag{9}$$

[12] If the set of characteristics for instrumenting exposures differed across factors, and if we had additional state variables for factor risk premiums, in the conditional intercept we could replace $\sum_l -\mu_{l,t} \times \boldsymbol{\phi}'_{i,l,t} \boldsymbol{b}_l$ with $\widetilde{\boldsymbol{\phi}}'_{i,t}\boldsymbol{q}$, where $\widetilde{\boldsymbol{\phi}}_{i,t}$ is a new TPRS basis defined on the complete set of characteristics and state variables.

pooled over the whole option panel.

3.3.1 Delta-hedging efficiency

We begin by examining the model's ability to delta-hedge option returns. In this section, $r_{i,t+1} = r^e_{i,t+1}$, the delevered excess return defined in equation (1). The fitted values are computed as:

$$\widehat{r}_{i,t+1} = \widehat{\beta}_{\mathrm{DLT},i,t}\mathrm{DLT}_{t+1}\,,$$

and $\widehat{\beta}_{\mathrm{DLT},i,t}$ is obtained from estimating the model with all six factors.

The values are plotted in Figure 1. The shaded column in each panel represents the R^2 of delta-hedging across the whole sample, and the dashed line plots it across maturities. First, delta-hedging is highly effective both in puts (∼94%) and calls (∼86%). Second, it remains effective even at the shortest maturities, including 0DTE options, and in fact rises only slightly from 0DTE to 1–2DTE only to drop again for longer maturities.

Table A.IV reports (in the columns labeled "DLT") results further disaggregated by moneyness. Naturally, delta-hedging is more effective for at-the-money (ATM) options and drops off further out-of-the-money (OTM). In 0DTE options, the drop-off is more pronounced in puts than in calls, and an opposite pattern holds in calls. At longer maturities, the delta-hedging effectiveness falls off faster for calls, with 4–15DTE OTM calls being effectively unhedgeable using only the underlying.

Overall, these results confirm that intraday delta-hedging is highly effective even at the shortest maturities, including 0DTE options.

3.3.2 Model explanatory power for delevered excess option returns

The residual variation after delta-hedging can be further explained by the remaining five factors in the model, and hence we report the model's total explanatory ability for option returns. In this section, the fitted values for R^2 (9) are computed as:

$$\widehat{r}_{i,t+1} = \widehat{c}_{i,t} + \sum_{l} \widehat{\beta}_{l,i,t} f_{l,t+1}\,.$$

The explained values are $r_{i,t+1} = r^e_{i,t+1}$.

Figure 1 presents the results for puts and calls; the blue column reporting the value for the whole sample, and the blue line plotting it across maturities. In puts, the six factors and conditional intercept explain over 99% of total return variation; in calls the figure is almost 98%. There is very little difference in explanatory power across maturities, with the R^2 for 0–1DTE options being between one and two percentage points lower than for longer maturities. The results are similarly strong across moneyness levels (cf. Table A.IV, in the columns labeled "6F"). The model performs well over the whole moneyness spectrum. In OTM options, the R^2 is 93.4% for calls and 97% for puts, and the sub-sample with the worst fit—0DTE OTM puts—still has an R^2 of 86.6%. We see a drop-off in explanatory power for DOTM options, to 61.2% for 0DTE puts to 85.6% for 4–15DTE puts, and 82.7% across the whole DOTM put sub-sample; the drop-off in calls is slower than in puts, except for the longest maturities.

3.3.3 Sources of variation in delevered delta-hedged option returns

We examine in detail the sources of variation in delta-hedged option returns. In this section, for the purpose of computing the R^2 in equation (9), the returns are delta-hedged delevered excess returns defined in equation (2); $r_{i,t+1} = r^{dh}_{i,t+1}$. The fitted values are computed as:

$$\widehat{r}^{dh}_{i,t+1} = \widehat{c}_{i,t} + \sum_{l \neq \text{DLT}} \widehat{\beta}_{l,i,t} f_{l,t+1} \,.$$

Table IV reports, for put and call options, by moneyness and maturity, the R^2 of the five-factor model in explaining delta-hedged delevered excess returns (in columns labeled "5F"). Furthermore, the table reports the incremental R^2 of each factor when added to a model that already includes DLT and other factors that are listed before it in the table.

Our first observation is that the five-factor model explains a significant portion of the variation in delta-hedged option returns, the R^2 is 84.7% in puts and 86% in calls. It is noteworthy that the explanatory power remains very high even at the shortest maturity and in OTM options (approximately 70% in both puts and calls), only dropping away in DOTM 0DTE contracts (55.6% in puts and 42.3% in calls). For 1+DTE options, the R^2 never drops below 76.8%. Even though delta-hedging removes up to 94% of return variation, the remaining five factors still explain a large portion of the residual variation. Their explanatory power for delta-hedged returns compares very favorably to, for instance, factor models for stock returns, which typically explain 30–40% of return variation.

A more significant empirical observation is the dramatic change in the sources of variation in delta-hedged option returns as we move from 0DTE to longer maturities. In 0DTE options, the dominant factor is GAM, the squared return on the underlying, which explains 58% of return variation in puts and 57.8% in calls. Already at 1–3DTE, the explanatory power of GAM drops by a factor of three: to 16.5% in puts and 15.9% in calls; the drop continues—albeit more slowly—at longer maturities. This finding is complemented by the opposite pattern in the explanatory power of dSV, the spot-variance change factor, which explains only 7.6% (puts) and 5.7% (calls) of return variation in 0DTE options, 43.3% (puts) and 51.1% (calls) already at 1–3DTE. A similar pattern holds for the other two variance dynamics factors, although their contributions are smaller in magnitude.

These results are in line with economic intuition: at ultra-short maturities, the realized variance over the interval is the main driver of option returns after delta-hedging, as options are primarily exposed to prevailing variance—they will expire before the onset of future variance. As maturity increases, the role of prevailing variance diminishes, and changes in variance expectations become the dominant drivers of option returns.

When moving across the moneyness spectrum, we observe additional patterns. First, the further away from ATM, the less important GAM becomes, even at 0DTE (albeit it remains the dominant factor at the shortest maturity). There are significant changes in the relative importance of the variance dynamics factors. The explanatory power of dSV slightly decreases as we move OTM in puts, but increases in calls. Importantly, the explanatory power of dVRP increases rapidly as we move OTM in puts (up to 36.1% in DOTM 4–15 DTE puts), while it decreases in calls (9.7% for DOTM 4–15 DTE calls). These patterns are consistent with the idea that dVRP captures compensation for short-term left-tail events. The explanatory power of dTRM is small across the board, increases with maturity (from about 1% to 5% in both puts and calls), and remains stable across moneyness.

The role of the JSK factor is negligible except for DOTM 0DTE options, where it explains approximately 9% of return variation in both puts and calls.

4. Compensation for risk

We estimate compensation for risk under minimal assumptions on premium dynamics while allowing for time variation in the premiums and accounting for the co-movement of premiums and exposures. A risk premium has two components: factor expectations under the physical and risk-neutral measures. In what follows, we separate the estimation of the conditional Q-expectations of the factors from the estimation of their physical means. Before examining the risk premiums, we first assess the plausibility of the estimated conditional Q-expectations.

4.1 Risk Premiums with non-traded factors

Risk premiums on non-traded factors are typically estimated by cross-sectional regressions of excess asset returns on their factor loadings. Similarly to Gagliardini, Ossola, and Scaillet (2016), we use a cross-sectional approach only to estimate the conditional Q-expectations of the factors, and then combine them with time-series estimates of the physical means to obtain risk premiums.

4.1.1 The conditional intercept and risk-neutral expectations

Let r denote the excess return on an asset, F_T an excess return factor and F_{NT} a non-traded factor, and β_T and β_{NT} the asset's exposures to the respective factors. Then, the following factor model for the asset holds in each period (we omit asset and time subscripts to simplify notation):

$$r = c + \beta_T F_T + \beta_{NT} F_{NT} + \varepsilon \,. \tag{10}$$

Given that both r and F_T are excess returns on traded assets, $E^Q[r] = E^Q[F_T] = 0$. Taking Q-expectations on both sides of equation (10) thus implies that

$$c = \beta_{NT} \times (-E^Q[F_{NT}]). \tag{11}$$

We leverage the multivariate generalization of the no-arbitrage restriction in equation (11) to estimate the Q-expectations of the factors from the conditional intercepts of the factor model for option returns estimated in Section 3.

4.1.2 Implementation

Using the notation of our factor model (5), the no-arbitrage restriction (11) becomes:

$$c_{i,t} = \sum_{l} \beta_{l,i,t} \times (-E^Q[f_{l,t+1}]) = -\sum_{l} \beta_{l,i,t} \times \mu^Q_{l,t} \,. \tag{12}$$

We estimate $\mu^Q_{l,t}$ period-by-period using cross-sectional regressions of the conditional intercepts estimated in Section 3, $\widehat{c}_{i,t}$, on the estimated factor loadings, $\widehat{\beta}_{l,i,t}$. Furthermore, to allow for potential mispricing of options with similar characteristics, we group options into buckets based on their maturity (0, 1–3 or 4–15 days) and moneyness (ATM, OTM, DOTM), and include bucket fixed effects in the cross-sectional regression:

$$\widehat{c}_{i,t} = \alpha_{b(i),t} - \sum_{l} \widehat{\beta}_{l,i,t} \times \mu^Q_{l,t} + \nu_{i,t} \,. \tag{13}$$

Finally, we include in the regression the option deltas ($\widehat{\beta}_{\mathrm{DLT},i,t}$), even if the DLT factor is traded. Theory suggests that the estimated $\mu^Q_{\mathrm{DLT},t}$ should be zero, but in practice it could deviate from zero due to frictions in the option market or misspecification of our model. In the next section (4.2), we discuss the estimates of $\mu^Q_{l,t}$ in the context of their plausibility, robustness, and economic interpretation. We further examine option mispricing in Section 5.

4.2 Risk-neutral expectations of the factors

Table II contains the averages of the conditional risk-neutral expectations of the factors, $\mu^Q_{l,t}$, estimated from call and put options, alongside with the average factor realizations and their average differences, estimates of unconditional risk premiums λ_l. In sub-panels, we report the estimates for three sub-samples: FOMC days, non-FOMC days, and excluding the COVID-19 market distress period (March 2020). Our first observation is that for each factor, the average $\mu^Q_{l,t}$ estimates from call and put are always of the same sign and indeed very close numerically. For instance, $\mu^Q_{\mathrm{DLT},t}$ is -0.76% per year in put options and -1.16% in call options, and $\mu^Q_{\mathrm{GAM},t}$ is 1.53% in puts and 1.39% in calls. Across all factors, the relative discrepancy between put- and call-based estimates is low, with the exception of dVRP, where the two estimates differ substantially. Figure 2 shows that the time-series of the estimates from puts and calls are also very similar. This is the first indication that our estimates are robust enough to be informative of the economic forces in the intraday SPX option market.

4.2.1 Plausibility of estimated risk-neutral expectations

The six factors in our model can be categorized in two ways: first, traded (DLT) and non-traded, and second, representing the underlying asset dynamics (DLT, GAM, and JSK), and aggregate option price dynamics (dSV, dVRP, dTRM). These categories help us further evaluate the plausibility of the estimated λ_t values.

That DLT is traded implies that $\mu^Q_{\text{DLT},t}$ should be zero in each period, and all deviations should be due to sampling noise. While the average of the $\mu^Q_{\text{DLT},t}$ estimates is statistically different from zero, its magnitude is modest at approximately -1% per year in both put and call options. Economically, these estimates are small enough that they could be due to market frictions. While we discuss risk premiums in more detail in Section 4, it is nonetheless worth noting here that, together with the P-expectations of DLT, the $\mu^Q_{\text{DLT},t}$ estimates imply an intraday equity risk premium of 5.39% per annum in puts and 5.78% in calls, matching the actual intraday equity premium in our sample.[13]

GAM is the square of DLT, and thus $\mu^Q_{\text{GAM},t} = E^Q_t[\text{DLT}^2_{t+1}]$ is the conditional Q-measure second moment of the high-frequency underlying return. As a consequence, $\mu^Q_{\text{GAM},t}$ should always be positive. The estimates of $\mu^Q_{\text{GAM},t}$ are indeed positive not only on average in our whole sample, but also on average in every intraday interval, and practically almost everywhere in the sample, as evident in Figure 2.

JSK is the third power of DLT and $\mu^Q_{\text{JSK},t}$ is the conditional Q-measure third moment of the high-frequency underlying return. At the frequency of our dataset–30 minutes–JSK can be largely attributed to jump movements in the underlying,[14] and hence we interpret $\mu^Q_{\text{JSK},t}$ as the risk-neutral conditional third moment of market index jumps. The estimates of $\mu^Q_{\text{JSK},t}$ are negative on average–in line with evidence on risk-neutral skewness of market returns (see, for instance, Dennis and Mayhew, 2002). Overall, our estimates of the conditional Q-expectations of the powers of S&P500 futures returns are in line with common sense and the stylized facts reported in the literature, and we consider them as the second indication

[13] In the asset pricing literature, the gap between cross-sectional and time-series estimates of risk premiums is often used an as informal gauge of whether a model is reasonable (see, e.g., Giglio, Kelly, and Xiu, 2022, and Barillas and Shanken (2017) for a formal statement).

[14] See, for instance, Jacod and Protter (2012): when taking powers of price increments of semimartingales at short intervals, jumps dominate the behavior.

that we can rely on our estimated alphas.

The interpretation of the Q-expectation estimates for the remaining three factors is less straightforward. Recall from Section 3.1 that these three factors decompose the dynamics of long-term risk-neutral variance into three components: pure spot variance shocks, short-term variance premium dynamics, and a term-structure component.[15] As the three factors are changes in the respective quantities, their conditional Q-expectations can be positive or negative. Indeed, we see that the average of $\mu^Q_{\mathrm{dSV},t}$ is negative, whereas the averages of $\mu^Q_{\mathrm{dVRP},t}$ and $\mu^Q_{\mathrm{dTRM},t}$ are positive. All three averages are of plausible magnitude. For instance, if the spot volatility of the S&P 500 is 20%, then spot variance is 0.04 per year, and the risk-neutral expected change in spot variance over a day is approximately -16bp (-0.0016), so approximately 4% of spot variance.

Overall, we conclude that our estimates of the conditional Q-expectations of the factors are plausible and in line with the stylized facts in the literature. This testifies to the robustness of our model and supports its use for the analysis of risk premiums and mispricing in intraday SPX options.

4.2.2 Dynamics

We further examine the time-series properties of the estimated risk-neutral moments. We plot the time-series in Figure 2, and report their 1-lag and 1-day autocorrelations in Table III. The time-series are sampled at 09:45 ET and 15:15 ET.

As in Section 4.2, we first focus on the three factors related to the underlying dynamics. $\mu^Q_{\mathrm{DLT},t}$ oscillates around zero most of the time, but in certain period deviates substantially from zero in both directions. Notably, in periods of market distress, the deviations tend to be negative, which suggests time variation in frictions in the option market. The time-series of $\mu^Q_{\mathrm{GAM},t}$ is markedly different–not only always positive, but also it bears a strong visual resemblance to other estimates of the second risk-neutral moment. We corroborate this observation by computing the correlation between $\mu^Q_{\mathrm{GAM},t}$ estimated from put and call options and CIV_{5+} with the shortest maturity exceeding 5DTE: 0.76/0.77 in the series sampled in the morning and 0.53/0.57 forty five minutes before the close. The time-series of $\mu^Q_{\mathrm{JSK},t}$ is

[15]To be rigorous, we note that our "variance" proxies are in fact entropy proxies (Martin, 2017). However, we allow ourselves to label them as variance proxies since (i) most of the literature does refer to those as variance proxies, and (ii) we here explicitly introduce JSK to account for higher order moments.

noisy, but it is clearly negative on average, and it exhibits downward spikes in periods of market distress. The dynamics of the third moment is also similar to estimates one can back out from the Cboe SKEW index and others provided in the literature. The interesting observation is that the series sampled in the morning spikes strongly negative in almost all distress periods, whereas the series sampled in the afternoon spikes positively in the COVID turmoil.

There are further observations of note related to FOMC announcements. On announcement days, $\mu^Q_{\text{DLT},t}$ tends to be more negative (about double the non-announcement day levels), albeit it never strays far from zero. While $\mu^Q_{\text{GAM},t}$ is slightly higher on announcement days than in the remainder of the sample, it is in μ^Q_{JSK} that we see the largest difference: the annualized magnitude of risk-neutral third moment of jumps changes from approximately -27% to between -60% and -70%.

We defer the discussion of the estimated Q-dynamics of the three variance dynamics factors to section 4.3 because they are easier to interpret in the context of associated changes in the factor P-dynamics–as risk premiums.

We also note that all risk-neutral moment estimates are persistent, with 1-lag autocorrelations between 0.82 and 0.97. They are not simply estimation noise, but measure meaningful market quantities. One-day persistence varies across factors: DLT, GAM, dVRP, and JSK one-day autocorrelations are high (between 0.32 and 0.76), but dSV and dTRM one-day autocorrelations are close to zero.

4.2.3 Seasonality

Figure 3 plots the intraday patterns of the estimated conditional risk-neutral expectations of the six factors. The patterns are similar between put- and call-based estimates, confirming the robustness of our results. The dynamics of μ^Q_{DLT} and μ^Q_{GAM} are in contrast, consistent with the negative correlation between the risk-neutrual return and its variance for the S&P 500 index. μ^Q_{DLT} is mildly negative throughout the day and drifts upward toward the close, whereas μ^Q_{GAM} is strictly positive and declines monotonically from the open to the close, mirroring the intraday behavior of 5+ DTE implied variance. μ^Q_{dVRP} and μ^Q_{dTRM} are both positive at the open and decline over the day. However, μ^Q_{dVRP} turns negative for puts late in the afternoon, whereas calls remain positive but compress toward zero. μ^Q_{dTRM} remains positive throughout the day for both puts and calls; its downward trend indicates an intraday flattening of the risk-neutral variance term structure. Finally, both μ^{Q}_{dSV} and μ^{Q}_{JSK} are negative on average throughout the day and rise toward zero toward the end of the day.

When 0DTE options are excluded from the estimation, the intraday patterns of the estimated conditional risk-neutral expectations remain qualitatively similar (Figure 4). This indicates that the intraday seasonality in the estimated risk-neutral expectations is not driven solely by 0DTE options, but rather reflects broader intraday dynamics in the short-maturity SPX option market.

4.3 Risk premiums

We combine the estimates of the conditional Q-expectations of the factors with time-series estimates of their physical means to examine unconditional risk premiums. The premiums–differences between the average realizations of the factors and averages of the estimated conditional Q-expectations–are reported in Table II alongside average factor realizations and estimates of conditional Q-expectations.

As already discussed above, the risk premium on DLT implied by our model is approximately 5.6% per year, in line with the equity risk premium estimates in the literature. The estimates of the premium for GAM are essentially zero: 10bp per year from puts and 20bp from calls; this result is in line with Fournier, Jacobs, and Orłowski (2024) who find that this risk premium is not significant in daily data. Finally, the negative estimates of $\mu_{\text{JSK},t}$ combined with the near-zero average realized values of JSK imply a positive jump skewness risk premium of approximately 37% per year. To put this estimate in context, one can compare it to the 10.8% reported in Orłowski, Schneider, and Trojani (2024), which is based on a model-free dynamic replication methodology, but uses a different definition of an option's return (with a notion of margin in the denominator).

To assess the compensation for variance dynamics, we first add the premiums on dSV, dVRP, and dTRM to obtain the premium for the change in long-term risk-neutral entropy–a quantity easiest to compare with the existing literature. The result is -9.6% per year from puts and -2.4% from calls. The most closely related estimates in the literature are from FJO who find a premium on the change in the Cboe VIX^2 index between -6.2% and -15.2% per year in daily option returns. Dickerson et al. (2025) find a similar gap to ours between estimates from weekly returns on put and call options on different underlying assets, but overall a more negative premium (approximately -20% per year). Both papers use more restrictive premium specifications. The smaller magnitude of our estimates might be due to our focus on intraday data, as a part of the literature argues that variance risk is not priced at high frequencies. Furthermore, our decomposition of variance dynamics into three components with a strong correlation structure yields different exposures to these components, and thus potentially offers more precise risk premium estimates.

Looking at the variance dynamics factors individually, we find a negative premium on dVRP of about -41% and positive premiums on dSV (about 18.7%) and dTRM (about 12.7%). The negative sign of the dVRP premium is in line with the extant empirical evidence and with economic theory. The positive sign of the dTRM premium aligns with economic intuition. A positive shock to dTRM increases the slope of the risk-neutral variance term structure, and thus increases the value of long-dated options relative to short-dated options. Typically, such shocks occur when short-term uncertainty drops sharply in market rebounds.

That the premium on dSV is positive is more surprising, as it implies that investors are willing to pay a premium to hedge against *negative* spot variance shocks. The sign of the dSV premium can be partially rationalized by the factor's behavior on FOMC days. Physical dSV realizations are substantially lower on FOMC days–consistent with the typical volatility drop that follows uncertainty resolution after the announcement. Risk-neutral expectations of dSV move much less (though they are slightly more negative on announcement days), so the realized decline in spot variance typically exceeds what is priced in, producing a negative dSV premium on FOMC days (while on non-FOMC days the smaller realized declines translate into a positive average dSV premium). By contrast, premiums on DLT, JSK, and dTRM are larger on FOMC days, consistent with higher compensation demanded for exposure to underlying return risk, jump skewness, and the slope of the variance term structure around announcements. Interestingly, both P- and Q-moments of dVRP move in parallel between FOMC and non-FOMC days and the premium remains unchanged. Altogether, these patterns imply that uncertainty resolution after FOMC announcements mechanically drives the negative dSV premium on announcement days while amplifying pricing of other factor risks.

We are the first to present such disaggregate and extensive evidence on the joint pricing of variance and jump dynamics risk in intraday trading of a proxy for the U.S. stock market factor.

5. Price dislocations in the SPX option market

In this section, we examine the potential mispricing of SPX options relative to the factor model. We estimate time-varying option alphas as described in Section 5.1 below. In the context of a factor model, a positive (negative) alpha signals that an option is cheap (expensive) and abnormal profits could be earned by buying (selling) the option and hedging its factor exposures.

5.1 Identifying price dislocations

5.1.1 Conditional intercept and *alpha*

Unless equation (11) in Section 4.1.1 holds, the asset's expected return is no longer solely determined by compensation for systematic risks. The difference between the estimated conditional intercept and $\beta_{NT} \times (-E^{Q}[F_{NT}])$ is an asset's "alpha"—mispricing of the asset relative to the assumed model:

$$\alpha := c - \beta_{NT} \times (-E^{Q}[F_{NT}]). \tag{14}$$

A non-zero alpha on a single asset is not a violation of no-arbitrage in the APT context, but the existence of persistent non-zero alphas across a broad set of assets would signal one.[16] To estimate alphas, consider first a simplified version of the cross-sectional regression (13) from Section 4.1.2, keeping only asset-specific indexing:

$$c_i = \alpha - \beta_{NT,i}\mu^{Q}_{NT} + \nu_i\,. \tag{15}$$

This cross-sectional regression at a given point in time does not allow recovering asset-specific alphas. However, in the cross-section of SPX options, it is likely that contracts with similar characteristics should have similar alphas. In the subsequent empirical analysis, we thus group options into buckets based on their characteristics and include bucket fixed effects in regression (13).

[16]Empirically, this could also arise from an omitted systematic factor; a priori, we consider *mispricing* as being relative to our model. We will later turn to studying whether one can profit from the mispricing.

5.1.2 Implementation

We return to regression (13) in Section 4.1.2 and recall it here:

$$\widehat{c}_{i,t} = \alpha_{b(i),t} - \sum_{l} \widehat{\beta}_{l,i,t} \times \mu^{Q}_{l,t} + \nu_{i,t}\,. \tag{16}$$

We now focus on the time-series of estimated $\widehat{\alpha}_{b(i),t}$, the bucket-specific alphas which measure local option mispricing. In what follows, we call them option price dislocations and analyze their variation in the cross-section, over time (in the context of the economic environment), and within the trading day. We obtain estimates of the dislocations from cross-sectional regressions estimated separately for every 30-minute trading period, using conditional intercepts and option exposures estimated in Section 3. Next, we analyze the following aspects of the dislocations: (i) Patterns across moneyness and maturity in Section 5.2, (ii) Their time-series variation in Section 5.3, (iii) Their relation to the economic environment in Section 5.4, (iv) Their intraday seasonal patterns in Section 5.5, and (v) The profitability of trading strategies exploiting these dislocations in Section 5.6.

5.2 The cross-section of price dislocations

As discussed in Section 4.1.2, we estimate option price dislocations, $\alpha_{b(i),t}$, by grouping options into buckets based on their maturity (0, 1–3 or 4–15 days) and moneyness (ATM, OTM, DOTM). Table V reports the summary statistics of the estimated option price dislocations in percent per annum. Numerous patterns are of interest. First, the mean dislocation (in columns labeled $\overline{\alpha}_{b(i),t}$) is positive on average in puts (except for A/OTM 0DTE contracts), and negative in calls. In 0DTE ATM and OTM options, it exceeds -6% per year in calls, while being about -1% in puts. The reading of this result is that, contrary to benchmarks based on the Black-Scholes model, among 0DTE options, calls are overpriced rather than puts, taking the pricing of the remaining options across all maturity and moneyness buckets as given. Beyond the 0DTE options, the mean dislocation is approximately 1% per year in puts and -1% in calls. The average magnitude of dislocations (in columns labeled $\overline{|\alpha|}_{b(i),t}$) exhibits similar patterns in calls and puts: it's largest in 0DTEs and decreases away from ATM, with the decrease faster in puts. 0DTE dislocations are an order of magnitude larger than those at longer maturities. The average magnitude is much higher than the average dislocation, signaling sign changes in dislocations over time, which we explore in the remainder of this section.

The dislocations are persistent. In columns of Table V labeled "AC^{30min}" and "AC^{1day}" we report the autocorrelation at 30 minutes (one lag) and at one day (i.e., between values at the same time of day on consecutive trading days). Almost all one-lag autocorrelations are above 0.80, and the coefficients increase with option maturity. The one-day autocorrelations are only slightly lower, with estimates between 0.47 and 0.61 for puts, and between 0.58 and 0.73 for calls. This long-horizon persistence pattern is similar across option maturities and moneyness ranges. Thus, dislocations are not pure noise, but rather reflect systematic mispricing of options relative to the factor model.

5.3 Time-series variation

Figures 5 and 6 plot the time-series of dislocations for 0DTE and non-0DTE options, respectively. In each figure, for each maturity bucket, the left (right) panel presents results for puts (calls). Within each panel moneyness-specific series are distinguished by color. From top to bottom, panels show time-series sampled at different times of the trading day: 09:45, 12:15, and 15:30 ET.

Dislocations vary substantially over time, are strongly correlated across option types and maturity and moneyness buckets, and exhibit pronounced negative spikes around two types of events: FOMC announcements and periods of market distress. The COVID-19 spike in March 2020 is 2–3 times larger than FOMC spikes across most buckets—for instance, for 0DTE options, the mispricing reaches 200% of the underlying SPX value. Interestingly, 0DTE dislocations become very volatile and spike in both directions starting in March 2022, which coincides with the start of the Fed's rate-hiking cycle, heightened market volatility, and a year-long market decline.

As noted in Section 5.2, dislocations are more pronounced and more volatile in 0DTE options. For 1+DTE options, the dynamics and average levels of dislocations do not vary substantially across different times of the trading day. In contrast, 0DTE dislocations exhibit pronounced changes in their time-series patterns under one hour to the options' expiration. In both puts and calls, they become strongly negative and more volatile at 15:15 ET.

Overall, we identify two patterns that warrant further investigation: the dislocations respond to the macroeconomic environment, and they exhibit intraday seasonality.

5.4 Price dislocations and the economic environment

In this section, we explore the economic mechanisms behind the time-series variation in option price dislocations. We estimate regressions of dislocations—and their magnitudes—measured at 15:15 ET on variables capturing different aspects of the economic environment:

$$\begin{aligned}\widehat{\alpha}_{b(i),t} = \beta_0 + &\beta_{ESF}\, ESF_{t-1} + \beta_{HKM}\, HKM_{t-1} + \beta_{\varepsilon_{HKM}} \varepsilon_{HKM,t} \\ &+ \beta_{OI}\, OI_{b,t-1} + \beta_{CIV}\, CIV_{b,t} + \beta_{SP500}\, SP500_t + \varepsilon_{b(i),t}\end{aligned} \tag{17}$$

We define the variables below. In addition to reporting the results from the above multivariate regression for ATM options, the top panel Table VI also reports the R^2 from univariate regressions of each variable (not the coefficient). The bottom panel of the table reports similar results, but with $\left|\widehat{\alpha}_{b(i),t}\right|$ as the dependent variable. Tables A.V to A.IX, discussed in Appendix E, demonstrate that results are robust across several dimensions.

First, we follow Siriwardane, Sunderam, and Wallen (2025) and construct an equity spot-futures (ESF) spread from the difference between an S&P 500 (ES) futures-implied forward rate and the 3-month OIS rate (details in Appendix D). A deviation of ESF from zero signals that funding costs in the equity index futures market differ from those implied by the OIS rate, and is interpreted by Siriwardane, Sunderam, and Wallen (2025) as a measure of limits to arbitrage. Hazelkorn, Moskowitz, and Vasudevan (2023) also document that ESF measures liquidity demand for exposure to global equity markets, often achieved via futures trading. The fact that ESF comoves only partially with spreads in other segments is central to Siriwardane, Sunderam, and Wallen's conclusion that arbitrage capital is not freely mobile across markets. Table VI reports that as ESF increases, dislocations on 0DTE puts and calls become increasingly negative. This supports a narrative in which, when limits to arbitrage are binding, 0DTE options tend to be more expensive. The explanatory power is however limited, at most 1.6%, and the ESF is mostly insignificant for non-0DTE options.

Second, the aggregate market equity ratio of NY Fed primary dealers, HKM, that we refer to as the capital ratio, and the realization of the associated risk factor, ε_{HKM}—the non-predictable innovation to the capital ratio, expressed as a growth rate—defined by He, Kelly, and Manela (2017). While the primary dealers are not market makers in SPX options anymore, they played this role for a significant fraction of our sample.[17] They are also active in these markets for other reasons: they remain central to the over-the-counter derivatives markets,[18] where they are likely to hold short volatility exposure, and some of their hedging activities are likely carried out via SPX options. We find that the capital ratio, HKM, significantly predicts dislocations in most option buckets—4-to-15 day puts excepted. The coefficient estimates are positive, indicating that higher capital ratios—signaling better risk-bearing capacity—are associated with more positive dislocations, i.e., cheaper options. The capital ratio has the strongest explanatory power (12–22%) at 1–3DTE in both puts and calls, and 5–6% at 0DTE. It is of note that this is a predictive relation, as the capital ratio is measured at the end of the previous trading day; this variable is, naturally, very persistent.

The contemporaneous evidence is weaker. The unpredictable component of the growth rate of the capital ratio, ε_{HKM}, is positive at the shortest maturity, but only significant in calls, with a small univariate R^2 of 2.91%. Although it is not significant in puts, its explanatory power for 0DTE puts is similar to calls: 3.31%. This is in stark contrast to the R^2 at longer maturities, never in excess of 0.4%. The impact of intermediary variables on the magnitude of dislocation is less clear. While at 0DTE, the level of the capital ratio is negatively and significantly related to absolute alphas, the capital ratio innovation is only significant in calls. The signs of the coefficients are as expected—higher capital ratios/increases thereof lead to smaller mispricing magnitudes. The capital ratio is also a significant predictor of absolute dislocations at 1–3DTE in both calls and puts, and at 4–15 DTE in puts, albeit with a positive sign, contrary to expectations. We note that the univariate R^2s are small in these cases, below 2.1%. Overall, we find the effect of intermediary leverage on option dislocations to be strongest at the shortest maturities; improvements in intermediary leverage are associated with cheaper and less mispriced options.

Third, we consider the total open interest in options in the given bucket at the end of the preceding trading day, OI. Option open interest is a proxy for the aggregate option inventory held by some market participants. While the aggregate supply of options is zero, the risk exposures of market participants holding long and short positions are not offsetting.

[17] For instance, Goldman Sachs shut down their market-making operation in 2017, [Bloomberg]; Morgan Stanley sold their electronic market making unit to Citadel Securities in 2025 [Financial Times].

[18] Goldman Sachs was instrumental in the creation of the global OTC volatility swap market [Financial Times]. The broader OTC equity derivatives is about $7T, 1.2% (in notional terms) of the whole OTC derivatives market, and trading activity is split evenly between swaps and options [ISDA, 2024].

Whereas option buyers are only exposed to factor risk, option sellers also face frictions such as, e.g., margin constraints. A higher open interest signals that more—or larger—positions are subject to potential margin calls. When option sellers face binding constraints, they may demand higher premiums to bear the risk, leading to more negative dislocations. Our results indeed support this narrative: option dislocations move systematically and significantly with like-contract open interest in puts, but the evidence is much weaker in calls. Put options are more expensive when aggregate inventories are higher. The most stark difference between the two option types lies in the explanatory power of open interest: in puts, the univariate R^2 ranges from 12.83% at 4–15DTE to 26.21% at 0DTE, while in calls it is essentially zero except for the longest maturity. The estimates from regressions of absolute dislocations are more difficult to interpret: at 0DTE and 1–3DTE in puts, the significant coefficients are similar in magnitude, but of opposite sign. However, the univariate R^2 is very high at 0DTE (27.01%) and negligible (0.1%) at 1–3DTE. In calls, only the 0DTE coefficient is significant—and positive, but with a very modest R^2 of 0.38%. To summarize, we present strong evidence that higher open interest—and, hence, aggregate option inventory—is associated with more expensive puts, and larger mispricing magnitudes at the shortest maturity.

Finally, we directly control for the conditions in the equity and the SPX option markets. The variable *SP500* captures the overall market return on the day, from open until 15:15 ET, which is likely correlated with delta-hedging activity in the option market. In all regression, we include the day's *CIV* index, computed from options at a given maturity bucket at 15:15 ET, as a control variable. Whereas we refrain from interpreting its coefficient, we note that it has significant explanatory power (20-60% R^2 in all regressions) for both dislocations and their magnitudes across all option types and maturities. While this is to be expected, as *CIV* is a measure of how expensive options are in general, and hence its calculation integrates dislocations themselves, it also indicates that our results on intermediary variables and open interest are not driven by omitted-variable bias related to overall option expensiveness.

Table VII repeats this analysis using an instrumental variable approach to address potential endogeneity concerns arising from the fact that ES futures are the natural delta-hedging environment for SPX option traders, and thus the dynamics of funding conditions in ES futures may arise from hedgers' demand. We instrument the equity spot-futures spread (ESF) using the corresponding spread for the Russell 2000 E-Mini futures. The IV estimates are qualitatively consistent with the OLS results, confirming the robustness of our findings.

All in all, these results suggest that the mispricing of 0DTE options is related to the diverse roles of the market participants, and to their ability to absorb risk.

5.5 Intraday seasonality in price dislocations

In Figure 7, we present a summary of the intraday seasonality in dislocations. At each time of the trading day, we compute the average of dislocations across the sample period for each option bucket. A strong seasonal pattern is only present in 0DTE options. Dislocations are initially negative for all moneyness categories at market open, between -2 and -10 bps after scaling to a per-day basis. They subsequently increase steadily until 13:15 ET, reaching positive values of up to 5 bps. Then, they decline rapidly to reach values between -5 and -15 bps at 15:15 ET, i.e., 45 minutes before expiration.

Figure 8 decomposes the intraday pattern of 0DTE dislocations into FOMC and non-FOMC days. On FOMC days, dislocations are uniformly negative throughout the trading day across all moneyness buckets, consistent with elevated demand for downside protection and tighter inventory-management constraints around monetary policy announcements. On non-FOMC days, the inverted U-shaped intraday pattern documented above is clearly present, with dislocations starting negative, turning positive around midday, and declining sharply toward the close. Figure 9 examines whether similar intraday patterns emerge in 1–3DTE options across different subsamples: pre- and post-April 2022, and—within the pre-April 2022 period—separately for Tuesdays and Thursdays versus the remaining weekdays. April 2022 marks the introduction of daily SPX expirations on additional weekdays. Unlike 0DTE options, 1–3DTE dislocations exhibit minimal intraday seasonality across all subsamples.

5.6 Exploiting the Mispricing

Finally, we assess the economic significance of 0DTE dislocations by constructing self-financing, six-factor-neutral portfolios. In particular, this section speaks to whether or not the documented mispricings could be exploited in a trading strategy. For each 0DTE option at each 30-minute timestamp, we hedge its six factor exposures using a basket of 18 longer-maturity instrument contracts—the three most liquid contracts from each of six buckets defined by maturity (1–3DTE, 4–15DTE) and moneyness (ATM, OTM, DOTM). The hedging weights are obtained by projecting each target option's exposure vector onto the factor-loading matrix of the instruments:

$$\boldsymbol{w}_{i,t} = \left(\widehat{\boldsymbol{B}}_t \widehat{\boldsymbol{B}}_t'\right)^{\dagger} \widehat{\boldsymbol{B}}_t \boldsymbol{e}_{i,t}\,, \tag{18}$$

where (i) $\widehat{\boldsymbol{B}}_t$ combines the matrix of factor loadings (18×5) with a 6^{th} column containing the DLT-hedged P&L of the 18 hedging instruments at time t, (ii) $\boldsymbol{e}_{i,t}$ is the (6×1)-vector with the additive inverse of (a) the 5 factor loadings and (b) the DLT-hedged P&L of each target option i, at time t, and (iii) $\dagger$ denotes the Moore-Penrose pseudo-inverse. The resulting portfolios are thus self-financing by construction.

A 0DTE option's 6-factor-neutral return is calculated as

$$r_{i,t}^{N} = r_{i,t}^{dh} + \boldsymbol{w}_{i,t}' \boldsymbol{r}_{i,t}^{H} \tag{19}$$

where $r_{i,t}^{dh}$ is time-t DLT-hedged return of 0DTE option i, and $\boldsymbol{r}_{i,t}^{H}$ is the vector of DLT-hedged returns of the hedging instruments. We average the factor-neutral returns cross-sectionally and then over time. Table VIII reports their summary statistics.

The delta-hedged returns of the target 0DTE options (in rows labeled "T") are significantly negative across all moneyness buckets, with Sharpe ratios between −1.0 and −1.3. After hedging, the magnitude of factor-neutral mean returns (rows labeled "N") shrink substantially: for ATM options, from −0.63% to −0.15% (puts) and from −0.55% to −0.12% (calls), confirming that a large share of the 0DTE overpricing is attributable to the six factors. Nonetheless, the residual factor-neutral returns remain negative in puts—statistically significant at ATM and OTM—with Sharpe ratios between −0.23 and −0.29, suggesting that part of the 0DTE overpricing survives factor-neutral hedging. In calls, the residual returns are smaller and statistically insignificant.

Figure 10 displays the intraday patterns of the factor-neutral returns across the full sample, then separately on FOMC and non-FOMC days. It is worth noting that these returns are obtained by opening 30-minutes per day over the (sub)sample. Consistent with the seasonality documented in Figure 7, the trading strategy yields negative returns at the beginning of the day, positive returns early afternoon, and large negative returns later in the afternoon. Only the late afternoon returns are statistically significant.

These results are further supported by Figure 11. The figure presents the cumulative returns of factor-neutral portfolios over the sample period for the three 30-minute periods ending at 10:15, 12:45 and 15:45 ET. The figure further reports the return of a (long) buy-and-hold position on ES futures over the same periods. The position in the option portfolio is normalized to exhibit the same standard deviation as the ES position. Whereas the return of factor-neutral portfolios are of comparable magnitude to those of the ES positions at 10:15 and 12:45, the magnitude of returns on a short position in the factor-neutral portfolio over the 15:15–15:45 period is roughly three times larger than that of an ES position over any 30-minutes period throughout the day.

6. Conclusion

Our study documents that the returns on ultra-short-maturity (USM) SPX options, and in particular zero-days-to-expiration (0DTE) contracts, are driven by a compact yet rich factor structure that combines powers of underlying returns with a decomposition of innovations in variance dynamics. The factor-model approach also enables recovering intraday time series of the factors' risk-neutral expectations and, from these, their risk premiums, thereby delivering a new perspective on the option market stochastic discount factor at high frequency. The time-series of Q-expectations are interesting objects of future study in their own right, as they embed real-time market perception of risk premiums and go beyond what is accessible via the static option replication approach.

Within the same framework, we uncover systematic mispricing in 0DTE options—price dislocations. Dislocations are highly seasonal within the trading day: options are underpriced at the open, overpriced around midday, and again underpriced near the close. They also co-move with market-wide measures of intermediary balance-sheet strength, becoming more negative (i.e., options becoming more expensive) when dealer leverage tightens. This pattern indicates that temporary constraints in intermediaries' risk-bearing capacity transmit directly into intraday option prices, shaping the cost of insuring against volatility and tail risk. The magnitude and persistence of these dislocations underscore that same-day-expiry options, while highly liquid, are not fully arbitraged even at the highest trading frequencies. In particular, holding a 6-factor-neutral short position in 0DTE options for 30 minutes per day, between 15:15 and 15:45 ET, yields a Sharpe ratio roughly three times higher than buying or selling ES futures for any half-hour period.

Our findings contribute to several areas of finance research. First, we extend the study of ultra-short-maturity options by documenting the economic sources of their returns and by quantifying how their risk compensation evolves throughout the day. Second, by estimating the Q-moments of return and volatility factors at high frequency, we show that conditional factor models can yield interpretable and robust insights into risk pricing in markets where exposures are complex and time-varying. Third, we link intraday mispricing in index options to intermediary constraints, providing direct evidence that financial institutions' balance-sheet dynamics influence the high-frequency pricing of volatility risk. Taken together, these results offer a comprehensive empirical framework to study the risk and pricing of 0DTE and other ultra-short-maturity options.

REFERENCES

Adams, Greg, Cherkashin Dim, Bjørn Eraker, Jean-Sébastien Fontaine, Chayawat Ornthanalai, and Grigory Vilkov, 2025, Do S&P 500 Options Increase Market Volatility? Evidence from 0DTEs, Working paper.

Aït-Sahalia, Yacine, and Jean Jacod, 2014, *High-Frequency Financial Econometrics* (Princeton University Press).

Almeida, Caio, Gustavo Freire, and Rodrigo Hizmeri, 2024, 0DTE Asset Pricing, *Available at SSRN 4701401.*

Andersen, Torben G., Oleg Bondarenko, and Maria T Gonzalez-Perez, 2015, Exploring Return Dynamics via Corridor Implied Volatility, *Review of Financial Studies* 28, 2902–2945.

Bandi, Federico M, Nicola Fusari, and Roberto Renò, 2024, 0dte option pricing, *Available at SSRN 4503344.*

Barillas, Francisco, and Jay Shanken, 2017, Which Alpha?, *The Review of Financial Studies* 30, 1316–1338.

Broadie, Mark, Mikhail Chernov, and Michael Johannes, 2009, Understanding Index Option Returns, *Review of Financial Studies* 22.

Carr, Peter, and Liuren Wu, 2020, Option Profit and Loss Attribution and Pricing: A New Framework, *Journal of Finance* 75, 2271–2316.

Chen, Hui, Yuhan Cheng, Yanchu Liu, and Ke Tang, 2023, Teaching Economics to the Machines, *Available at SSRN 4642167* .

Dennis, Patrick, and Stewart Mayhew, 2002, Risk-neutral skewness: Evidence from stock options, *Journal of Financial and Quantitative Analysis* 37, 471–493.

Dickerson, Alexander, Mathieu Fournier, Kris Jacobs, and Piotr Orłowski, 2025, Systematic variance risk everywhere in equity option markets, *HEC Montréal / Canadian Derivatives Institute Working Paper* .

Dickerson, Alexander, Philippe Mueller, and Cesare Robotti, 2023, Priced risk in corporate bonds, *Journal of Financial Economics* 150, 103707.

Duarte, Jefferson, Christopher S Jones, Haitao Mo, and Mehdi Khorram, 2024, Too Good to Be True: Look-ahead Bias in Empirical Option Research, *Available at SSRN 4590083* .

Duarte, Jefferson, Christopher S. Jones, and Junbo L. Wang, 2024, Very noisy option prices and inference regarding the volatility risk premium, *The Journal of Finance* .

Fournier, Mathieu, Kris Jacobs, and Piotr Orłowski, 2024, Modeling conditional factor risk premia implied by index option returns, *The Journal of Finance* 79, 2289–2338.

Fu, Lei, Su Li, David K. Musto, and Neil D. Pearson, 2024, Trading Like There's No Tomorrow: Uncovering the S&P 500 0DTE Options Market Dynamics

Gagliardini, Patrick, Elisa Ossola, and Olivier Scaillet, 2016, Time-Varying Risk Premium in Large Cross-Sectional Equity Data Sets, *Econometrica* 84, 985–1046.

Giglio, Stefano, Bryan Kelly, and Dacheng Xiu, 2022, Factor models, machine learning, and asset pricing, *Annual Review of Financial Economics* 14, 337–368.

Hazelkorn, Todd M., Tobias J. Moskowitz, and Kaushik Vasudevan, 2023, Beyond basis basics: Liquidity demand and deviations from the law of one price, *The Journal of Finance* 78, 301–345.

He, Zhiguo, Bryan Kelly, and Asaf Manela, 2017, Intermediary asset pricing: New evidence from many asset classes, *Journal of Financial Economics* .

Jacod, J, and P Protter, 2012, *Discretization of Processes*, volume 67 of *Stochastic Modelling and Applied Probability* (Springer-Verlag, Heidelberg).

Lipson, Marc L., Davide Tomio, and Jiajun Zhang, 2023, A Real Cost of Free Trades: Retail Option Trading Increases the Volatility of Underlying Securities, Working paper, Darden School of Business.

Martin, Ian, 2017, What is the Expected Return on the Market?*, *The Quarterly Journal of Economics* 132, 367–433.

Muravyev, Dmitriy, and Xuechuan (Charles) Ni, 2019, Why do option returns change sign from day to night?, *Journal of Financial Economics* In Press.

Ni, Shangkun X., Neil D. Pearson, Allen M. Poteshman, and Joshua White, 2020, Does Option Trading Have a Pervasive Impact on Underlying Stock Prices?, *Review of Financial Studies* 34, 1952–1986.

Orłowski, Piotr, Paul Schneider, and Fabio Trojani, 2024, On the nature of (jump) skewness risk premia, *Management Science* 70, 1154–1174.

Siriwardane, Emil, Aditya Sunderam, and Jonathan Wallen, 2025, Segmented Arbitrage, *The Journal of Finance* 80, 2543–2590.

Todorov, Viktor, 2019, Nonparametric spot volatility from options, *The Annals of Applied Probability* 29, 3590–3636.

Figure 1. The R Squared of the Factor Model across DTEs

The figure plots R^2% of the factor model with specification from Section 3.1 for the delevered unhedged returns (left-axis) and DLT-hedged option returns (right-axis) across DTEs. The blue bar plot of total ${R_{6f}^{\mathrm{Uh}}}^2$% of the 6 factors (DLT, GAM, dSV, dVRP, dTRM and dS3) for all DTE (A in x-axis) is the fraction of variance in delevered unhedged option returns explained by all the factors. The hatched blue bar (middle bar) represents the ${R_{\mathrm{DLT}}}^2$%, the R square of the DLT factor alone, obtained from the six-factor model for all DTE (A in x-axis). The orange bar reports the total ${R_{5f}^{\mathrm{Dh}}}^2$% of DLT-hedged option returns explained by the 5 factors (GAM, dSV, dVRP, dTRM and dS3) for all DTE (A in x-axis). The line plot of total ${R_{6f}^{\mathrm{Uh}}}^2$%, ${R_{\mathrm{DLT}}}^2$%, and ${R_{5f}^{\mathrm{Dh}}}^2$% for each DTE are calculated within the DTE subsample. The sample period is from 2016/09 to 2023/12.

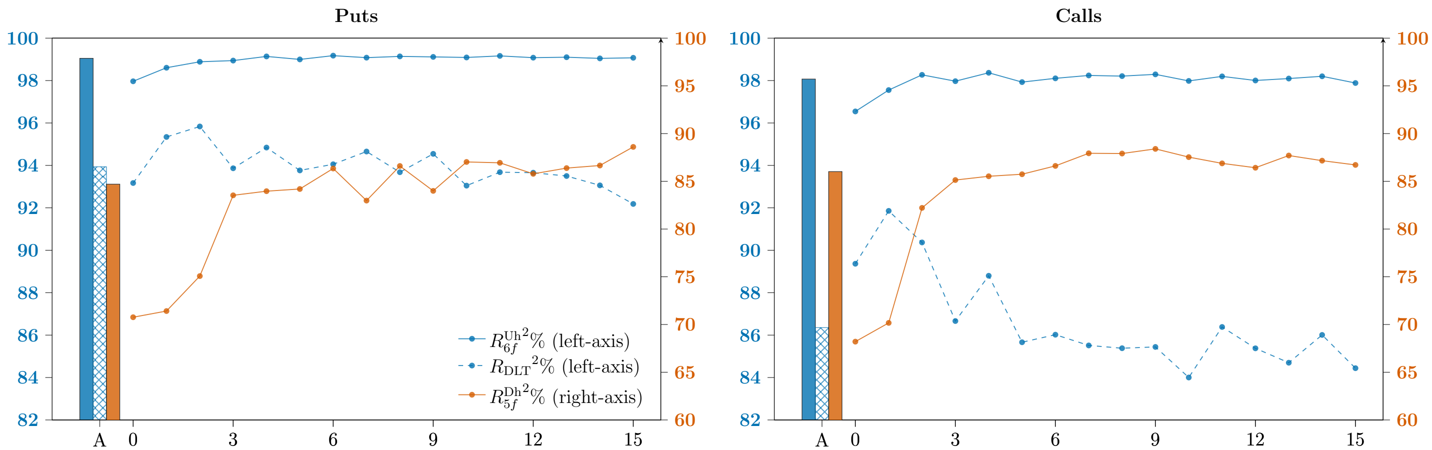

Figure 2. Time-series of Estimated Conditional Risk-neutral Expectations of Risk Factors

The figure presents time-series plots of conditional risk-neutral expectations of risk factors estimated from put and call options at 10:15 ET and 15:45 ET. They are obtained from the cross-sectional regression (14) of the conditional intercepts on option exposures at each 30-minute timestamp for puts and calls, respectively. The ordinate axis labels are in annualized percentage points. The sample period is from 2016/09 to 2023/12.

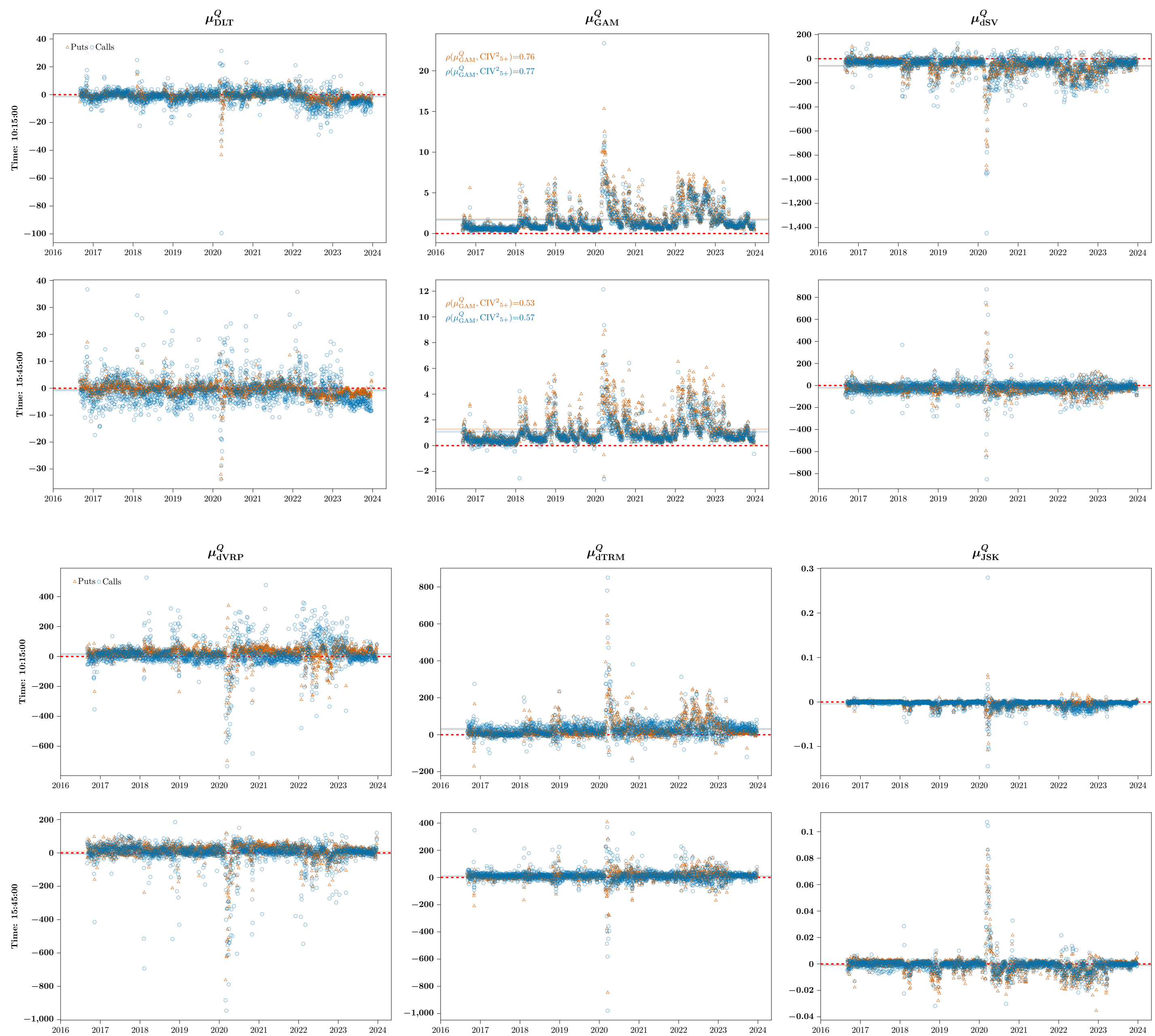

Figure 3. The Intraday Pattern of Estimated Conditional Risk-neutral Expectations of Risk Factors

The figure plots the intraday average conditional risk-neutral expectation, μ_t^Q, of each risk factor, estimated from puts and calls. They are obtained from the cross-sectional regression (14) of the conditional intercepts on option exposures at each 30-minute timestamp for puts and calls, respectively. The ordinate axis labels are in annualized percentage points. The sample period is from 2016/09 to 2023/12.

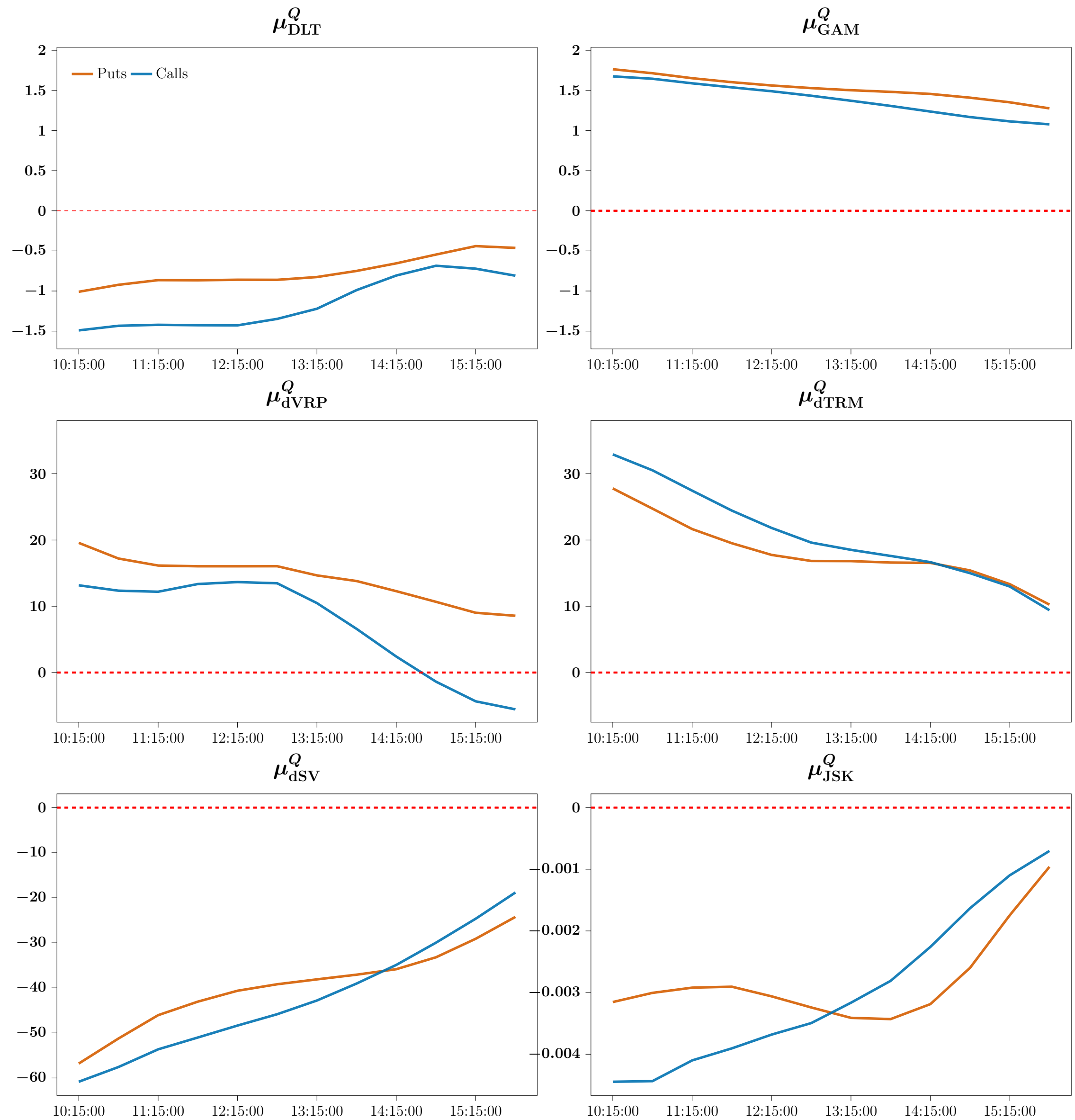

Figure 4. The Intraday Pattern of Estimated Conditional Risk-neutral Expectations of Risk Factors from Non-0DTE Options

The figure plots the intraday average conditional risk-neutral expectation, μ_t^Q, of each risk factor,estimated from non-0DTE puts and calls. They are obtained from the cross-sectional regression (14) of the conditional intercepts on option exposures at each 30-minute timestamp for puts and calls, excluding 0DTEs. The ordinate axis labels are in annualized percentage points. The sample period is from 2016/09 to 2023/12.

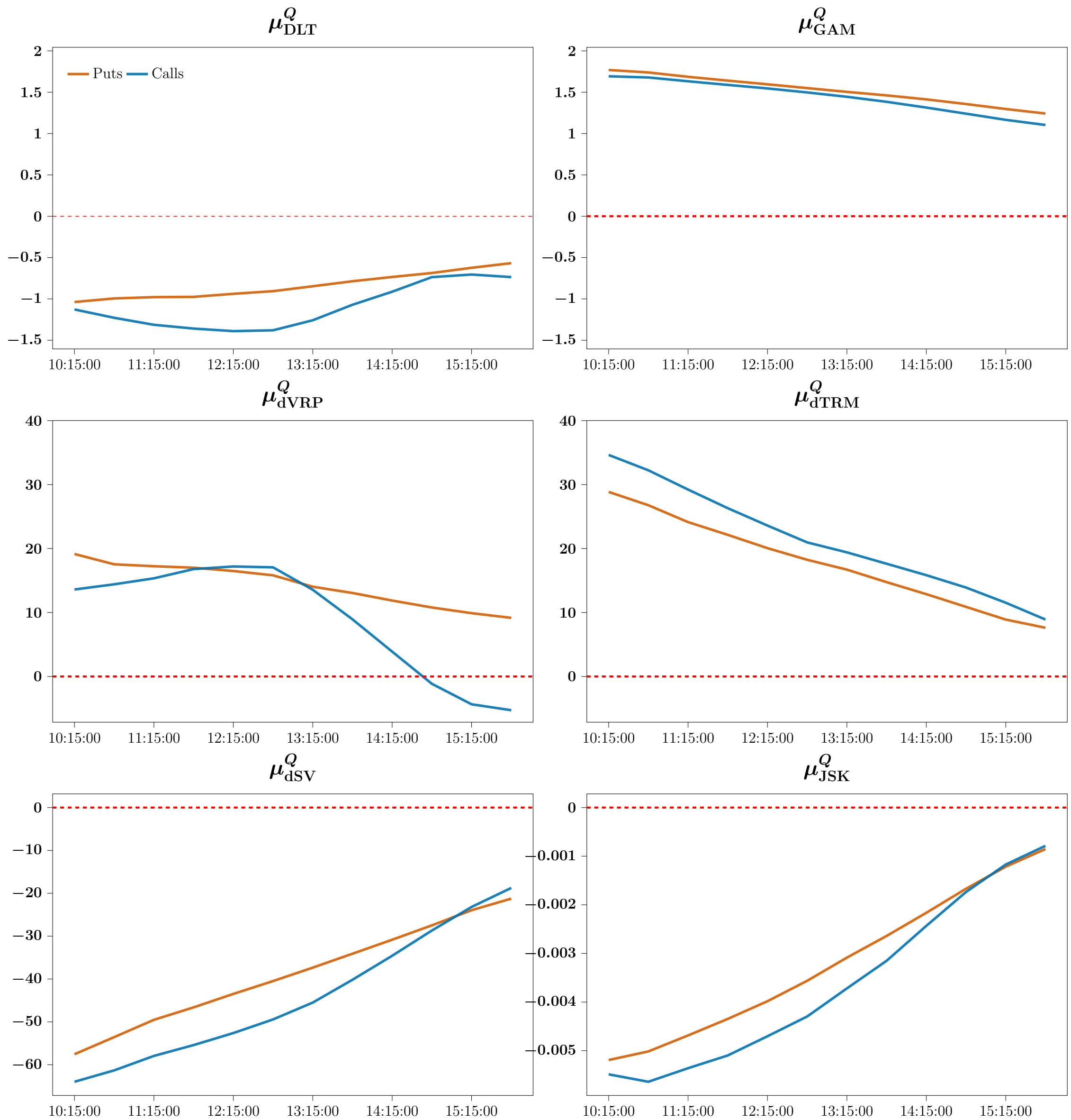

Figure 5. Time-series of 0DTE Estimated Alphas

The figure plots the time-series of 0DTE bucket-specific alphas, $\widehat{\alpha}_{b(i),t}$, estimated from puts and calls. They are obtained from the cross-sectional regression (17) of the conditional intercepts on option exposures at each 30-minute timestamp for puts and calls, respectively. The options are assigned into 9 buckets based on option maturities (0DTE, 1–3DTE, 4–15DTE) and moneyness (DOTM, OTM, ATM). This figure displays the estimated $\widehat{\alpha}_{b(i),t}$ for the 0DTE buckets only at 10:15, 12:45 and 15:45 ET, respectively. The vertical red dashed line marks April 1, 2022, while the new Tuesday and Thursday expirations began trading on April 18 and May 11, 2022, respectively. The vertical gray dashed lines indicate the FOMC days (the second day of FOMC meetings). The ordinate axis labels are in annualized percentage points. The sample period is from 2016/09 to 2023/12.

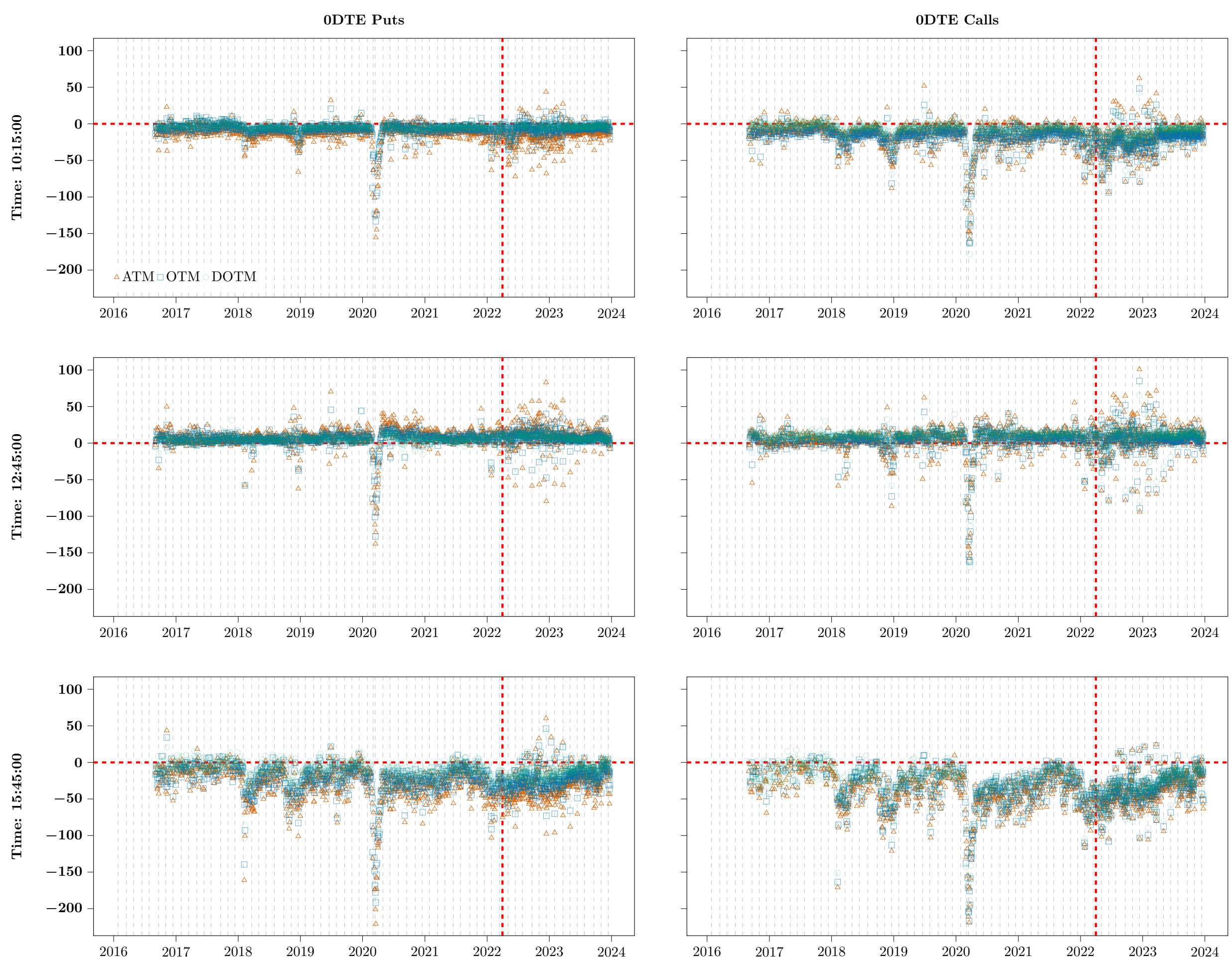

Figure 6. Time-series of Non-0DTE Estimated Alphas

The figure plots the time-series of 1+DTE bucket-specific alphas, $\widehat{\alpha}_{b(i),t}$, estimated from puts and calls. They are obtained from the cross-sectional regression (17) of the conditional intercepts on option exposures at each 30-minute timestamp for puts and calls, respectively. The options are assigned into 9 buckets based on option maturities (0DTE, 1–3DTE, 4–15DTE) and moneyness (DOTM, OTM, ATM). This figure displays the estimated $\widehat{\alpha}_{b(i),t}$ for the non-0DTE buckets only at 10:15, 12:45 and 15:45 ET, respectively. The vertical red dashed line marks April 1, 2022, while the new Tuesday and Thursday expirations began trading on April 18 and May 11, 2022, respectively. The vertical gray dashed lines indicate the FOMC days (the second day of FOMC meetings). The ordinate axis labels are in annualized percentage points. The sample period is from 2016/09 to 2023/12.

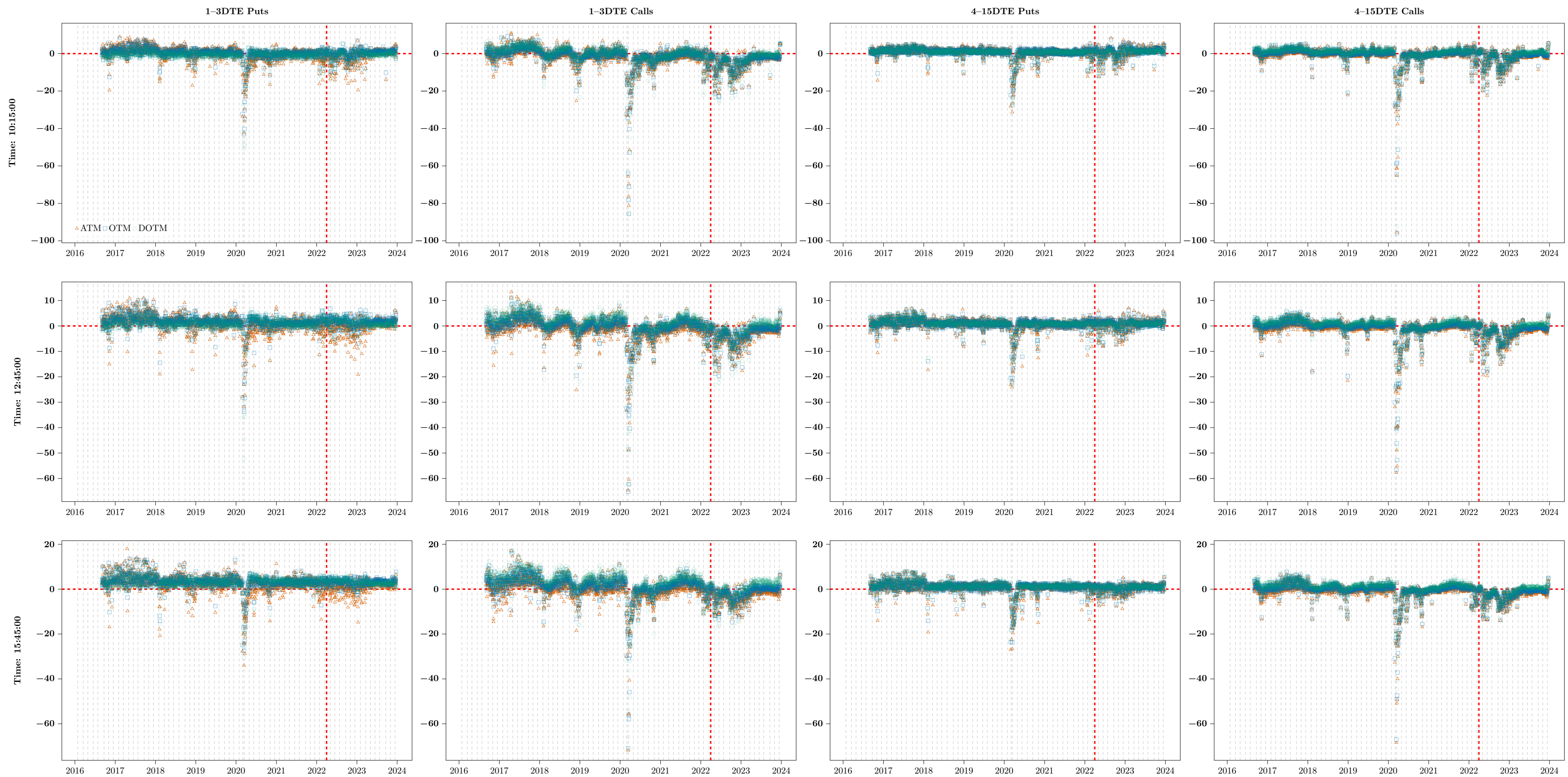

Figure 7. The Intraday Pattern of Estimated Alphas

The figure plots the intraday average bucket-specific alphas, $\widehat{\alpha}_{b(i),t}$, at each intraday timestamp across days for puts and calls, respectively. The bucket-specific alphas are estimated from the cross-sectional regression (17) of the conditional intercepts on option exposures for puts and calls, at each 30-minute timestamp. The options are assigned into 9 buckets based on option maturities (0DTE, 1–3DTE, 4–15DTE) and moneyness (DOTM, OTM, ATM). The ordinate axis labels are in annualized percentage points. The sample period is from 2016/09 to 2023/12.

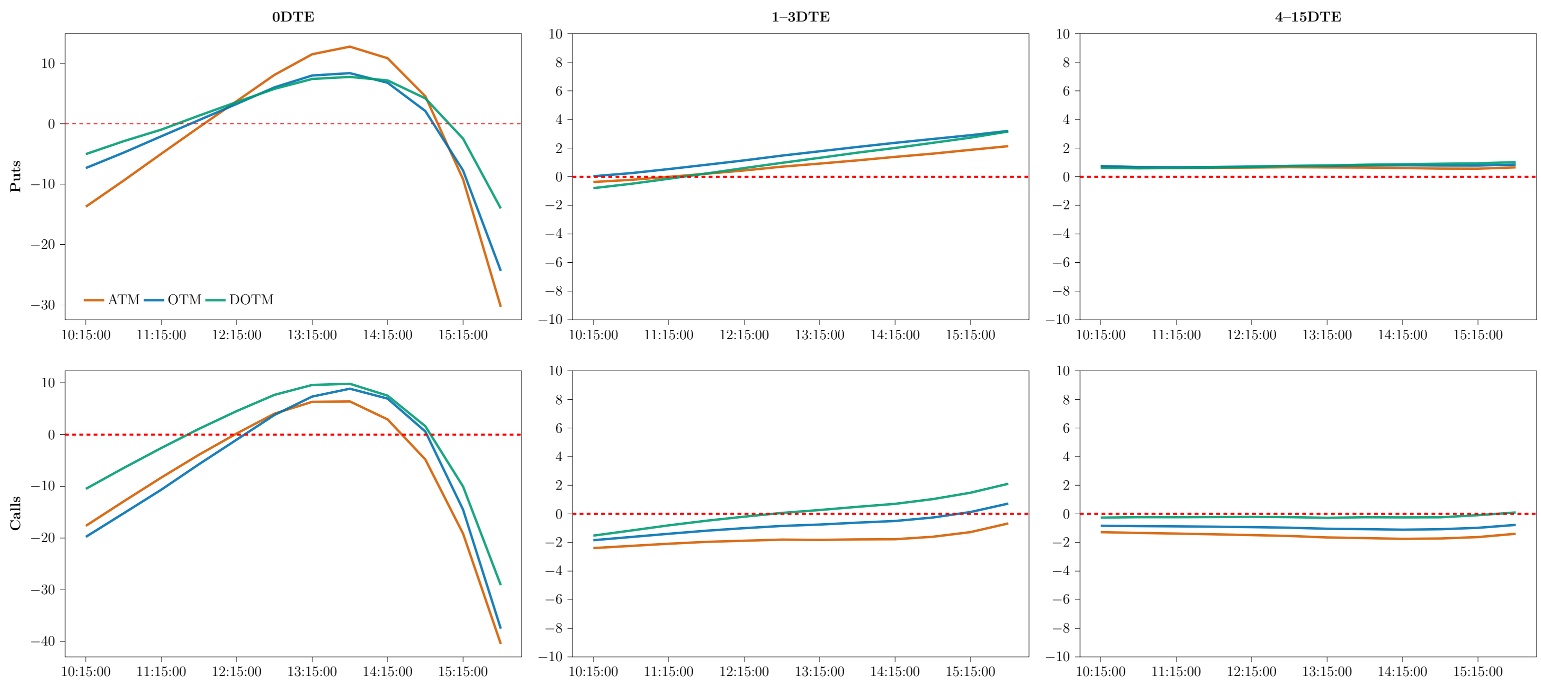

Figure 8. The Intraday Pattern of 0DTE Estimated Alphas on FOMC and Non-FOMC Days

The figure plots the intraday average 0DTE alphas, $\widehat{\alpha}_{b(i),t}$, at each intraday timestamp across FOMC and non-FOMC days for puts and calls, respectively. The bucket-specific alphas are estimated from the cross-sectional regression (17) of the conditional intercepts on option exposures for puts and calls, at each 30-minute timestamp. The options are assigned into 9 buckets based on option maturities (0DTE, 1–3DTE, 4–15DTE) and moneyness (DOTM, OTM, ATM). This figure plots the intraday average $\widehat{\alpha}_{b(i),t}$ for the 0DTE buckets only, computed across FOMC days (the second day of FOMC meetings) and non-FOMC days. The ordinate axis labels are in annualized percentage points. The sample period is from 2016/09 to 2023/12.

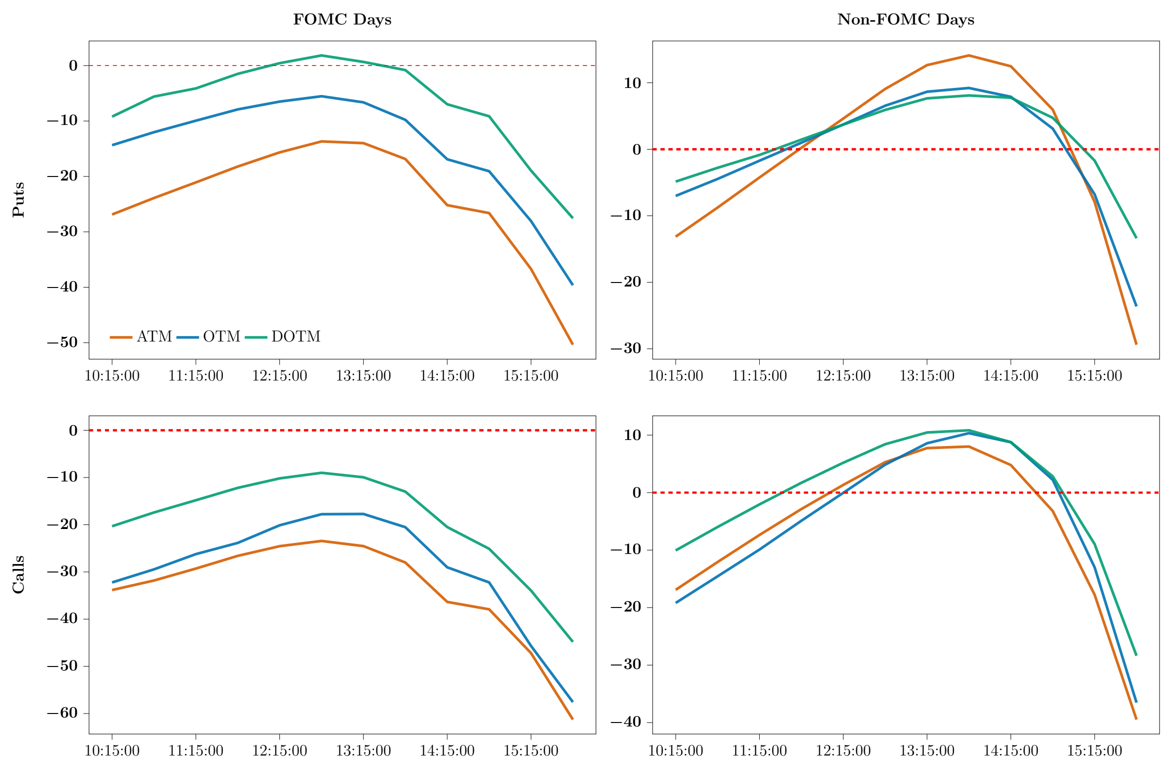

Figure 9. The Intraday Pattern of 1–3DTE Estimated Alphas across Different Periods

The figure plots the intraday average 1–3DTE alphas, $\widehat{\alpha}_{b(i),t}$, at each intraday timestamp across different periods for puts and calls, respectively. The bucket-specific alphas are estimated from the cross-sectional regression (17) of the conditional intercepts on option exposures for puts and calls, at each 30-minute timestamp. The options are assigned into 9 buckets based on option maturities (0DTE, 1–3DTE, 4–15DTE) and moneyness (DOTM, OTM, ATM). This figure plots the intraday average $\widehat{\alpha}_{b(i),t}$ for the 1–3DTE buckets only, computed across four subsamples: pre-April 2022, post-April 2022, pre-April 2022 Tuesdays and Thursdays, and pre-April 2022 Mondays, Wednesdays and Fridays. All the subsamples include only normal trading days (non-FOMC days and excluding March 2020). The ordinate axis labels are in annualized percentage points. The sample period is from 2016/09 to 2023/12.

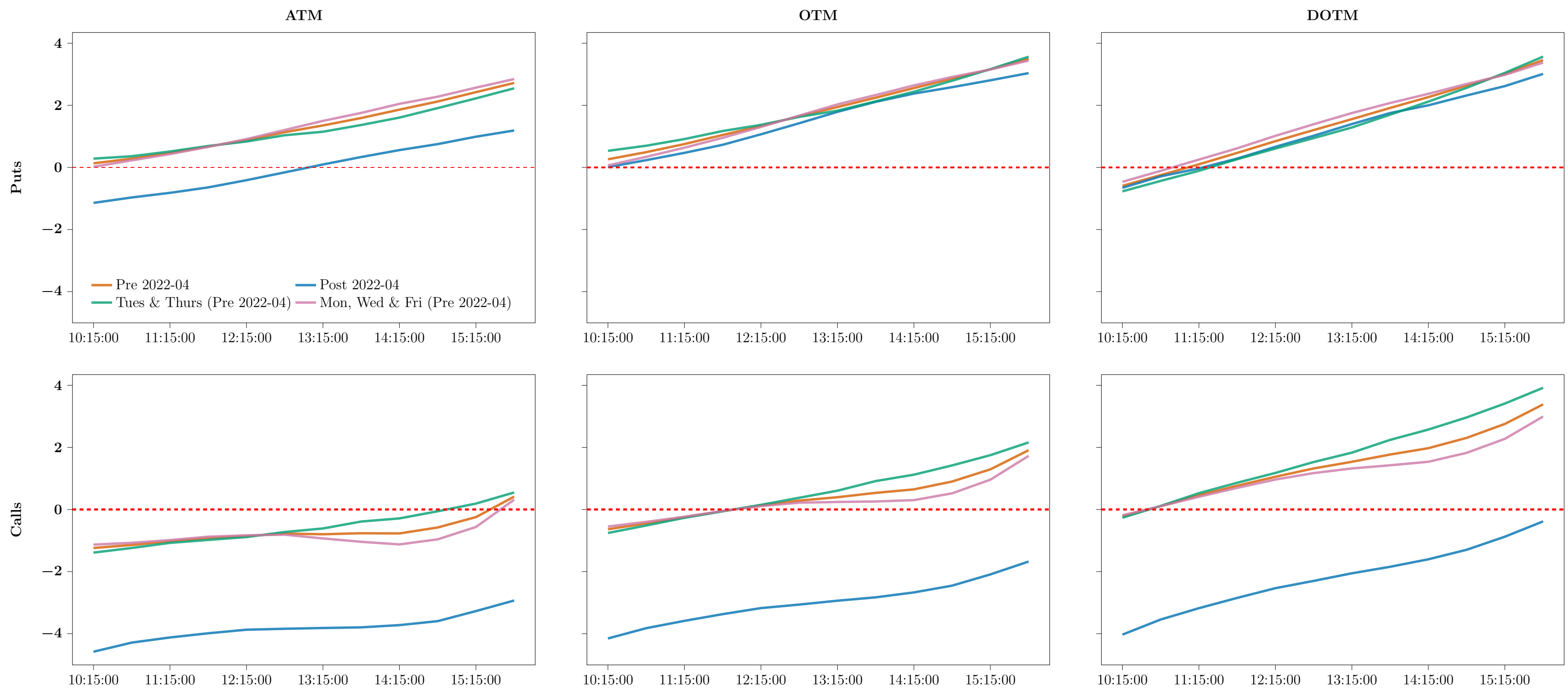

Figure 10. Intraday Patterns of Self-financing Six-factor-neutral Portfolio Returns

This figure plots the intraday patterns of the six-factor-neutral returns of the 0DTE options hedged by instrument option contracts across different periods using self-financing strategy. The hedging procedure is implemented foreach individual 0DTE put and call contract, within each moneyness bucket (ATM ,OTM, DOTM), at each 30-min timestamp. The non-zero options are assigned into 6 buckets based on option maturities (1–3 DTE, 4–15DTE) and moneyness (ATM, OTM, DOTM). The hedging instrument contracts are constructed, at each 30-min timestamp, by selecting top 3 traded contracts from each bucket of non-zero puts and calls, yielding a total of 18 instrument contracts. The factor-neutral returns are averaged cross-sectionally at each timestamp, and then averaged over days to obtain the intraday patterns. The mean return is then calculated by $\frac{1}{T}\sum_{t\in T}\frac{1}{n_t}\sum_{i\in n_t} R^{dh}_{N,i,t}$. The top row plots show the intraday patterns during the full sample period, while the middle and bottom rows plot the intraday patterns during the FOMC days and non-FOMC days, respectively. The shaded areas represent the 95% confidence intervals of the intraday means. The ordinate axis labels are in annualized percentage points (multiplied by 252 × 100). The sample period is from 2016/09 to 2023/12.

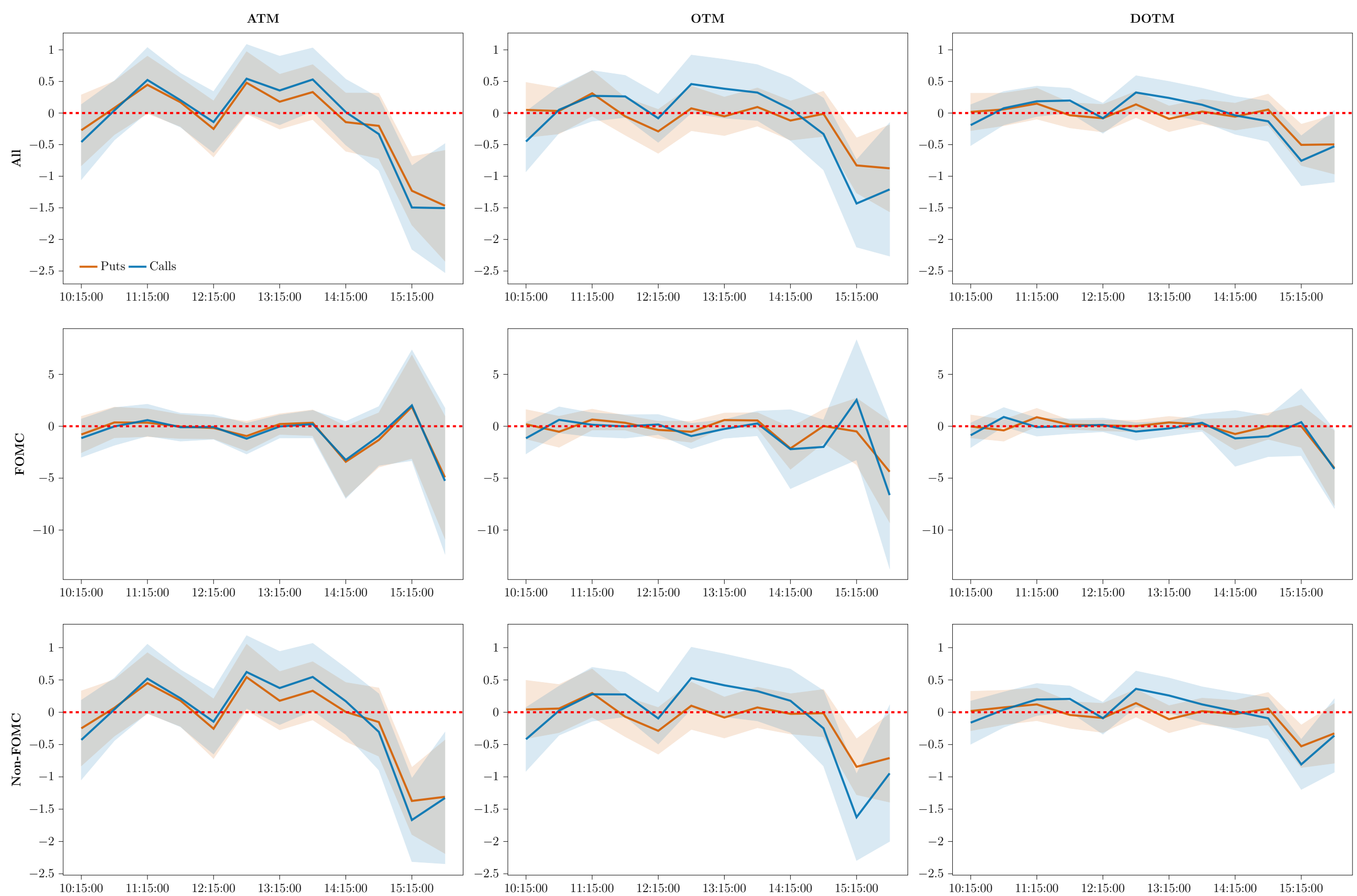

Figure 11. Cumulative Returns of Self-financing Six-factor-neutral Portfolio

This figure plots the time-series of the cumulative six-factor-neutral returns of the 0DTE options hedged by instrument option contracts using self-financing strategy, at 10:15, 12:45 and 15:45 ET, respectively. The hedging procedure is implemented for each individual 0DTE put and call contract, within each moneyness bucket (ATM ,OTM, DOTM), at each 30-min timestamp. The non-zero options are assigned into 6 buckets based on option maturities (1–3 DTE, 4–15DTE) and moneyness (ATM, OTM, DOTM). The hedging instrument contracts are constructed, at each 30-min timestamp, by selecting top 3 traded contracts from each bucket of non-zero puts and calls, yielding a total of 18 instrument contracts. The factor-neutral returns are averaged cross-sectionally at each timestamp. We also report the cumulative return of a long position of ES futures initiated at the same intraday time and hold for the same period as the option trade. The hedging portfolios are leveraged such that the unconditional (whole sample) volatility of the hedged returns matches that of the corresponding ES futures returns. It means that the factor-neutral return is multiplied by $\frac{\sigma_{ES}}{\sigma_{b,N}}$, where σ_{ES} is the unconditional volatility of ES futures returns, and $\sigma_{b,N}$ is the unconditional volatility of the risk-factor-neutral returns within each moneyness bucket b. The cumulative returns are summed across previous days at each intraday timepoint. The ordinate axis labels are in percentage (multiplied by 100). The sample period is from 2016/09 to 2023/12.

Table I

Summary Statistics of Intraday Delevered Returns on S&P 500 Index Options

The table reports the summary statistics of intraday delevered returns on S&P 500 index options, before and after delta-hedging. The column labeled Moneyness indicates how options are grouped by their moneyness level. The column labeled DTE indicates how options are grouped by their remaining days to expiration. Further columns report: the number of observation in each sub-sample (N), the mean return (Mean) and standard deviation (SD) of unhedged and delta-hedged delevered returns (reported in percent per annum), respectively. The annualization factors account for 12 intraday periods per trading day and 252 trading days per year. We delta-hedge the options with the S&P 500 E-Mini futures returns as in equation (2), and we estimate the option delta using our main specification of the model in Section 3. In the rare case an estimated delta has an incorrect sign, we set it to zero. We measure moneyness as $\kappa_{t,\tau} = \frac{\ln(K/F_{t,\tau})}{\sqrt{\tau CIV_{t,\tau}}}$, and we supply all details about the calculations in Appendix C. The option moneyness categories are: DOTM puts (calls) for $\kappa_{t,\tau} \leq -2.2$ ($\kappa_{t,\tau} > 1$), OTM puts (calls) for $-2.2 < \kappa_{t,\tau} \leq -1$ ($-0.5 < \kappa_{t,\tau} \leq 1$) and ATM puts (calls) for $-1 < \kappa_{t,\tau} \leq 1$ ($-0.5 < \kappa_{t,\tau} \leq 0.5$). The sample period is from 2016/09 to 2023/12.

		Puts					Calls				
		Unhedged		DLT-hedged			Unhedged		DLT-hedged		
Moneyness	DTE	Mean	SD	Mean	SD	N	Mean	SD	Mean	SD	N
All	All	-4.12^{***}	7.07	-1.46^{***}	1.74	14,025,137	2.84^{***}	5.52	-1.22^{***}	2.04	6,824,692
	0	-9.10^{***}	7.55	-6.99^{***}	1.97	200,728	-5.11^{***}	6.16	-7.13^{***}	2.00	127,742
	1–3	-5.46^{***}	7.41	-1.86^{***}	1.67	1,729,571	2.28^{***}	5.96	-1.98^{***}	1.93	914,663
	4–15	-3.85^{***}	7.01	-1.31^{***}	1.75	12,094,838	3.10^{***}	5.44	-0.97^{***}	2.06	5,782,287
ATM	All	-7.00^{***}	9.66	-2.20^{***}	2.22	7,302,345	4.30^{***}	7.03	-0.70^{***}	2.13	3,832,225
	0	-13.32^{***}	10.28	-9.58^{***}	2.45	105,146	-6.26	9.01	-9.24^{***}	2.53	52,589
	1–3	-9.47^{***}	10.13	-3.02^{***}	2.08	897,875	3.75^{**}	8.05	-1.87^{***}	2.10	450,544
	4–15	-6.55^{***}	9.58	-1.96^{***}	2.23	6,299,324	4.54^{***}	6.85	-0.41^{***}	2.12	3,329,092
OTM	All	-1.38^{***}	2.11	-0.87^{***}	1.20	4,047,581	1.75^{***}	2.97	-2.13^{***}	2.24	1,972,603
	0	-5.55^{***}	2.23	-5.04^{***}	1.47	61,694	-4.52^{*}	4.19	-7.33^{***}	2.11	26,525
	1–3	-1.72^{***}	2.21	-0.89^{***}	1.23	524,776	2.15^{**}	3.50	-2.29^{***}	2.15	235,556
	4–15	-1.26^{***}	2.09	-0.80^{***}	1.19	3,461,111	1.79^{***}	2.87	-2.03^{***}	2.25	1,710,522
DOTM	All	-0.41^{***}	0.65	-0.33^{***}	0.56	2,675,211	-0.55^{***}	1.07	-1.43^{***}	1.11	1,019,864
	0	-2.48^{***}	0.69	-2.47^{***}	0.63	33,888	-4.18^{***}	1.53	-4.73^{***}	1.09	48,628
	1–3	-0.14	0.73	-0.12	0.66	306,920	-0.48	1.26	-1.87^{***}	1.23	228,563
	4–15	-0.41^{***}	0.63	-0.33^{***}	0.54	2,334,403	-0.34^{***}	0.96	-1.08^{***}	1.06	742,673

$\star$ denotes statistically significant difference from zero at the 10% level, $\star\star$ at the 5% level, and $\star\star\star$ at the 1% level.

Table II
Risk Factors under P and Q Measures

This table reports the sample averages of the risk factor realizations ($\overline{f}$), the sample averages of the factors' conditional risk-neutral expectations ($\overline{\mu}^Q$), and the risk premiums, i.e., differences between the two ($\widehat{\lambda} = \overline{f} - \overline{\mu}^Q$). The construction of the factors is described in Section 3.1. The conditional risk-neutral expectations, μ_t^Q, are estimated from cross-sectional regressions of option-specific conditional intercepts on estimated exposures at each 30-minute timestamp for puts and calls, respectively, as specified in equation (13). The table reports these summary statistics for four sub-samples: our entire dataset (All), FOMC (FOMC) and non-FOMC days (Non-FOMC), and the subsample excluding March 2020 (Ex-COVID). All the values are reported in percent per annum (multiplied by 12×252). The sample period is from 2016/09 to 2023/12.

		DLT		GAM		dSV		dVRP		dTRM		JSK × 100	
Period	Qty	Puts	Calls	Puts	Calls	Puts	Calls	Puts	Calls	Puts	Calls	Puts	Calls
All	$\overline{f}$	4.5		1.6***		−21.0***		−26.6***		30.9***		0.1	
	$\overline{\mu}^Q$	−0.8***	−1.1***	1.5***	1.4***	−39.6***	−42.3***	14.2***	7.2***	18.1***	20.6***	−0.3***	−0.3***
	$\widehat{\lambda}$	5.3	5.7	0.1	0.2**	18.6***	21.4***	−40.8***	−33.9***	12.8**	10.3*	0.4***	0.4***
FOMC	$\overline{f}$	0.2		2.7***		−86.1***		−15.9		81.5***		−0.1	
	$\overline{\mu}^Q$	−1.2***	−1.6***	2.2***	1.8***	−66.5***	−45.4***	21.3***	−0.5	28.2***	22.7***	−0.6***	−0.5***
	$\widehat{\lambda}$	1.5	1.8	0.5	0.9**	−19.7	−40.7	−37.2	−15.4	53.3**	58.8**	0.5	0.4
Non-FOMC	$\overline{f}$	4.7		1.6***		−18.8***		−27.0***		29.3***		0.1	
	$\overline{\mu}^Q$	−0.7***	−1.1***	1.5***	1.4***	−38.7***	−42.2***	13.9***	7.5***	17.8***	20.5***	−0.3***	−0.3***
	$\widehat{\lambda}$	5.4	5.8	0.1	0.2*	19.9***	23.4***	−40.9***	−34.5***	11.5**	8.7	0.4***	0.4***
Ex-COVID	$\overline{f}$	2.4		1.3***		−18.5***		−19.3***		27.8***		−0.0	
	$\overline{\mu}^Q$	−0.7***	−1.1***	1.4***	1.3***	−37.6***	−39.4***	15.7***	9.1***	18.0***	20.2***	−0.3***	−0.3***
	$\widehat{\lambda}$	3.0	3.4	−0.1***	0.0	19.1***	20.9***	−35.0***	−28.4***	9.7***	7.6**	0.2***	0.3***

⋆ denotes statistically significant difference from zero at the 10% level, ⋆⋆ at the 5% level, and ⋆⋆⋆ at the 1% level.

Table III
Persistence of Risk Factors and their Risk-Neutral Expectations

The table reports the autocorrelation coefficients of the risk factor realizations (f_t) and their risk-neutral expectations (μ_t^Q). The column labeled "30 minutes" reports the 1-lag autocorrelation calculated from all intraday observations at 30-minute frequency, while the column labeled "1 day" reports the autocorrelation calculated from observations at 15:15 ET on each day, i.e., with a 24-hour lag. The construction of the factors is described in Section 3.1. The conditional risk-neutral expectations, μ_t^Q, are estimated from cross-sectional regressions of option-specific conditional intercepts on estimated exposures at each 30-minute timestamp for puts and calls, respectively, as specified in equation (13). The sample period is from 2016/09 to 2023/12.

		30 minutes		1 day	
Factor	Qty	Puts	Calls	Puts	Calls
DLT	f_t	−0.03		−0.05	
	μ_t^Q	0.91	0.88	0.40	0.33
GAM	f_t	0.28		0.31	
	μ_t^Q	0.97	0.95	0.76	0.56
dSV	f_t	−0.10		−0.09	
	μ_t^Q	0.86	0.86	−0.07	−0.23
dVRP	f_t	−0.00		0.08	
	μ_t^Q	0.90	0.88	0.47	0.32
dTRM	f_t	−0.08		−0.29	
	μ_t^Q	0.87	0.82	0.02	−0.12
JSK	f_t	−0.09		−0.01	
	μ_t^Q	0.85	0.82	0.75	0.65

Table IV
Model Explanatory Power for Delta-Hedged Delevered Option Returns

This table reports the incremental $R^2\%$ of the five risk factors for delta-hedged delevered option returns, calculated as follows:

$$R^2\% = \left[1 - \frac{\sum_{i,t}\left(r^{dh}_{i,t+1} - \left(\widehat{c}_{i,t} + \sum_l \widehat{\beta}_{l,i,t} f_{l,t+1}\right)\right)^2}{\sum_{i,t}(r^{dh}_{i,t+1})^2}\right] \times 100,$$

where $\widehat{c}_{i,t}$ is an option's conditional intercept, and $\widehat{\beta}_{i,l,t}$ is the estimated option exposure. We give a breakdown of the results for puts and calls, respectively, and across option moneyness and maturity buckets. In each sub-panel, each column labeled with a factor name reports the increment in $R^2\%$ after adding that factor to a model that already includes the preceding factors. The column labeled "5F" represents the total explanatory power of the model. We delta-hedge the options with the S&P 500 E-Mini futures returns as in equation (2), and we estimate the option delta using our main specification of the model in Section 3. In the rare case an estimated delta has an incorrect sign, we set it to zero. We measure moneyness as $\kappa_{t,\tau} = \frac{\ln(K/F_{t,\tau})}{\sqrt{\tau CIV_{t,\tau}}}$, and we supply all details about the calculations in Appendix C. The option moneyness categories are: DOTM puts (calls) for $\kappa_{t,\tau} \leq -2.2$ ($\kappa_{t,\tau} > 1$), OTM puts (calls) for $-2.2 < \kappa_{t,\tau} \leq -1$ ($-0.5 < \kappa_{t,\tau} \leq 1$) and ATM puts (calls) for $-1 < \kappa_{t,\tau} \leq 1$ ($-0.5 < \kappa_{t,\tau} \leq 0.5$). The sample period is from 2016/09 to 2023/12.

		Puts						Calls					
Moneyness	DTE	GAM	dSV	dVRP	dTRM	JSK	5F	GAM	dSV	dVRP	dTRM	JSK	5F
All	All	9.7	53.0	17.0	4.5	0.6	84.7	10.5	59.3	10.6	4.6	0.9	86.0
	0	58.0	7.6	2.3	0.6	2.3	70.8	57.8	5.7	1.1	1.0	2.7	68.2
	1–3	16.5	43.3	15.7	1.6	1.1	78.2	15.9	52.1	10.0	1.3	1.4	80.8
	4–15	7.8	55.2	17.4	5.0	0.5	85.8	8.8	61.4	10.9	5.2	0.8	87.1
ATM	All	9.9	54.7	13.9	4.6	0.6	83.7	12.1	55.3	12.4	5.2	0.3	85.4
	0	61.0	6.4	1.9	0.5	1.5	71.3	65.7	4.0	0.9	0.6	0.8	72.0
	1–3	17.2	45.1	11.9	1.7	0.9	76.8	20.1	45.2	11.5	1.8	0.5	79.1
	4–15	8.0	56.9	14.4	5.0	0.5	84.8	9.9	57.7	12.8	5.8	0.2	86.5
OTM	All	9.4	43.4	33.0	4.6	0.5	90.8	9.2	66.2	7.5	4.0	1.5	88.3
	0	46.1	13.1	3.9	1.1	5.4	69.7	54.0	8.5	1.5	1.6	4.5	70.2
	1–3	15.2	35.1	31.5	1.7	1.9	85.3	11.1	62.8	7.7	0.7	2.0	84.3
	4–15	7.5	45.5	34.0	5.2	0.2	92.3	8.3	67.4	7.5	4.4	1.4	89.1
DOTM	All	1.8	43.4	35.0	3.0	0.7	83.8	−0.7	61.5	9.0	1.7	5.4	76.9
	0	32.7	9.6	5.9	−1.5	8.9	55.6	19.6	9.4	1.6	2.1	9.5	42.3
	1–3	3.5	41.8	31.8	−2.1	2.0	77.1	6.8	58.1	8.6	0.5	5.4	79.4
	4–15	0.8	44.4	36.1	4.0	0.2	85.6	−5.3	66.5	9.7	2.2	5.2	78.3

Table V
Summary Statistics of Option Price Dislocations

The table collects the summary statistics of option price dislocations estimated at the option maturity and moneyness bucket level, $\widehat{\alpha}_{b(i),t}$, for puts and calls, respectively. The dislocations are estimated as bucket-level fixed effects in cross-sectional regressions of the conditional intercepts on option exposures (as in equation (16)) for puts and calls, at each 30-minute timestamp. The options are assigned to one of nine buckets based on option maturities (0DTE, 1–3DTE, 4–15DTE) and moneyness (DOTM, OTM, ATM). The reported statistics include the number of observations (N), mean ($\overline{\widehat{\alpha}}$), mean of the absolute values ($\overline{|\widehat{\alpha}|}$), standard deviation (SD), 1-lag autocorrelation at 30 minutes ($\text{AC}^{30\text{min}}$) and at one day ($\text{AC}^{1\text{day}}$) calculated from observations at 15:15 ET on each day. Means and standard deviations are reported in percent per annum (scaled by 12×252). The sample period is from 2016/09 to 2023/12.

	Puts						Calls					
Factor	$\overline{\widehat{\alpha}}$	$\overline{\lvert\widehat{\alpha}\rvert}$	SD	$\text{AC}^{30\text{min}}$	$\text{AC}^{1\text{day}}$	N	$\overline{\widehat{\alpha}}$	$\overline{\lvert\widehat{\alpha}\rvert}$	SD	$\text{AC}^{30\text{min}}$	$\text{AC}^{1\text{day}}$	N
$\alpha_{0,A}$	$-1.28^{\star\star}$	14.28	21.26	0.84	0.57	15,527	$-6.93^{\star\star\star}$	16.35	24.52	0.86	0.63	15,024
$\alpha_{0,O}$	$-0.76^{\star}$	9.92	15.95	0.82	0.61	15,278	$-6.11^{\star\star\star}$	16.02	23.87	0.86	0.65	13,508
$\alpha_{0,D}$	$1.01^{\star\star\star}$	7.54	11.79	0.79	0.58	14,711	$-1.36^{\star\star}$	13.43	21.57	0.86	0.72	15,584
$\alpha_{1\sim3,A}$	$0.82^{\star\star\star}$	2.65	3.80	0.93	0.56	21,974	$-1.77^{\star\star\star}$	3.27	5.20	0.93	0.58	21,974
$\alpha_{1\sim3,O}$	$1.60^{\star\star\star}$	2.44	3.11	0.89	0.46	21,974	$-0.76^{\star\star\star}$	2.99	5.27	0.94	0.67	21,974
$\alpha_{1\sim3,D}$	$1.13^{\star\star\star}$	2.28	3.56	0.88	0.47	21,688	0.16	3.77	6.07	0.95	0.73	21,940
$\alpha_{4\sim15,A}$	$0.63^{\star\star\star}$	1.79	2.74	0.94	0.53	21,998	$-1.52^{\star\star\star}$	2.26	4.59	0.94	0.58	21,998
$\alpha_{4\sim15,O}$	$0.75^{\star\star\star}$	1.65	2.42	0.94	0.53	21,998	$-0.95^{\star\star\star}$	2.05	4.47	0.95	0.62	21,998
$\alpha_{4\sim15,D}$	$0.77^{\star\star\star}$	1.59	2.36	0.95	0.57	21,998	-0.20	2.24	4.07	0.95	0.72	21,812

$\star$ denotes statistically significant difference from zero at the 10% level, $\star\star$ at the 5% level, and $\star\star\star$ at the 1% level.

Table VI
Option Dislocations and Intermediary Frictions

The table reports the coefficients and R^2 of the regressions of ATM option dislocations measured at 15:45 ET on variables related to frictions faced by financial intermediaries and on controls. The top panel reports the results for dislocations, $\widehat{\alpha}_{b(i),t}$, while the bottom panel reports the results for absolute dislocations, $|\widehat{\alpha}_{b(i),t}|$. The dislocations are estimated as bucket-level fixed effects in cross-sectional regressions of the conditional intercepts on option exposures (as in equation (16)) for puts and calls, at each 30-minute timestamp. *ESF* is the spread between the forward interest rate implied by the S&P 500 E-Mini futures and the three-month OIS rate, as in Siriwardane, Sunderam, and Wallen (2025) and Appendix D, estimated using futures prices at the futures closing time, 16:15 ET, of the previous day. *HKM* is the level of the aggregate market equity ratio of primary dealers at the end of the previous day as defined by He, Kelly, and Manela (2017). ε_{HKM} proposed therein is the AR(1) innovation to the capital ratio, scaled by the lagged ratio, on the current day. *CIV* is the corridor implied variance calculated from options with the given maturity at 15:15 ET on the current day. *OI* is the open interest of all the puts (calls) within each bucket at the end of the previous day. *SP500* is the intraday return of the S&P 500 ES futures from 9:45 ET to 15:15 ET on the current day. For each combination of option maturity and type, the table reports the estimated coefficients, their robust standard errors (in parentheses) and adjusted R^2 (in %) in the first column, and the $R^2_{\text{univ.}}$ (in %) from a univariate regression in the second column. All the variables are normalized using their full-sample standard deviations. The sample period is from 2016/09 to 2023/12.

	$\widehat{\alpha}_{b(i),t}$											
	0DTE				1–3DTE				4–15DTE			
	Puts		Calls		Puts		Calls		Puts		Calls	
	Coef.	$R^2_{\text{univ.}}$	Coef.	$R^2_{\text{univ.}}$	Coef.	$R^2_{\text{univ.}}$	Coef.	$R^2_{\text{univ.}}$	Coef.	$R^2_{\text{univ.}}$	Coef.	$R^2_{\text{univ.}}$
ESF	−0.09*	1.42	−0.09**	1.45	−0.03	0.73	−0.07***	1.11	−0.01	0.88	−0.04	1.47
	(0.05)		(0.04)		(0.02)		(0.02)		(0.03)		(0.03)	
HKM	0.10**	4.92	0.14**	6.05	0.16***	12.23	0.28***	22.23	0.03	9.44	0.11***	17.37
	(0.05)		(0.06)		(0.03)		(0.03)		(0.04)		(0.03)	
ε_{HKM}	0.02	3.31	0.08***	2.91	−0.01	0.31	−0.04	0.00	−0.03	0.39	−0.10	0.15
	(0.03)		(0.03)		(0.02)		(0.05)		(0.03)		(0.08)	
CIV	−0.50***	41.94	−0.59***	41.85	−0.59***	49.44	−0.63***	52.04	−0.67***	51.03	−0.72***	58.03
	(0.10)		(0.13)		(0.10)		(0.07)		(0.10)		(0.07)	
OI	−0.30***	26.21	−0.06***	0.40	−0.18***	15.50	−0.04**	0.01	−0.09*	12.83	−0.01	4.22
	(0.03)		(0.02)		(0.03)		(0.02)		(0.05)		(0.03)	
SP500	0.04*	3.82	0.09***	3.87	0.07***	0.70	0.03*	−0.04	0.08***	0.68	0.03	−0.04
	(0.02)		(0.03)		(0.02)		(0.02)		(0.02)		(0.03)	
Const.	−1.37***		−2.09***		0.06		−1.43***		0.64**		−0.48*	
	(0.31)		(0.38)		(0.23)		(0.21)		(0.28)		(0.26)	
R^2	52.20		46.11		54.92		59.31		52.24		59.96	

	$\lvert\widehat{\alpha}_{b(i),t}\rvert$											
	0DTE				1–3DTE				4–15DTE			
	Puts		Calls		Puts		Calls		Puts		Calls	
	Coef.	$R^2_{\text{univ.}}$	Coef.	$R^2_{\text{univ.}}$	Coef.	$R^2_{\text{univ.}}$	Coef.	$R^2_{\text{univ.}}$	Coef.	$R^2_{\text{univ.}}$	Coef.	$R^2_{\text{univ.}}$
ESF	0.09**	1.58	0.09**	1.44	−0.04	−0.04	0.01	0.43	−0.03	0.34	0.03	1.63
	(0.05)		(0.04)		(0.03)		(0.03)		(0.04)		(0.03)	
HKM	−0.11**	5.55	−0.15***	6.38	0.33***	1.78	0.09***	2.09	0.25***	0.36	0.03	8.87
	(0.05)		(0.06)		(0.03)		(0.03)		(0.04)		(0.04)	
ε_{HKM}	−0.01	3.10	−0.08***	2.81	0.04	0.32	0.09	0.38	0.06	−0.03	0.11	0.12
	(0.03)		(0.03)		(0.03)		(0.06)		(0.05)		(0.08)	
CIV	0.52***	45.05	0.59***	42.96	0.66***	22.22	0.74***	50.14	0.74***	35.76	0.79***	58.41
	(0.10)		(0.13)		(0.04)		(0.05)		(0.07)		(0.06)	
OI	0.30***	27.01	0.06***	0.38	−0.23***	0.12	−0.02	−0.05	−0.06	5.26	0.03	2.31
	(0.03)		(0.02)		(0.03)		(0.02)		(0.05)		(0.03)	
SP500	−0.05**	3.96	−0.10***	3.94	0.04*	0.11	0.01	0.01	−0.06**	0.12	−0.04	−0.05
	(0.02)		(0.03)		(0.02)		(0.02)		(0.03)		(0.03)	
Const.	1.50***		2.16***		−0.90***		−0.11		−1.11***		−0.25	
	(0.32)		(0.38)		(0.19)		(0.22)		(0.24)		(0.25)	
R^2	55.52		47.27		36.66		51.53		40.86		59.57	

Table VII
Option Dislocations and Intermediary Frictions: Instrumental Variable Approach

This table repeats the analysis of Table VI using an instrumental variable (IV) approach to address potential endogeneity concerns arising from the fact that time variation in frictions in the SPX option market and ES futures market (the primary hedging instrument) may be correlated. We instrument *ESF*, the spread between the forward interest rate implied by the S&P 500 E-Mini futures and the three-month OIS rate, using the corresponding spread for the Russell 2000 E-Mini futures. Since the latter are only available from 2017/07, the sample period is from 2017/07 to 2023/12.

	$\widehat{\alpha}_{b(i),t}$											
	0DTE				1–3DTE				4–15DTE			
	Puts		Calls		Puts		Calls		Puts		Calls	
	Coef.	$R^2_{\text{univ.}}$	Coef.	$R^2_{\text{univ.}}$	Coef.	$R^2_{\text{univ.}}$	Coef.	$R^2_{\text{univ.}}$	Coef.	$R^2_{\text{univ.}}$	Coef.	$R^2_{\text{univ.}}$
ESF	−0.14**	1.41	−0.17***	1.38	−0.09**	0.55	−0.14***	0.45	−0.05	0.67	−0.07*	1.05
	(0.05)		(0.06)		(0.04)		(0.03)		(0.04)		(0.04)	
HKM	0.08	3.48	0.12**	4.92	0.15***	11.04	0.29***	23.06	0.02	8.59	0.13***	17.56
	(0.05)		(0.06)		(0.04)		(0.03)		(0.04)		(0.04)	
ε_{HKM}	0.02	3.57	0.08***	3.09	0.00	0.42	−0.04	0.02	−0.02	0.46	−0.10	0.17
	(0.03)		(0.03)		(0.03)		(0.06)		(0.04)		(0.08)	
CIV	−0.51***	43.11	−0.59***	42.61	−0.63***	53.61	−0.65***	55.64	−0.70***	54.30	−0.72***	59.30
	(0.09)		(0.13)		(0.10)		(0.07)		(0.10)		(0.07)	
OI	−0.30***	26.31	−0.06**	0.32	−0.17***	15.30	−0.02	−0.06	−0.07	13.14	−0.02	4.99
	(0.03)		(0.02)		(0.03)		(0.02)		(0.05)		(0.03)	
SP500	0.05**	4.11	0.10***	3.99	0.07***	0.74	0.03	−0.06	0.09***	0.67	0.04	−0.04
	(0.02)		(0.03)		(0.02)		(0.02)		(0.02)		(0.03)	
Const.	−1.16***		−1.83***		0.23		−1.41***		0.77***		−0.49**	
	(0.31)		(0.38)		(0.22)		(0.18)		(0.27)		(0.24)	
R^2	52.53		45.61		57.92		62.83		55.14		61.29	

	$\lvert\widehat{\alpha}_{b(i),t}\rvert$											
	0DTE				1–3DTE				4–15DTE			
	Puts		Calls		Puts		Calls		Puts		Calls	
	Coef.	$R^2_{\text{univ.}}$	Coef.	$R^2_{\text{univ.}}$	Coef.	$R^2_{\text{univ.}}$	Coef.	$R^2_{\text{univ.}}$	Coef.	$R^2_{\text{univ.}}$	Coef.	$R^2_{\text{univ.}}$
ESF	0.14**	1.48	0.17***	1.36	−0.09**	−3.64	−0.01	−0.61	−0.09*	−1.03	0.00	1.48
	(0.05)		(0.06)		(0.04)		(0.05)		(0.05)		(0.04)	
HKM	−0.08*	3.93	−0.13**	5.22	0.32***	0.98	0.07*	2.89	0.23***	0.79	0.01	9.14
	(0.05)		(0.06)		(0.03)		(0.04)		(0.04)		(0.04)	
ε_{HKM}	−0.01	3.52	−0.08***	2.99	0.05	0.44	0.10	0.49	0.07	−0.05	0.11	0.16
	(0.03)		(0.03)		(0.03)		(0.07)		(0.05)		(0.09)	
CIV	0.53***	46.09	0.60***	43.79	0.72***	29.41	0.77***	55.12	0.77***	41.56	0.80***	59.89
	(0.10)		(0.13)		(0.06)		(0.05)		(0.09)		(0.07)	
OI	0.30***	27.21	0.05**	0.30	−0.22***	−0.04	0.00	−0.06	−0.03	7.23	0.04	2.50
	(0.03)		(0.02)		(0.03)		(0.02)		(0.05)		(0.03)	
SP500	−0.06**	4.31	−0.10***	4.07	0.03	0.07	0.00	−0.01	−0.06**	0.14	−0.04	−0.06
	(0.03)		(0.03)		(0.02)		(0.02)		(0.03)		(0.03)	
Const.	1.29***		1.91***		−0.76***		0.01		−0.95***		−0.16	
	(0.32)		(0.39)		(0.20)		(0.21)		(0.25)		(0.24)	
R^2	55.74		46.87		42.75		56.22		45.48		61.08	

Table VIII
Statistics Summary of Self-financing Six-factor-neutral Portfolio Returns

This table reports the summary statistics of the risk-factor-neutral returns of 0DTE options hedged by instrument option contracts using self-financing strategy and the returns of longing ES futures. The "Object" column indicates the return type. "T" (for target) denotes DLT-hedged returns of 0DTE options without additional hedging; "H" denotes returns on the instrument option contracts used for hedging; and "N" denotes six-factor-neutral portfolio returns obtained by hedging 0DTE options with the instrument contracts using a self-financing strategy. The hedging procedure described in Section 5.6 is implemented for each individual 0DTE put and call contract, within each moneyness bucket (ATM ,OTM, DOTM), at each 30-min timestamp. The factor-neutral returns of option i are averaged cross-sectionally and then over time. The (e.g.) mean return reported below is then calculated by $\frac{1}{T}\sum_{t\in T}\frac{1}{n_t}\sum_{i\in n_t} r^N_{i,t}$. All the statistics are reported in percent per annum (multiplied by $252 \times 100(\sqrt{252} \times 100)$). The sample period is from 2016/09 to 2023/12.

		Puts						Calls					
Mny	Object	Mean	SD	SR	25th	50th	75th	Mean	SD	SR	25th	50th	75th
ATM	T	-0.63^{***}	0.50	-1.27	-3.58	-1.48	0.81	-0.55^{***}	0.55	-1.00	-3.91	-1.60	1.08
	H	0.48^{***}	0.73	0.66	-2.15	1.13	4.26	0.43^{***}	0.81	0.53	-2.34	1.24	4.74
	N	-0.15^{**}	0.59	-0.25	-2.70	-0.17	2.49	-0.12	0.66	-0.18	-2.93	-0.12	2.73
OTM	T	-0.36^{***}	0.33	-1.09	-2.08	-0.95	0.24	-0.50^{***}	0.45	-1.09	-3.31	-1.44	0.86
	H	0.23^{***}	0.54	0.42	-1.83	0.78	3.23	0.39^{***}	0.67	0.58	-1.89	1.04	3.76
	N	-0.13^{**}	0.44	-0.29	-2.21	-0.10	2.11	-0.11	0.56	-0.19	-2.32	-0.11	2.18
DOTM	T	-0.19^{***}	0.15	-1.23	-0.91	-0.41	0.06	-0.30^{***}	0.23	-1.31	-1.39	-0.58	0.20
	H	0.12^{**}	0.35	0.34	-1.31	0.40	2.04	0.25^{***}	0.42	0.60	-1.13	0.55	2.21
	N	-0.07^{*}	0.30	-0.23	-1.54	0.06	1.61	-0.05	0.36	-0.12	-1.38	0.06	1.46

Appendix A. Data

Our dataset comprises high-frequency records of quotes of S&P 500 Index options from September 2016 to December 2023. We obtain this data from the Chicago Board Options Exchange (CBOE)'s Option Intervals dataset, which includes option quotes aggregated to a 1-minute frequency alongside synchronized intraday records of the underlying S&P 500 index. We use the midpoint of the high-frequency quotes as the option price and then compute returns over thirty-minute intervals. Since the S&P 500 index is costly to replicate at a high frequency, we use the E-mini S&P 500 (ES) futures as the tradable hedging asset; these are the most actively traded futures on the S&P 500 index. We obtain the millisecond-frequency quotes for ES futures from Tickdata Inc. Finally, we obtain risk-free rates from the Fama-French Data Library.[1] We assume that the risk-free rates remain constant across all timestamps within each day.

To study the performance of investments in short-term, continuously hedged options, we construct an investment period which starts 15 business days before expiration and ends at expiration. We avoid irregular option quotes and anomalies in bid-ask spreads shortly after the market opens by setting 9:45 a.m. ET as the time of the first trade, and 3:45 p.m. ET as the time of the last trade to demarcate the intraday and overnight periods. To reduce the impact of microstructure noise, we subsample these datasets at a 30-minute frequency.

Throughout this period, whenever an option contract satisfies the selection conditions stated below, it is considered to be held by an investor for the next 30-minute or overnight period. We only consider PM-settled options. For each option position with 15 or fewer DTE the first 30-minute or overnight return included in our sample is the earliest interval in which the option has positive trading volume and a positive bid price at the outset, and is neither in-the-money (ITM)[2] nor extremely deep out-of-the-money (DOTM)[3] indicating real trading activity. Subsequently, we do not require the option to have positive trading volume at the start of each 30-minute or overnight interval. Once the option becomes ITM or extreme DOTM, the investment position is assumed to be closed and the option is excluded from the sample. However, it may re-enter the sample if it satisfies the prior conditions again.

Finally, we track an option's value until expiration in the following manner. If the option has a positive bid price at the end of each trading period, we keep all 30-minute and overnight returns satisfying prior criteria, and calculate the final return at expiration using the (potentially zero) settlement payoff of the option. If the option's bid price reaches zero prior to expiration, we apply the following procedure: we track all trading periods where the

[1] See https://mba.tuck.dartmouth.edu/pages/faculty/ken.french/data_library.html

[2] The trading of short-term options is skewed toward OTM options (Andersen, Fusari, and Todorov, 2017). We keep options with $\kappa_{t,\tau} > -0.5$ for calls and $\kappa_{t,\tau} \leq 1$ for puts where $\kappa_{t,\tau}$ is the relative strike with maturity τ at time t as defined in Section C.

[3] We exclude the options in the 1% extreme left and right tails, due to their illiquidity and lack of meaningful informational content. The tail ratio and strike boundary are defined in Section B.

start-of-period bid price is positive and the end-of-period bid price is zero; in the last such period before expiration, we consider the option to become valueless, i.e., we consider the investor writes the option off and realizes a -100% raw return on the option; in prior such periods, we use half of the ask price to calculate returns.

Appendix B. Local Variance Proxy

The implementation of our model requires proxies of market variance at all maturities. This proxy has two uses: first, it serves as a normalization factor for option moneyness (in Section C); second, we use its high-frequency evolution to decompose variance dynamics into three orthogonal components. Whereas the the VIX index calculated at selected maturities is an obvious candidate, Andersen, Bondarenko, and Gonzalez-Perez (2015) highlight sudden fluctuations in the high-frequency VIX series due to the cut-off rule for including options in the VIX calculation used by the CBOE. Following their work, we employ the square of the model-free corridor implied variance (CIV) index as the expected market variance measure. For option time to expiration τ, CIV is defined as

$$CIV = 2e^{r\tau}\left[\int_{\kappa_L}^{F_0} \frac{P_{t,\tau}(K)}{K^2}dK + \int_{F_0}^{\kappa_H} \frac{C_{t,\tau}(K)}{K^2}dK\right] \times \frac{252}{\tau} \tag{B1}$$

where $P_{t,\tau}(K)$ and $C_{t,\tau}(K)$ are put and call prices with strike K and time to expiration τ at time t respectively, and to compute it we must define the boundary strikes κ_L and κ_H.

To compute the CIV at each timestamp t, we first select all options with maturity τ. Then, we select all OTM options with positive bid quotes.[4] We determine the strike truncation level with the use of the following ratio statistic $R_{t,\tau}(K)$:

$$R_{t,\tau}(K) := \frac{P_{t,\tau}(K)}{P_{t,\tau}(K) + C_{t,\tau}(K)} \tag{B2}$$

which naturally runs from zero to one across the strike range for a fixed time to expiration. To maximize data retention, we set the constant 1% cut-off level; this ensures valid quotes spanning the corridor in each high-frequency interval. Then we set the lower integration boundary to $\kappa_L = R_{t,\tau}(K)^{-1}(0.01)$ and the upper boundary to $\kappa_H = R_{t,\tau}(K)^{-1}(0.99)$, which also serves as our criterion for identifying the extreme DOTM options, as described in prior sample selection conditions.

[4]We define OTM as $\frac{K}{F_t} \geq 1$ for calls and $\frac{K}{F_t} \leq 1$ for puts where K represents the strike and F_t is the forward price at time t.

Appendix C. Option Time to Expiration and Moneyness

These two quantities are key inputs to our modeling of option exposures. With our focus on intraday option return dynamics, we carefully describe their calculation in this section.

First, in the calculation of time to expiration (TTE) we account for the intraday passage of time. We define the days to expiration (DTE) in terms of business days, treating the period from Friday to Monday as a single business day. Then we measure the intraday time change by the duration in seconds between each timestamp and the option market's official closing time on each date.[5] This duration is further divided by 24×3600 to obtain a fraction representing the portion of one day. We add this intraday time duration to the DTE to compute the total TTE, which subsequently yields the annualized time to expiration, $\tau = TTE/252$.

To account for the fact that investors trade narrower strike ranges as options approach expiration, we adjust the logarithmic moneyness by incorporating volatility and define moneyness as:

$$\kappa_{t,\tau} = \frac{\ln\left(K/F_{t,\tau}\right)}{\sqrt{\tau CIV_{t,\tau}}} \tag{C3}$$

where CIV is the maturity-specific aggregate market variance proxy which captures the market conditions, described in Section B, $F_{t,\tau}$ is the forward price of the index computed from put-call parity using ATM option pairs, $F_{t,\tau} = K_{ATM} + e^{r\tau}(C_{t,\tau}(K_{ATM}) - P_{t,\tau}(K_{ATM}))$, at time t with time to expiration τ.

Considering the narrower moneyness ranges for calls, as shown in Figure A.I, we divide moneyness into finer intervals for calls in our analysis. We define at-the-money (ATM) puts (calls) as $-1 < \kappa_{t,\tau} \leq 1$ ($-0.5 < \kappa_{t,\tau} \leq 0.5$), OTM puts (calls) as $-2.2 < \kappa_{t,\tau} \leq -1$ ($0.5 < \kappa_{t,\tau} \leq 1$), and DOTM puts (calls) as $\kappa_{t,\tau} \leq -2.2$ ($\kappa_{t,\tau} > 1$).

Appendix D. Spot-futures Spread

To proxy for liquidity conditions in the underlying futures market, we follow Siriwardane, Sunderam, and Wallen (2025) and construct the spot-futures spread, defined as the difference between the forward rate implied by the futures and the 3-month OIS swap rate.

Let F_{t,τ_1} and F_{t,τ_2} denote, respectively, the nearby and first-deferred futures prices at date t, with maturities $\tau_1 < \tau_2$. Under no-arbitrage condition, the implied forward rate yields

$$f_t^{\tau_1,\tau_2} = \left(\frac{F_{t,\tau_2} + \mathbb{E}_t^Q[D_{t,\tau_2}]}{F_{t,\tau_1} + \mathbb{E}_t^Q[D_{t,\tau_1}]} - 1\right)\frac{1}{\tau_2 - \tau_1} \tag{D4}$$

where $\mathbb{E}t^Q[D_{t,\tau}]$ denotes the risk-neutral expectation of cumulative dividends over $[t, t+\tau]$.

[5] We use the real option expiration time (4:00 p.m.) to calculate the accurate time to expiration in seconds.

We implement this construction for S&P 500 E-mini (ES) and Russell 2000 E-mini (RUT) futures using the nearby and first-deferred contract close prices at 16:15 ET on each day. ES futures prices are obtained from TickData Inc., and RUT futures prices are obtained from Bloomberg. Following Siriwardane, Sunderam, and Wallen (2025), we proxy for $\mathbb{E}_t^Q[D_{t,\tau}]$ using realized dividends, obtained from Bloomberg. We compute the future values of dividends using the risk-free rate, measured by SOFR; missing observations are filled using LIBOR. Finally, the spot-futures spread is defined as the difference between the implied forward rate and the 3-month OIS swap rate:

$$ESF_t = f_t^{\tau_1,\tau_2} - OIS_t^{3M} \tag{D5}$$

where all the interest-rate series are obtained from Bloomberg. Figure A.II plots the *ESF* series.

Appendix E. Robustness of the Dislocation Regressions

Section 5.4 discusses the economic mechanisms behind the time-series variation in option price dislocations. In particular, Table VI reports results for dislocations and their magnitudes in ATM options with different maturities.

We here provide evidence that those results are robust along the moneyness dimension, as evidenced by Tables A.V (for OTM options), and A.VI (for DOTM options).

In Tables A.VII to A.IX, we also address a concern that dislocations could be mechanically related to the day's underlying return, *o2c*, via our estimation process. We split the *SP500* variable into two components: the return from market open until 14:45 ET ($SP500_{[09:45,14:45]}$) and from 14:45 to 15:15 ET ($SP500_{[14:45,15:15]}$). The return in the last 30 minutes of trading before dislocation measurement is not significant in any of the regressions, except for certain DOTM put cases, where it's only significant at the 10% level. Negative market returns are associated with a decrease in alphas of 0DTE options of both types, and of longer-maturity puts, with the changes much larger in 0DTEs, and with the highest explanatory power in this bucket–up to 4%, vs. below 1% in longer maturities. In other words, options become more expensive when the market declines. The magnitude of 0DTE mispricing also increases on down days, with patterns broadly similar to those for the level of dislocations.

Figure A.I. The Distribution Density of Moneyness

The figure displays the Gaussian kernel-estimated density of option moneyness, defined as $\kappa_{t,\tau} = \frac{\log(K/F)}{\sqrt{\tau CIV_{t,\tau}}}$, for our sample across three maturity groups (0DTE, 1–3DTE, and 4–15DTE) at three intraday timestamps. The left column shows the moneyness density for puts, while the right column shows the corresponding densities for calls. Each row corresponds to a different intraday time: 9:45, 12:15, and 15:15 ET, respectively. The sample period is from 2016/09 to 2023/12.

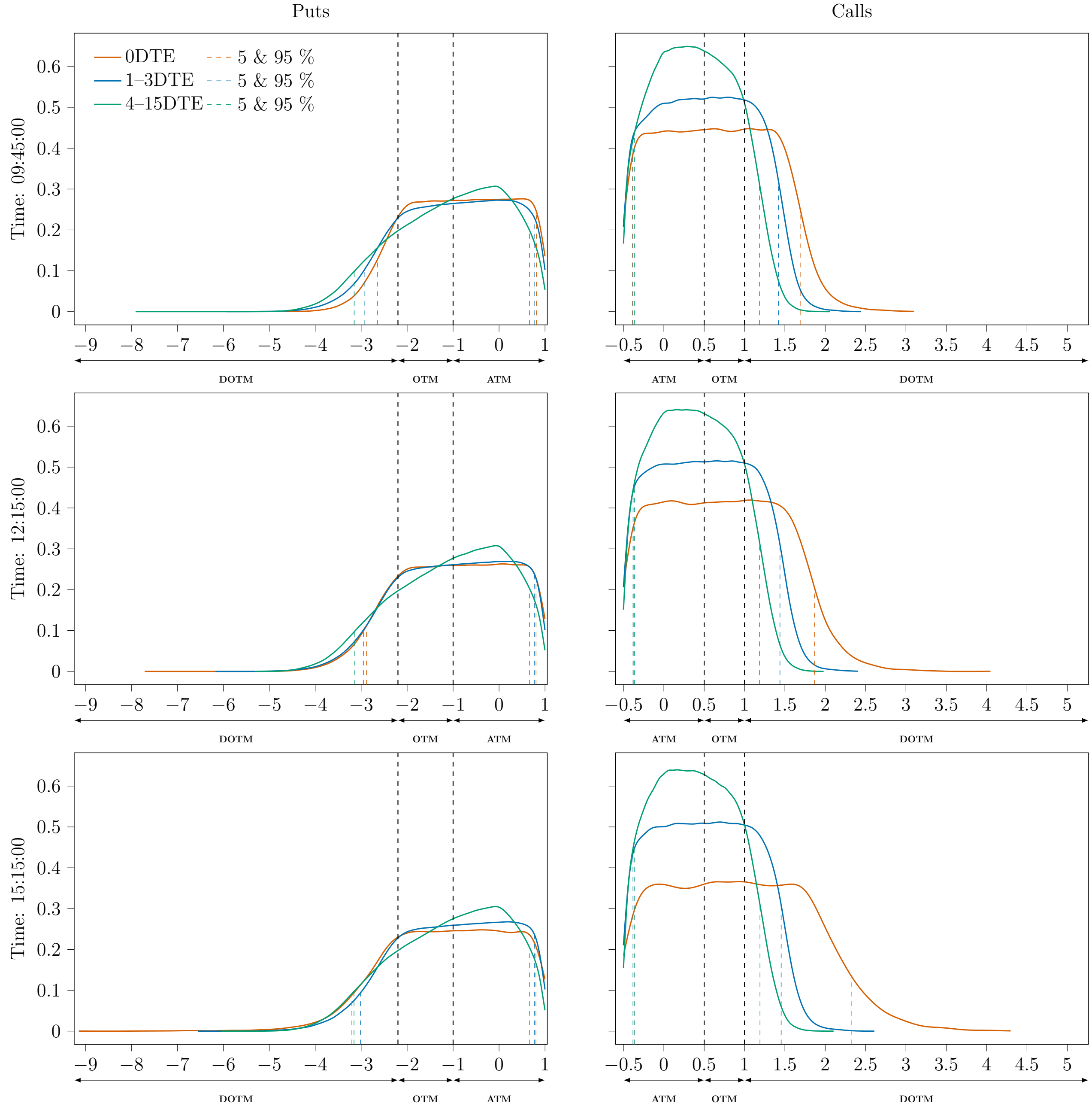

Figure A.II. Time-series of ESF (bps)

The figure plots the time-series of the daily spot-futures spread, *ESF*, in basis points (bps). The spot-futures spread is the spread between the forward interest rate implied by futures and the three-month OIS rate, as in Siriwardane, Sunderam, and Wallen (2025) and Appendix D, estimated using futures prices at the futures closing time, 16:15 ET. The blue line represents the *ESF* estimated using S&P 500 E-Mini futures, while the orange line represents the *ESF* estimated using Russell 2000 E-Mini futures. The latter are only available from 2017/07. The sample period is from 2016/09 to 2023/12.

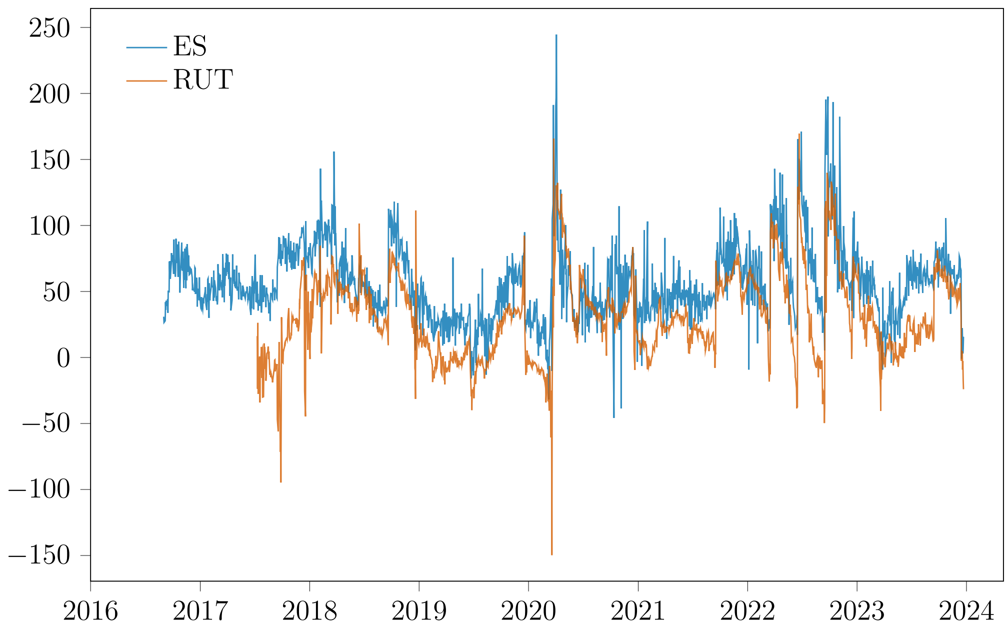

Table A.I
Summary Statistics of Intraday 0DTE DLT-hedged Delevered Returns

The table reports the summary statistics of 0DTE intraday delevered returns at each 30-minute interval. The number of observations is labeled as N. The table reports the average return (Mean), 25th percentile, median (50th), and 75th percentile, all reported in percent per annum (multiplied by 12×252). We delta-hedge the options with the S&P 500 E-Mini futures returns as in equation (2). The option delta, $\widehat{\beta}_{\mathrm{DLT},i,t}$, is estimated using the factor model described in Section 3. The sample period is from 2016/09 to 2023/12.

	Puts					Calls				
Time	N	Mean	25th	50th	75th	N	Mean	25th	50th	75th
10:15:00	23,034	-11.17^{***}	-56.14	-18.92	9.73	14,361	-14.93^{***}	-61.24	-20.48	15.96
10:45:00	21,569	-10.95^{***}	-46.09	-16.38	6.45	13,531	-12.03^{***}	-49.45	-17.17	9.25
11:15:00	20,272	-5.25^{***}	-38.49	-13.15	7.89	12,691	-4.76^{*}	-42.27	-13.99	10.74
11:45:00	19,167	3.38	-33.11	-10.11	10.24	12,045	0.29	-35.38	-11.79	9.32
12:15:00	18,237	-5.81^{***}	-33.73	-11.05	5.76	11,490	-5.59^{***}	-35.04	-12.75	6.99
12:45:00	17,241	-2.66^{*}	-30.07	-9.40	6.60	10,946	-0.37	-29.44	-9.73	8.57
13:15:00	16,321	-5.42^{***}	-30.36	-8.75	7.05	10,431	-6.64^{***}	-30.77	-9.60	8.13
13:45:00	15,517	1.63	-26.57	-7.48	8.86	9,894	1.96	-27.46	-8.63	9.43
14:15:00	14,625	-12.53^{***}	-36.60	-11.37	4.41	9,390	-9.51^{***}	-39.01	-12.46	6.27
14:45:00	13,379	-6.51^{**}	-41.06	-14.58	1.55	8,649	-10.58^{***}	-41.54	-14.24	5.13
15:15:00	11,831	-6.80^{**}	-44.75	-15.70	1.63	7,779	-0.48	-50.04	-14.76	8.57
15:45:00	9,535	-31.60^{***}	-78.81	-24.90	-2.54	6,535	-26.63^{***}	-77.68	-21.68	2.65

$\star$ denotes statistically significant difference from zero at the 10% level, $\star\star$ at the 5% level, and $\star\star\star$ at the 1% level.

Table A.II
Incremental Explanatory Power of Higher-order Factors Estimated per Each Maturity

We start from a baseline five-factor model that includes the risk factors: DLT, GAM, dSV, dVRP, dTRM. This table reports the incremental $R^2\%$ of the higher-order risk factor in addition to the baseline five-factor model for delevered option returns, estimated separately for each maturity from 0DTE to 15DTE. The R square is defined as

$$R^2\% = \left[1 - \frac{\sum_{i,t}\left(r_{i,t+1} - \left(\widehat{c}_{i,t} + \sum_l \widehat{\beta}_{l,i,t} f_{l,t+1}\right)\right)^2}{\sum_{i,t}(r_{i,t+1})^2}\right] \times 100,$$

where $\widehat{c}_{i,t}$ is the factor model's conditional intercept for each option, i, and $\widehat{\beta}_{i,l,t}$ is the estimated option exposure to higher-order risk factor l. The 5F^{Base} column represents the total $R^2\%$ explained by the baseline five-factor model. The risk factors associated with vanna are set to the production of DLT and the two components of the variance risk factors: VaS, computed as DLT $\times$ dSV, and VaV, computed as DLT $\times$ dVRP, respectively. Similarly, the risk factors associated with volga are set to the two squared components of the variance risk factors: VlS, measured as dSV^2, and VlV,measured as dVRP^2, respectively. JSK and dS4 represent the third- and fourth-order risks measured by the cubic and quadratic E-mini futures returns, respectively. Each factor reports the incremental $R^2\%$ in addition to the baseline five-factor model. The $R^2\%$ are reported for aggregates 0, 1–3, 4–15 DTEs and moneyness groups. The moneyness is defined as $\kappa_{t,\tau} = \frac{ln(K/F_{t,\tau})}{\text{CIV}_{t,\tau}\sqrt{\tau}}$, where $\text{CIV}_{t,\tau}$ is the corridor implied volatility with maturity τ. We divide options into six moneyness groups: DOTM puts (calls) for $\kappa_{t,\tau} \leq -2.2(\kappa_{t,\tau} > 1)$, OTM puts (calls) for $-2.2 < \kappa_{t,\tau} \leq -1(-0.5 < \kappa_{t,\tau} \leq 1)$ and ATM puts (calls) for $-1 < \kappa_{t,\tau} \leq 1(-0.5 < \kappa_{t,\tau} \leq 0.5)$. The sample period is from 2016/09 to 2023/12.

		Puts							Calls						
Moneyness	DTE	5F^{Base}	Δ_+VaS	Δ_+VlS	Δ_+VaV	Δ_+VlV	Δ_+JSK	Δ_+dS4	5F^{Base}	Δ_+VaS	Δ_+VlS	Δ_+VaV	Δ_+VlV	Δ_+JSK	Δ_+dS4
All	All	99.0	0.0	0.0	0.0	0.0	0.0	0.0	97.9	0.1	0.1	0.1	0.1	0.1	0.0
	0	97.8	0.1	0.0	0.0	0.1	0.2	0.0	96.3	0.2	0.2	0.1	0.1	0.3	0.1
	1–3	98.8	0.0	0.0	0.0	0.1	0.1	0.0	97.8	0.1	0.1	0.1	0.1	0.2	0.1
	4–15	99.1	0.0	0.0	0.0	0.0	0.0	0.0	98.0	0.1	0.0	0.1	0.1	0.1	0.0
ATM	All	99.1	0.0	0.0	0.0	0.0	0.0	0.0	98.6	0.0	0.0	0.1	0.1	0.0	0.0
	0	98.3	0.0	0.0	0.0	0.0	0.1	0.0	97.7	0.1	0.1	0.0	0.1	0.0	0.1
	1–3	99.0	0.0	0.0	0.0	0.1	0.0	0.0	98.5	0.1	0.1	0.1	0.1	0.0	0.0
	4–15	99.2	0.0	0.0	0.0	0.0	0.0	0.0	98.7	0.0	0.0	0.1	0.1	0.0	0.0
OTM	All	96.9	0.0	0.0	0.0	0.1	0.1	0.0	92.5	0.4	0.3	0.4	0.3	0.9	0.2
	0	84.5	0.8	0.8	0.7	0.9	2.2	0.1	91.5	0.6	0.5	0.3	0.2	0.8	0.4
	1–3	94.9	0.1	0.0	0.2	0.3	0.5	0.1	93.3	0.6	0.3	0.6	0.4	0.7	0.3
	4–15	97.5	0.0	0.0	0.0	0.0	0.0	0.0	92.3	0.4	0.3	0.4	0.2	0.9	0.2
DOTM	All	72.9	0.3	0.3	0.4	−0.2	9.7	0.9	67.2	0.8	0.5	0.8	0.0	7.3	0.9
	0	31.8	0.5	−2.1	4.2	2.3	29.4	−2.0	63.4	2.7	1.7	0.6	−0.3	6.9	1.3
	1–3	42.9	1.1	0.8	1.6	0.4	25.4	3.0	74.1	1.1	0.4	0.5	−0.1	5.3	0.9
	4–15	78.9	0.2	0.3	0.1	−0.4	6.6	0.5	64.1	0.3	0.4	1.0	0.1	8.4	0.8

Table A.III
Correlation Matrix of Physical Risk Factors and Risk-neutral Expectations

The table presents the correlation matrices for risk factors under the physical values and conditional risk-neutral expectations. DLT is the market risk measured by the E-mini futures return. GAM denotes the gamma risk factor, computed by the squared DLT. The variance risk factors are decomposed to three components: (i) dSV denotes the change in spot variance proposed by Todorov (2019). (ii) dVRP captures the change in the difference between average expected variance, CIV_{2_+DTE}, at the two shortest available maturities, satisfying DTE $>$ 2 and calendar maturity $>$ 4 and the corresponding spot variance, $\text{dVRP} = (CIV_{2_+DTE,t+1} - \text{SV}_{\text{t+1}}) - (CIV_{2_+DTE,t} - \text{SV}_{\text{t}})$. (iii) dTRM represents the shifts in the term structure of CIV_τ: $\text{dTRM} = (CIV_{15DTE,t+1} - CIV_{2_+DTE,t+1}) - (CIV_{15DTE,t} - CIV_{2_+DTE,t})$, where CIV_{15DTE} denotes the CIV with the longest available maturity. The aggregated variance risk factor, dVAR, is the sum of the three variance components: $\text{dVAR} = \text{dSV} + \text{dVRP} + \text{dTRM}$. JSK is the cubic return of the S&P 500 E-mini futures, defined as $\text{dS3} = \text{DLT}^3$. The conditional risk-neutral expectations, μ_t^Q, are estimated from the cross-sectional regression, as specified in equation (13), by regressing the six-factor model conditional intercepts on estimated exposures at each 30-minute timestamp for puts and calls, respectively. The risk-neutral expectation of aggregated variance is also the sum of expectations of the three variance components: $\mu^Q_{\text{dVAR}} = \mu^Q_{\text{dSV}} + \mu^Q_{\text{dVRP}} + \mu^Q_{\text{dTRM}}$. The sample period is from 2016/09 to 2023/12.

	DLT	GAM	dSV	dVRP	dTRM	JSK	dVAR
DLT	1.00						
GAM	0.04	1.00					
dSV	−0.56	−0.08	1.00				
dVRP	−0.38	−0.07	0.44	1.00			
dTRM	0.41	0.09	−0.80	−0.81	1.00		
JSK	0.42	0.37	−0.50	−0.36	0.45	1.00	
dVAR	−0.65	−0.08	0.80	0.81	−0.80	−0.51	1.00

Puts

	μ^Q_{DLT}	μ^Q_{GAM}	μ^Q_{dSV}	μ^Q_{dVRP}	μ^Q_{dTRM}	μ^Q_{JSK}	μ^Q_{dVAR}
μ^Q_{DLT}	1.00						
μ^Q_{GAM}	−0.16	1.00					
μ^Q_{dSV}	0.43	−0.68	1.00				
μ^Q_{dVRP}	−0.06	−0.35	0.04	1.00			
μ^Q_{dTRM}	−0.19	0.49	−0.72	−0.49	1.00		
μ^Q_{JSK}	−0.06	−0.59	0.48	−0.26	−0.23	1.00	
μ^Q_{dVAR}	0.27	−0.74	0.56	0.70	−0.46	0.06	1.00

Calls

	μ^Q_{DLT}	μ^Q_{GAM}	μ^Q_{dSV}	μ^Q_{dVRP}	μ^Q_{dTRM}	μ^Q_{JSK}	μ^Q_{dVAR}
μ^Q_{DLT}	1.00						
μ^Q_{GAM}	−0.15	1.00					
μ^Q_{dSV}	0.24	−0.74	1.00				
μ^Q_{dVRP}	−0.54	0.02	−0.27	1.00			
μ^Q_{dTRM}	0.13	0.35	−0.57	−0.39	1.00		
μ^Q_{JSK}	0.01	−0.45	0.43	−0.37	−0.12	1.00	
μ^Q_{dVAR}	−0.28	−0.62	0.45	0.62	−0.45	−0.02	1.00

Table A.IV
Explanatory Power of DLT and Aggregated Six Factors for Unhedged Delevered Option Returns

This table reports the explanatory power of the S&P E-Mini futures returns (DLT) and the full model with six risk factors to delevered intraday returns of S&P 500 index options with maturity from 0DTE to 15DTE, estimated separately for each maturity. The R square of DLT is defined as

$$R^2_{\text{DLT}}\% = \left[1 - \frac{\sum_{i,t}\left(r_{i,t+1} - \widehat{\beta}_{\text{DLT},i,t}\text{DLT}_{t+1}\right)^2}{\sum_t (r_{i,t+1})^2}\right] \times 100$$

The exposure of DLT, $\widehat{\beta}_{\text{DLT},i,t}$, is estimated from the six-factor model. Any $\widehat{\beta}_{\text{DLT},i,t}$ with an incorrect sign is set to zero, which means the negative delta for calls and positive delta for puts. The R square of the six-factor model is defined as

$$R^2\% = \left[1 - \frac{\sum_{i,t}\left(r_{i,t+1} - \left(\widehat{c}_{i,t} + \sum_l \widehat{\beta}_{l,i,t} f_{l,t+1}\right)\right)^2}{\sum_{i,t} (r_{i,t+1})^2}\right] \times 100,$$

where $\widehat{c}_{i,t}$ is the factor model's conditional intercept for each option, i, and $\widehat{\beta}_{i,l,t}$ is the estimated option exposure to factor l. The risk factors l include: DLT, GAM, dSV, dVRP, dTRM, JSK. The $R^2\%$ are reported for aggregates 0, 1–3, 4–15 DTEs and moneyness groups. The moneyness is defined as $\kappa_{t,\tau} = \frac{ln(K/F_{t,\tau})}{\text{CIV}_{t,\tau}\sqrt{\tau}}$, where $\text{CIV}_{t,\tau}$ is the corridor implied volatility with maturity τ. We divide options into six moneyness groups: DOTM puts (calls) for $\kappa_{t,\tau} \leq -2.2(\kappa_{t,\tau} > 1)$, OTM puts (calls) for $-2.2 < \kappa_{t,\tau} \leq -1(-0.5 < \kappa_{t,\tau} \leq 1)$ and ATM puts (calls) for $-1 < \kappa_{t,\tau} \leq 1(-0.5 < \kappa_{t,\tau} \leq 0.5)$. The sample period is from 2016/09 to 2023/12.

		Puts		Calls	
Moneyness	DTE	DLT	6F	DLT	6F
All	All	93.9	99.1	86.3	98.1
	0	93.2	98.0	89.4	96.6
	1–3	94.9	98.9	89.4	97.9
	4–15	93.8	99.1	85.6	98.1
ATM	All	94.7	99.1	90.8	98.7
	0	94.3	98.4	92.1	97.8
	1–3	95.8	99.0	93.2	98.6
	4–15	94.6	99.2	90.4	98.7
OTM	All	67.8	97.0	43.3	93.4
	0	56.7	86.6	74.5	92.3
	1–3	69.0	95.3	62.1	94.1
	4–15	67.8	97.5	38.5	93.2
DOTM	All	25.2	82.7	−7.5	74.5
	0	16.7	61.2	48.6	70.3
	1–3	18.5	68.4	4.0	79.4
	4–15	26.5	85.6	−22.9	72.6

Table A.V
OTM Option Dislocations and Intermediary Frictions

The table reports the coefficients and R^2 of the regressions of OTM option dislocations measured at 15:45 ET on variables related to frictions faced by financial intermediaries and on controls. The top panel reports the results for dislocations, $\widehat{\alpha}_{b(i),t}$, while the bottom panel reports the results for absolute dislocations, $|\widehat{\alpha}_{b(i),t}|$. The dislocations are estimated as bucket-level fixed effects in cross-sectional regressions of the conditional intercepts on option exposures (as in equation (16)) for puts and calls, at each 30-minute timestamp. *SP500* is the intraday return of the S&P 500 ES futures from 9:45 ET to 15:15 ET on the current day. *HKM* is the level of the aggregate market equity ratio of primary dealers at the end of the previous day as defined by He, Kelly, and Manela (2017). ε_{HKM} proposed therein is the AR(1) innovation to the capital ratio, scaled by the lagged ratio, on the current day. *ESF* is the spread between the forward interest rate implied by the S&P 500 E-Mini futures and the three-month OIS rate, as in Siriwardane, Sunderam, and Wallen (2025) and Appendix D, estimated using futures prices at the futures closing time, 16:15 ET, of the previous day. *OI* is the open interest of all the puts (calls) within each bucket at the end of the previous day. CIV^2 is the corridor implied variance calculated from options with the given maturity at 15:15 ET on the current day. For each combination of option maturity and type, the table reports the estimated coefficients, their robust standard errors (in parentheses) and adjusted R^2 (in %) in the first column, and the $R^2_{\text{univ.}}$ (in %) from a univariate regression in the second column. All the variables are normalized using their full-sample standard deviations. The sample period is from 2016/09 to 2023/12.

	$\widehat{\alpha}_{b(i),t}$											
	0DTE				1–3DTE				4–15DTE			
	Puts		Calls		Puts		Calls		Puts		Calls	
	Coef.	$R^2_{\text{univ.}}$	Coef.	$R^2_{\text{univ.}}$	Coef.	$R^2_{\text{univ.}}$	Coef.	$R^2_{\text{univ.}}$	Coef.	$R^2_{\text{univ.}}$	Coef.	$R^2_{\text{univ.}}$
ESF	−0.07	1.17	−0.10**	1.54	0.02	0.09	−0.10***	1.91	0.01	0.61	−0.05	1.76
	(0.05)		(0.05)		(0.03)		(0.02)		(0.03)		(0.03)	
HKM	0.06	3.39	0.12**	5.00	0.03	5.82	0.27***	23.78	0.01	9.08	0.13***	20.29
	(0.05)		(0.06)		(0.04)		(0.03)		(0.04)		(0.04)	
ε_{HKM}	0.02	3.32	0.11***	4.18	−0.03	−0.04	−0.03	−0.03	−0.03	0.22	−0.09	0.06
	(0.03)		(0.03)		(0.02)		(0.04)		(0.03)		(0.07)	
CIV	−0.59***	48.99	−0.62***	46.62	−0.65***	46.16	−0.69***	61.29	−0.71***	50.32	−0.74***	62.98
	(0.11)		(0.14)		(0.06)		(0.07)		(0.07)		(0.08)	
OI	−0.28***	19.93	−0.07***	2.05	−0.11***	4.36	−0.03**	1.08	−0.02	−0.05	0.01	0.09
	(0.03)		(0.02)		(0.03)		(0.01)		(0.02)		(0.02)	
SP500	0.09***	3.47	0.07***	4.10	0.03	0.07	0.02	−0.04	0.08***	0.41	0.04	−0.05
	(0.02)		(0.03)		(0.02)		(0.02)		(0.02)		(0.03)	
Const.	−0.91***		−1.69***		1.34***		−1.07***		0.81***		−0.47*	
	(0.33)		(0.37)		(0.23)		(0.21)		(0.27)		(0.26)	
R^2	57.66		50.97		47.34		68.81		50.72		65.36	

	$\lvert\widehat{\alpha}_{b(i),t}\rvert$											
	0DTE				1–3DTE				4–15DTE			
	Puts		Calls		Puts		Calls		Puts		Calls	
	Coef.	$R^2_{\text{univ.}}$	Coef.	$R^2_{\text{univ.}}$	Coef.	$R^2_{\text{univ.}}$	Coef.	$R^2_{\text{univ.}}$	Coef.	$R^2_{\text{univ.}}$	Coef.	$R^2_{\text{univ.}}$
ESF	0.07	1.21	0.10**	1.45	−0.02	−0.05	−0.01	0.25	−0.03	0.30	0.02	1.47
	(0.05)		(0.05)		(0.02)		(0.04)		(0.04)		(0.03)	
HKM	−0.06	3.80	−0.12**	5.23	0.25***	0.82	0.23***	−0.03	0.29***	0.09	0.08**	6.69
	(0.05)		(0.06)		(0.04)		(0.04)		(0.04)		(0.04)	
ε_{HKM}	−0.01	3.07	−0.10***	4.04	0.05	0.53	0.09	0.39	0.07*	−0.05	0.11	0.09
	(0.03)		(0.03)		(0.04)		(0.06)		(0.04)		(0.08)	
CIV	0.62***	52.52	0.64***	48.45	0.50***	15.00	0.78***	48.20	0.71***	33.82	0.81***	58.68
	(0.11)		(0.14)		(0.05)		(0.04)		(0.06)		(0.06)	
OI	0.27***	19.99	0.07***	2.00	−0.20***	2.08	−0.05**	−0.01	−0.08***	−0.05	0.01	0.12
	(0.04)		(0.02)		(0.03)		(0.02)		(0.02)		(0.02)	
SP500	−0.09***	3.57	−0.07***	4.16	0.07***	0.49	0.02	0.07	−0.04	−0.04	−0.04	−0.05
	(0.03)		(0.03)		(0.02)		(0.02)		(0.03)		(0.03)	
Const.	1.03***		1.77***		0.16		−0.93***		−1.19***		−0.57**	
	(0.33)		(0.37)		(0.24)		(0.27)		(0.24)		(0.25)	
R^2	60.89		52.62		25.48		53.83		40.24		60.22	

Table A.VI
DOTM Option Dislocations and Intermediary Frictions

The table reports the coefficients and R^2 of the regressions of DOTM option dislocations measured at 15:45 ET on variables related to frictions faced by financial intermediaries and on controls. The top panel reports the results for dislocations, $\widehat{\alpha}_{b(i),t}$, while the bottom panel reports the results for absolute dislocations, $|\widehat{\alpha}_{b(i),t}|$. The dislocations are estimated as bucket-level fixed effects in cross-sectional regressions of the conditional intercepts on option exposures (as in equation (16)) for puts and calls, at each 30-minute timestamp. *SP500* is the intraday return of the S&P 500 ES futures from 9:45 ET to 15:15 ET on the current day. *HKM* is the level of the aggregate market equity ratio of primary dealers at the end of the previous day as defined by He, Kelly, and Manela (2017). ε_{HKM} proposed therein is the AR(1) innovation to the capital ratio, scaled by the lagged ratio, on the current day. *ESF* is the spread between the forward interest rate implied by the S&P 500 E-Mini futures and the three-month OIS rate, as in Siriwardane, Sunderam, and Wallen (2025) and Appendix D, estimated using futures prices at the futures closing time, 16:15 ET, of the previous day. *OI* is the open interest of all the puts (calls) within each bucket at the end of the previous day. CIV^2 is the corridor implied variance calculated from options with the given maturity at 15:15 ET on the current day. For each combination of option maturity and type, the table reports the estimated coefficients, their robust standard errors (in parentheses) and adjusted R^2 (in %) in the first column, and the $R^2_{\text{univ.}}$ (in %) from a univariate regression in the second column. All the variables are normalized using their full-sample standard deviations. The sample period is from 2016/09 to 2023/12.

	$\widehat{\alpha}_{b(i),t}$											
	0DTE				1–3DTE				4–15DTE			
	Puts		Calls		Puts		Calls		Puts		Calls	
	Coef.	$R^2_{\text{univ.}}$	Coef.	$R^2_{\text{univ.}}$	Coef.	$R^2_{\text{univ.}}$	Coef.	$R^2_{\text{univ.}}$	Coef.	$R^2_{\text{univ.}}$	Coef.	$R^2_{\text{univ.}}$
ESF	−0.10**	0.89	−0.11***	2.06	0.03	−0.05	−0.12***	2.61	0.00	0.68	−0.09***	3.72
	(0.05)		(0.04)		(0.04)		(0.02)		(0.03)		(0.03)	
HKM	0.16***	5.74	0.23***	12.30	−0.04	2.25	0.29***	25.52	−0.01	12.29	0.21***	24.61
	(0.05)		(0.05)		(0.04)		(0.03)		(0.04)		(0.04)	
ε_{HKM}	0.05**	1.39	0.10***	4.01	−0.03	−0.06	0.00	−0.02	−0.03	0.20	−0.04	0.12
	(0.02)		(0.03)		(0.03)		(0.04)		(0.03)		(0.03)	
CIV	−0.64***	48.65	−0.60***	46.43	−0.67***	42.34	−0.68***	61.32	−0.74***	56.65	−0.69***	62.63
	(0.14)		(0.15)		(0.05)		(0.11)		(0.07)		(0.11)	
OI	−0.20***	4.94	−0.05***	0.95	−0.06***	0.29	−0.02	0.02	0.07***	6.88	−0.09***	0.00
	(0.03)		(0.02)		(0.02)		(0.01)		(0.03)		(0.02)	
SP500	0.08***	2.84	0.09***	4.85	0.04	0.12	0.04***	0.10	0.07***	0.27	0.02	−0.05
	(0.03)		(0.03)		(0.03)		(0.02)		(0.02)		(0.02)	
Const.	−1.21***		−2.23***		1.69***		−0.96***		0.83***		−0.54	
	(0.36)		(0.36)		(0.27)		(0.25)		(0.26)		(0.34)	
R^2	55.77		54.80		43.01		70.19		57.37		66.95	

	$\lvert\widehat{\alpha}_{b(i),t}\rvert$											
	0DTE				1–3DTE				4–15DTE			
	Puts		Calls		Puts		Calls		Puts		Calls	
	Coef.	$R^2_{\text{univ.}}$	Coef.	$R^2_{\text{univ.}}$	Coef.	$R^2_{\text{univ.}}$	Coef.	$R^2_{\text{univ.}}$	Coef.	$R^2_{\text{univ.}}$	Coef.	$R^2_{\text{univ.}}$
ESF	0.09*	0.82	0.11***	2.08	−0.01	0.03	−0.04	−0.01	−0.05	0.16	0.03	2.20
	(0.05)		(0.04)		(0.03)		(0.04)		(0.04)		(0.04)	
HKM	−0.13**	4.93	−0.22***	11.95	0.17***	0.01	0.28***	0.15	0.23***	−0.02	0.15***	3.71
	(0.05)		(0.05)		(0.04)		(0.04)		(0.04)		(0.04)	
ε_{HKM}	−0.04	1.20	−0.10***	4.01	0.04	0.59	0.08	0.35	0.09**	0.07	0.05	0.06
	(0.03)		(0.03)		(0.03)		(0.05)		(0.04)		(0.04)	
CIV	0.69***	54.04	0.61***	47.88	0.52***	22.20	0.72***	39.00	0.69***	29.19	0.78***	50.36
	(0.15)		(0.15)		(0.04)		(0.04)		(0.06)		(0.07)	
OI	0.18***	3.98	0.04**	0.85	−0.10***	0.53	−0.01	−0.02	0.15***	0.90	−0.02	0.05
	(0.03)		(0.02)		(0.02)		(0.02)		(0.04)		(0.03)	
SP500	−0.08***	2.86	−0.09***	4.90	0.10***	1.13	0.02	0.05	0.01	0.01	−0.02	−0.03
	(0.03)		(0.03)		(0.02)		(0.02)		(0.02)		(0.03)	
Const.	1.23***		2.23***		0.48*		−0.93***		−1.15***		−0.74**	
	(0.36)		(0.35)		(0.28)		(0.28)		(0.26)		(0.30)	
R^2	59.28		55.84		26.20		46.57		39.11		52.32	

Table A.VII
ATM Option Dislocations and Intraday ES Futures Returns Decomposition

The table reports the coefficients and R^2 of the regressions of ATM option dislocations at 15:45 ET on the decomposition of intraday ES futures return at daily frequency across option types and maturity buckets. The top panel reports the results for dislocations, $\alpha_{b(i),t}$, while the bottom panel reports the results for absolute dislocations, $|\alpha_{b(i),t}|$. The dislocations are estimated as bucket-level fixed effects in cross-sectional regressions of the conditional intercepts on option exposures (as in equation (16)) for puts and calls, at each 30-minute timestamp. $SP500_{t,[09:45,14:45]}$ and $SP500_{t,[14:45,15:15]}$ denote the intraday returns of the S&P 500 ES futures from 9:45 ET to 14:45 ET and from 14:45 ET to 15:15 ET, respectively, on the current day. For each combination of option maturity and type, the table reports the estimated coefficients, their robust standard errors (in parentheses) and adjusted R^2 (in %) in the first column, and the $R^2_{\text{univ.}}$ (in %) from a univariate regression in the second column. All the variables are normalized using their full-sample standard deviations. The sample period is from 2016/09 to 2023/12.

	$\widehat{\alpha}_{b(i),t}$											
	0DTE				1–3DTE				4–15DTE			
	Puts		Calls		Puts		Calls		Puts		Calls	
	Coef.	$R^2_{\text{univ.}}$	Coef.	$R^2_{\text{univ.}}$	Coef.	$R^2_{\text{univ.}}$	Coef.	$R^2_{\text{univ.}}$	Coef.	$R^2_{\text{univ.}}$	Coef.	$R^2_{\text{univ.}}$
$SP500_{[09:45,14:45]}$	0.19***	3.35	0.19***	3.42	0.08	0.49	0.00	−0.05	0.07	0.45	−0.02	0.00
	(0.05)		(0.05)		(0.05)		(0.07)		(0.06)		(0.07)	
$SP500_{[14:45,15:15]}$	0.07	0.36	0.07	0.34	0.05	0.17	0.04	0.09	0.05	0.20	0.03	0.04
	(0.05)		(0.05)		(0.04)		(0.04)		(0.04)		(0.05)	
Const.	−1.32***		−1.59***		0.56***		−0.13*		0.24***		−0.33***	
	(0.07)		(0.08)		(0.06)		(0.07)		(0.06)		(0.07)	
R^2	3.74		3.78		0.69		0.03		0.69		0.04	

	$\lvert\widehat{\alpha}_{b(i),t}\rvert$											
	0DTE				1–3DTE				4–15DTE			
	Puts		Calls		Puts		Calls		Puts		Calls	
	Coef.	$R^2_{\text{univ.}}$	Coef.	$R^2_{\text{univ.}}$	Coef.	$R^2_{\text{univ.}}$	Coef.	$R^2_{\text{univ.}}$	Coef.	$R^2_{\text{univ.}}$	Coef.	$R^2_{\text{univ.}}$
$SP500_{[09:45,14:45]}$	−0.19***	3.53	−0.19***	3.53	0.05	0.27	0.04	0.11	−0.03	0.00	0.01	−0.03
	(0.05)		(0.05)		(0.04)		(0.07)		(0.06)		(0.08)	
$SP500_{[14:45,15:15]}$	−0.07	0.32	−0.06	0.30	−0.04	0.12	−0.04	0.11	−0.06	0.26	−0.03	0.07
	(0.05)		(0.05)		(0.04)		(0.04)		(0.05)		(0.05)	
Const.	1.42***		1.62***		1.21***		0.79***		0.85***		0.57***	
	(0.07)		(0.08)		(0.05)		(0.06)		(0.06)		(0.07)	
R^2	3.88		3.85		0.37		0.20		0.28		0.03	

Table A.VIII
OTM Option Dislocations and Intraday ES Futures Returns Decomposition

The table reports the coefficients and R^2 of the regressions of OTM option dislocations at 15:45 ET on the decomposition of intraday ES futures return at daily frequency across option types and maturity buckets. The top panel reports the results for dislocations, $\alpha_{b(i),t}$, while the bottom panel reports the results for absolute dislocations, $|\alpha_{b(i),t}|$. The dislocations are estimated as bucket-level fixed effects in cross-sectional regressions of the conditional intercepts on option exposures (as in equation (16)) for puts and calls, at each 30-minute timestamp. $SP500_{t,[09:45,14:45]}$ and $SP500_{t,[14:45,15:15]}$ denote the intraday returns of the S&P 500 ES futures from 9:45 ET to 14:45 ET and from 14:45 ET to 15:15 ET, respectively, on the current day. For each combination of option maturity and type, the table reports the estimated coefficients, their robust standard errors (in parentheses) and adjusted R^2 (in %) in the first column, and the $R^2_{\text{univ.}}$ (in %) from a univariate regression in the second column. All the variables are normalized using their full-sample standard deviations. The sample period is from 2016/09 to 2023/12.

	$\widehat{\alpha}_{b(i),t}$											
	0DTE				1–3DTE				4–15DTE			
	Puts		Calls		Puts		Calls		Puts		Calls	
	Coef.	$R^2_{\text{univ.}}$	Coef.	$R^2_{\text{univ.}}$	Coef.	$R^2_{\text{univ.}}$	Coef.	$R^2_{\text{univ.}}$	Coef.	$R^2_{\text{univ.}}$	Coef.	$R^2_{\text{univ.}}$
$SP500_{[09:45,14:45]}$	0.17***	2.93	0.19***	3.61	0.02	−0.03	0.00	−0.05	0.05	0.21	−0.01	−0.03
	(0.05)		(0.05)		(0.06)		(0.07)		(0.06)		(0.08)	
$SP500_{[14:45,15:15]}$	0.07	0.44	0.07	0.37	0.06	0.30	0.04	0.13	0.06	0.25	0.04	0.09
	(0.05)		(0.05)		(0.04)		(0.04)		(0.05)		(0.05)	
Const.	−1.24***		−1.41***		1.13***		0.14**		0.35***		−0.18***	
	(0.07)		(0.08)		(0.06)		(0.07)		(0.06)		(0.07)	
R^2	3.40		4.01		0.28		0.07		0.49		0.05	

	$\lvert\widehat{\alpha}_{b(i),t}\rvert$											
	0DTE				1–3DTE				4–15DTE			
	Puts		Calls		Puts		Calls		Puts		Calls	
	Coef.	$R^2_{\text{univ.}}$	Coef.	$R^2_{\text{univ.}}$	Coef.	$R^2_{\text{univ.}}$	Coef.	$R^2_{\text{univ.}}$	Coef.	$R^2_{\text{univ.}}$	Coef.	$R^2_{\text{univ.}}$
$SP500_{[09:45,14:45]}$	−0.18***	3.06	−0.20***	3.69	0.09**	0.88	0.05	0.20	0.01	−0.05	0.01	−0.04
	(0.05)		(0.05)		(0.04)		(0.08)		(0.06)		(0.08)	
$SP500_{[14:45,15:15]}$	−0.07	0.41	−0.07	0.35	−0.06	0.30	−0.04	0.10	−0.07	0.38	−0.04	0.11
	(0.05)		(0.05)		(0.04)		(0.04)		(0.05)		(0.05)	
Const.	1.33***		1.46***		1.64***		0.81***		0.92***		0.56***	
	(0.07)		(0.08)		(0.04)		(0.06)		(0.06)		(0.07)	
R^2	3.50		4.06		1.13		0.28		0.33		0.07	

Table A.IX
DOTM Option Dislocations and Intraday ES Futures Returns Decomposition

The table reports the coefficients and R^2 of the regressions of DOTM option dislocations at 15:45 ET on the decomposition of intraday ES futures return at daily frequency across option types and maturity buckets. The top panel reports the results for dislocations, $\alpha_{b(i),t}$, while the bottom panel reports the results for absolute dislocations, $|\alpha_{b(i),t}|$. The dislocations are estimated as bucket-level fixed effects in cross-sectional regressions of the conditional intercepts on option exposures (as in equation (16)) for puts and calls, at each 30-minute timestamp. $SP500_{t,[09:45,14:45]}$ and $SP500_{t,[14:45,15:15]}$ denote the intraday returns of the S&P 500 ES futures from 9:45 ET to 14:45 ET and from 14:45 ET to 15:15 ET, respectively, on the current day. For each combination of option maturity and type, the table reports the estimated coefficients, their robust standard errors (in parentheses) and adjusted R^2 (in %) in the first column, and the $R^2_{\text{univ.}}$ (in %) from a univariate regression in the second column. All the variables are normalized using their full-sample standard deviations. The sample period is from 2016/09 to 2023/12.

	$\widehat{\alpha}_{b(i),t}$											
	0DTE				1–3DTE				4–15DTE			
	Puts		Calls		Puts		Calls		Puts		Calls	
	Coef.	$R^2_{\text{univ.}}$	Coef.	$R^2_{\text{univ.}}$	Coef.	$R^2_{\text{univ.}}$	Coef.	$R^2_{\text{univ.}}$	Coef.	$R^2_{\text{univ.}}$	Coef.	$R^2_{\text{univ.}}$
$SP500_{[09:45,14:45]}$	0.17***	2.88	0.21***	4.33	0.02	−0.03	0.03	0.03	0.04	0.11	−0.01	−0.04
	(0.04)		(0.04)		(0.08)		(0.07)		(0.07)		(0.09)	
$SP500_{[14:45,15:15]}$	0.02	−0.07	0.07	0.42	0.08*	0.53	0.04	0.06	0.05	0.22	0.02	−0.01
	(0.08)		(0.05)		(0.05)		(0.04)		(0.05)		(0.05)	
Const.	−0.85***		−1.20***		1.11***		0.36***		0.44***		0.03	
	(0.07)		(0.08)		(0.06)		(0.07)		(0.06)		(0.07)	
R^2	2.85		4.78		0.51		0.10		0.35		−0.06	

	$\lvert\widehat{\alpha}_{b(i),t}\rvert$											
	0DTE				1–3DTE				4–15DTE			
	Puts		Calls		Puts		Calls		Puts		Calls	
	Coef.	$R^2_{\text{univ.}}$	Coef.	$R^2_{\text{univ.}}$	Coef.	$R^2_{\text{univ.}}$	Coef.	$R^2_{\text{univ.}}$	Coef.	$R^2_{\text{univ.}}$	Coef.	$R^2_{\text{univ.}}$
$SP500_{[09:45,14:45]}$	−0.18***	2.95	−0.21***	4.39	0.13**	1.60	0.05	0.18	0.04	0.16	0.02	0.01
	(0.04)		(0.04)		(0.06)		(0.08)		(0.06)		(0.10)	
$SP500_{[14:45,15:15]}$	−0.02	−0.07	−0.07	0.41	−0.04	0.15	−0.04	0.12	−0.05	0.26	−0.02	0.00
	(0.08)		(0.05)		(0.05)		(0.04)		(0.05)		(0.05)	
Const.	1.01***		1.24***		1.60***		1.10***		0.95***		0.78***	
	(0.07)		(0.08)		(0.05)		(0.06)		(0.06)		(0.06)	
R^2	2.90		4.83		1.71		0.28		0.39		0.00	

Table A.X
OTM Option Dislocations and Intermediary Frictions: Instrumental Variable Approach

This table repeats the analysis of Table A.V using an instrumental variable (IV) approach to address potential endogeneity concerns arising from the fact that time variation in frictions in the SPX option market and ES futures market (the primary hedging instrument) may be correlated. We instrument *ESF*, the spread between the forward interest rate implied by the S&P 500 E-Mini futures and the three-month OIS rate, using the corresponding spread for the Russell 2000 E-Mini futures. Since the latter are only available from 2017/07, the sample period is from 2017/07 to 2023/12.

	$\widehat{\alpha}_{b(i),t}$											
	0DTE				1–3DTE				4–15DTE			
	Puts		Calls		Puts		Calls		Puts		Calls	
	Coef.	$R^2_{\text{univ.}}$	Coef.	$R^2_{\text{univ.}}$	Coef.	$R^2_{\text{univ.}}$	Coef.	$R^2_{\text{univ.}}$	Coef.	$R^2_{\text{univ.}}$	Coef.	$R^2_{\text{univ.}}$
ESF	−0.12**	0.99	−0.18***	1.54	−0.01	−0.01	−0.16***	1.47	−0.03	0.51	−0.09**	1.16
	(0.06)		(0.06)		(0.04)		(0.03)		(0.05)		(0.04)	
HKM	0.04	2.57	0.11**	4.65	0.01	4.76	0.28***	24.01	−0.02	7.89	0.15***	20.14
	(0.05)		(0.05)		(0.04)		(0.03)		(0.05)		(0.04)	
ε_{HKM}	0.02	3.35	0.11***	4.26	−0.02	−0.03	−0.04	−0.02	−0.02	0.27	−0.10	0.08
	(0.03)		(0.03)		(0.03)		(0.05)		(0.04)		(0.08)	
CIV	−0.61***	50.11	−0.62***	46.98	−0.70***	51.31	−0.70***	64.01	−0.74***	53.49	−0.73***	63.67
	(0.10)		(0.13)		(0.06)		(0.07)		(0.08)		(0.08)	
OI	−0.26***	19.17	−0.07***	1.99	−0.08***	3.17	−0.02*	0.87	0.00	−0.06	0.00	0.03
	(0.04)		(0.02)		(0.03)		(0.01)		(0.02)		(0.02)	
SP500	0.09***	3.55	0.08***	4.26	0.02	0.05	0.03	−0.06	0.08***	0.40	0.05	−0.06
	(0.02)		(0.03)		(0.02)		(0.02)		(0.03)		(0.03)	
Const.	−0.76**		−1.50***		1.52***		−1.03***		0.98***		−0.47**	
	(0.32)		(0.37)		(0.23)		(0.18)		(0.26)		(0.23)	
R^2	57.87		50.55		51.69		71.43		53.75		66.06	

	$\lvert\widehat{\alpha}_{b(i),t}\rvert$											
	0DTE				1–3DTE				4–15DTE			
	Puts		Calls		Puts		Calls		Puts		Calls	
	Coef.	$R^2_{\text{univ.}}$	Coef.	$R^2_{\text{univ.}}$	Coef.	$R^2_{\text{univ.}}$	Coef.	$R^2_{\text{univ.}}$	Coef.	$R^2_{\text{univ.}}$	Coef.	$R^2_{\text{univ.}}$
ESF	0.11*	0.87	0.17***	1.41	−0.11**	−3.83	−0.04	−2.10	−0.11**	−1.63	−0.01	1.21
	(0.06)		(0.06)		(0.05)		(0.06)		(0.05)		(0.05)	
HKM	−0.04	2.81	−0.11**	4.88	0.23***	0.21	0.21***	0.09	0.27***	0.53	0.08**	6.86
	(0.05)		(0.05)		(0.04)		(0.04)		(0.04)		(0.04)	
ε_{HKM}	−0.02	3.26	−0.10***	4.12	0.07*	0.82	0.10	0.50	0.08*	−0.05	0.12	0.12
	(0.03)		(0.03)		(0.04)		(0.06)		(0.04)		(0.08)	
CIV	0.63***	53.48	0.64***	48.87	0.57***	20.75	0.81***	53.51	0.77***	40.81	0.82***	60.39
	(0.11)		(0.13)		(0.04)		(0.04)		(0.07)		(0.07)	
OI	0.26***	19.36	0.06***	1.94	−0.19***	1.73	−0.03*	0.04	−0.06**	−0.06	0.01	0.18
	(0.04)		(0.02)		(0.03)		(0.02)		(0.03)		(0.02)	
SP500	−0.09***	3.68	−0.08***	4.33	0.07***	0.49	0.02	0.04	−0.04	−0.04	−0.05	−0.06
	(0.03)		(0.03)		(0.02)		(0.02)		(0.03)		(0.03)	
Const.	0.88***		1.60***		0.43*		−0.82***		−0.98***		−0.49**	
	(0.33)		(0.38)		(0.23)		(0.24)		(0.24)		(0.24)	
R^2	61.03		52.37		29.53		58.28		45.37		61.76	

Table A.XI
DOTM Option Dislocations and Intermediary Frictions: Instrumental Variable Approach

This table repeats the analysis of Table A.VI using an instrumental variable (IV) approach to address potential endogeneity concerns arising from the fact that time variation in frictions in the SPX option market and ES futures market (the primary hedging instrument) may be correlated. We instrument *ESF*, the spread between the forward interest rate implied by the S&P 500 E-Mini futures and the three-month OIS rate, using the corresponding spread for the Russell 2000 E-Mini futures. Since the latter are only available from 2017/07, the sample period is from 2017/07 to 2023/12.

	$\widehat{\alpha}_{b(i),t}$											
	0DTE				1–3DTE				4–15DTE			
	Puts		Calls		Puts		Calls		Puts		Calls	
	Coef.	$R^2_{\text{univ.}}$	Coef.	$R^2_{\text{univ.}}$	Coef.	$R^2_{\text{univ.}}$	Coef.	$R^2_{\text{univ.}}$	Coef.	$R^2_{\text{univ.}}$	Coef.	$R^2_{\text{univ.}}$
ESF	−0.16***	0.22	−0.20***	1.88	0.03	−0.41	−0.22***	1.78	−0.04	0.41	−0.16***	2.42
	(0.06)		(0.06)		(0.05)		(0.04)		(0.05)		(0.04)	
HKM	0.15***	4.57	0.21***	10.72	−0.07	1.68	0.30***	25.43	−0.03	10.95	0.22***	24.54
	(0.05)		(0.05)		(0.04)		(0.03)		(0.04)		(0.04)	
ε_{HKM}	0.05*	1.37	0.10***	4.25	−0.02	−0.06	−0.01	−0.04	−0.02	0.24	−0.03	0.10
	(0.02)		(0.03)		(0.03)		(0.04)		(0.04)		(0.03)	
CIV	−0.65***	49.69	−0.61***	47.57	−0.70***	46.36	−0.68***	62.84	−0.76***	60.07	−0.68***	62.87
	(0.14)		(0.14)		(0.06)		(0.10)		(0.08)		(0.10)	
OI	−0.20***	4.47	−0.04*	0.64	−0.04**	0.14	−0.02	0.08	0.08***	6.47	−0.09***	0.33
	(0.03)		(0.02)		(0.02)		(0.01)		(0.03)		(0.02)	
SP500	0.09***	2.96	0.10***	5.01	0.03	0.11	0.05***	0.08	0.07***	0.26	0.02	−0.06
	(0.03)		(0.03)		(0.03)		(0.02)		(0.02)		(0.02)	
Const.	−1.02***		−1.98***		1.83***		−0.88***		1.02***		−0.54*	
	(0.35)		(0.36)		(0.26)		(0.21)		(0.24)		(0.29)	
R^2	55.62		54.31		47.14		71.34		60.48		67.21	

	$\lvert\widehat{\alpha}_{b(i),t}\rvert$											
	0DTE				1–3DTE				4–15DTE			
	Puts		Calls		Puts		Calls		Puts		Calls	
	Coef.	$R^2_{\text{univ.}}$	Coef.	$R^2_{\text{univ.}}$	Coef.	$R^2_{\text{univ.}}$	Coef.	$R^2_{\text{univ.}}$	Coef.	$R^2_{\text{univ.}}$	Coef.	$R^2_{\text{univ.}}$
ESF	0.14**	0.42	0.20***	1.99	−0.07	−1.57	−0.07	−2.63	−0.16***	−3.32	0.00	1.98
	(0.06)		(0.06)		(0.05)		(0.07)		(0.05)		(0.06)	
HKM	−0.12**	3.92	−0.21***	10.43	0.14***	0.34	0.27***	0.01	0.20***	0.00	0.14***	3.97
	(0.05)		(0.05)		(0.05)		(0.05)		(0.04)		(0.05)	
ε_{HKM}	−0.04*	1.28	−0.10***	4.25	0.05	0.91	0.09*	0.41	0.10**	0.09	0.05	0.04
	(0.03)		(0.03)		(0.03)		(0.05)		(0.04)		(0.04)	
CIV	0.69***	54.40	0.62***	48.80	0.57***	27.83	0.75***	43.90	0.76***	36.42	0.79***	52.82
	(0.14)		(0.14)		(0.04)		(0.04)		(0.06)		(0.08)	
OI	0.18***	3.79	0.03	0.58	−0.09***	0.47	0.00	−0.03	0.16***	0.61	−0.03	−0.03
	(0.03)		(0.02)		(0.03)		(0.02)		(0.04)		(0.03)	
SP500	−0.08***	2.97	−0.10***	5.04	0.10***	1.21	0.02	0.01	0.01	0.00	−0.02	−0.04
	(0.03)		(0.03)		(0.02)		(0.02)		(0.03)		(0.03)	
Const.	1.06***		1.98***		0.71***		−0.85***		−0.84***		−0.66**	
	(0.35)		(0.36)		(0.27)		(0.27)		(0.23)		(0.29)	
R^2	59.02		55.34		30.91		50.76		44.06		54.50	

Table A.XII
The First-stage Results of IV Regressions

This table reports the first-stage regression results for the instrumental variable (IV) approach used in Tables VII, A.X, and A.XI. Since the puts and calls with different maturities are not available on the exactly same dates, we report the first-stage regression results separately for each option type and maturity group. We instrument *ESF*, the spread between the forward interest rate implied by the S&P 500 E-Mini futures and the three-month OIS rate, using the corresponding spread for the Russell 2000 E-Mini futures. Since the latter are only available from 2017/07, the sample period is from 2017/07 to 2023/12.

	0DTE		1–3DTE		4–15DTE	
	R^2	$Fstats.$	R^2	$Fstats.$	R^2	$Fstats.$
P	57.4	298.2	53.1	203.8	53.3	200.6
C	58.3	310.4	53.2	209.8	53.2	211.5